eport No. DOT-TSC-OST-77-10

DYNAMIC CENTRALIZED AND DECENTRALIZED CONTROL SYSTEMS

Douglas P. Looze
Paul K. Houpt
Michael Athans

Massachusetts Institute of Technology
Cambridge MA 02139

SEPTEMBER 1977

FINAL REPORT

Prepared for
U.S. DEPARTMENT OF TRANSPORTATION
OFFICE OF THE SECRETARY

Office of the Assistant Secretary for
Systems Development and Technology
Office of Systems Engineering
Washington DC 20590

NOTICE

This document is disseminated under the sponsorship of the Department of Transportation in the interest of information exchange. The United States Government assumes no liability for its contents or use thereof.

NOTICE

The United States Government does not endorse products or manufacturers. Trade or manufacturers' names appear herein solely because they are considered essential to the object of this report.

Technical Report Documentation Page

1. Report No.	2. Government Accession No.	3. Recipient's Catalog No.
DOT-TSC-OST-77-10		

4. Title and Subtitle
DYNAMIC CENTRALIZED AND DECENTRALIZED CONTROL SYSTEMS

5. Report Date
September 1977

6. Performing Organization Code

7. Author(s)
D.P. Looze, P.K. Houpt, M. Athans

8. Performing Organization Report No.
DOT-TSC-OST-77-5

9. Performing Organization Name and Address
Massachusetts Institute of Technology*
Electronic Systems Laboratory
Dept. of Electrical Engineering & Computer Science
Cambridge MA 02139

10. Work Unit No. (TRAIS)
OS750/R8526

11. Contract or Grant No.
DOT-TSC-849

12. Sponsoring Agency Name and Address
U.S. Department of Transportation
Office of the Assistant Secretary for Systems Development and Technology
Office of Systems Engineering
Washington DC 20590

13. Type of Report and Period Covered
Final Report
Sep 1975 - Sep 1976

14. Sponsoring Agency Code

15. Supplementary Notes
*Under contract to: U.S. Department of Transportation
Transportation Systems Center
Kendall Square
Cambridge MA 02142

16. Abstract

This report develops a systematic method for designing suboptimal decentralized control systems. The method is then applied to the design of a decentralized controller for a freeway-corridor system.

A freeway corridor is considered to be a system of parallel freeways and arterials connecting two locations. A centralized control system is designed for a freeway corridor using the Linear Quadratic Gaussian (LQG) regulator-design technique. It is found that the centralized design works well, subject to the validity of the model that is used.

An approach similar to the LQG method is used to develop the decentralized design method. A linearized model is used, and the subsystem filters and control laws are assumed to be linear. Communication between subsystems is specified before the filter and control gains are designed. The problem is formed as a static minimization constrained by a Lyapunov matrix equation. The variables over which the cost is minimized are the elements of the filter and control gains. A computer solution to the constrained static minimization is developed.

The design method is applied to a freeway-corridor system, and resulting design is compared to the centralized solution. It is found that the decentralized control system works almost as well as the centralized control system.

17. Key Words		18. Distribution Statement
Freeway corridor	Estimation	DOCUMENT IS AVAILABLE TO THE U.S. PUBLIC THROUGH THE NATIONAL TECHNICAL INFORMATION SERVICE, SPRINGFIELD, VIRGINIA 22161
Traffic	Assignment	
Control	Dynamic	
Centralized	Stochastic	
Decentralized		

19. Security Classif. (of this report)	20. Security Classif. (of this page)	21. No. of Pages	22. Price
Unclassified	Unclassified	114	

Form DOT F 1700.7 (8-72) Reproduction of completed page authorized

PREFACE

The current study is being performed under the Transportation Advanced Research Program (TARP) which is aimed at investigating the applicability of advanced techniques to large-scale transportation systems.

This report is based in part on the S.M. thesis by Douglas P. Looze, "Decentralized Control of a Freeway Traffic Corridor".

The research conducted at the M.I.T. Electronic Systems Laboratory has been supported by the U.S. Department of Transportation (DOT), and monitored by the Transportation Systems Center (TSC). We thank Diarmuid O'Mathuna and Ann Muzyka of TSC, and John Fearnsides of DOT for their helpful criticism, considered remarks, and welcome encouragement.

METRIC CONVERSION FACTORS

Approximate Conversions to Metric Measures

Symbol	When You Know	Multiply by	To Find	Symbol
	LENGTH			
in	inches	2.5	centimeters	cm
ft	feet	30	centimeters	cm
yd	yards	0.9	meters	m
mi	miles	1.6	kilometers	km
	AREA			
in^2	square inches	6.5	square centimeters	cm^2
ft^2	square feet	0.09	square meters	m^2
yd^2	square yards	0.8	square meters	m^2
mi^2	square miles	2.6	square kilometers	km^2
	acres	0.4	hectares	ha
	MASS (weight)			
oz	ounces	28	grams	g
lb	pounds	0.45	kilograms	kg
	short tons (2000 lb)	0.9	tonnes	t
	VOLUME			
tsp	teaspoons	5	milliliters	ml
Tbsp	tablespoons	15	milliliters	ml
fl oz	fluid ounces	30	milliliters	ml
c	cups	0.24	liters	l
pt	pints	0.47	liters	l
qt	quarts	0.95	liters	l
gal	gallons	3.8	liters	l
ft^3	cubic feet	0.03	cubic meters	m^3
yd^3	cubic yards	0.76	cubic meters	m^3
	TEMPERATURE (exact)			
°F	Fahrenheit temperature	5/9 (after subtracting 32)	Celsius temperature	°C

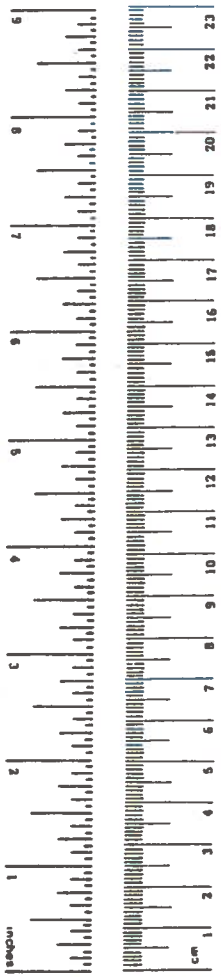

Approximate Conversions from Metric Measures

Symbol	When You Know	Multiply by	To Find	Symbol
	LENGTH			
mm	millimeters	0.04	inches	in
cm	centimeters	0.4	inches	in
m	meters	3.3	feet	ft
m	meters	1.1	yards	yd
km	kilometers	0.6	miles	mi
	AREA			
cm^2	square centimeters	0.16	square inches	in^2
m^2	square meters	1.2	square yards	yd^2
km^2	square kilometers	0.4	square miles	mi^2
ha	hectares (10,000 m^2)	2.5	acres	
	MASS (weight)			
g	grams	0.035	ounces	oz
kg	kilograms	2.2	pounds	lb
t	tonnes (1000 kg)	1.1	short tons	
	VOLUME			
ml	milliliters	0.03	fluid ounces	fl oz
l	liters	2.1	pints	pt
l	liters	1.06	quarts	qt
l	liters	0.26	gallons	gal
m^3	cubic meters	35	cubic feet	ft^3
m^3	cubic meters	1.3	cubic yards	yd^3
	TEMPERATURE (exact)			
°C	Celsius temperature	9/5 (then add 32)	Fahrenheit temperature	°F

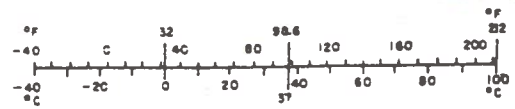

TABLE OF CONTENTS

SECTION		PAGE
1.	INTRODUCTION	1
2.	CENTRALIZED CONTROLLER	6
	2.1 Introduction	6
	2.2 Freeway-Corridor Model	6
	2.3 Centralized Solution	11
	2.4 Centralized Control Example	24
	2.5 Conclusion	43
3.	AN APPROACH TO DECENTRALIZED CONTROL	44
	3.1 Introduction	44
	3.2 The Decentralized Control Problem	44
	3.3 Method of Solution	50
	3.4 An Example	53
	3.5 Choosing the Parameters	64
	3.6 Existence of Solutions	67
4.	IMPLEMENTATION OF THE DECENTRALIZED CONTROL ALGORITHM	72
	4.1 Introduction	72
	4.2 Corridor and Controller Structure	72
	4.3 A Specific Corridor Structure	74
	4.4 Decentralized Control Example	80
5.	CONCLUSIONS	93
6.	BIBLIOGRAPHY	96
APPENDIX A:	DIRECT METHOD FOR SOLVING LYAPUNOV EQUATIONS	A-1
APPENDIX B:	LINEARIZED SYSTEM AND CENTRALIZED GAIN MATRICES	B-1
APPENDIX C:	DECENTRALIZED GAIN MATRICES	C-1
APPENDIX D:	REPORT OF INVENTIONS	D-1

ILLUSTRATIONS

FIGURE		PAGE
2.1	Interpretation of Aggregate Variables	7
2.2	Definition of Freeway Variables	8
2.3	Control Algorithm Flow Chart	22
2.4	Block Diagram of Centralized Control System	23
2.5	Freeway Corridor Structure for Example	25
2.6	Driver-Desired Velocity Curve	27
2.7	Centralized Control System Results for Example (Density) (Links 1 and 2)	33
2.8	Centralized Control System Results for Example (Density) (Links 3 and 4)	34
2.9	Centralized Control System Results for Example (Density) (Links 5 and 6)	35
2.10	Centralized Control System Results for Example (Velocity) (Links 1 and 2)	36
2.11	Centralized Control System Results for Example (Velocity) (Links 3 and 4)	37
2.12	Centralized Control System Results for Example (Velocity) (Links 5 and 6)	38
2.13	Centralized Control System Results for Example (Controls)	39
2.14	Uncontrolled Flow Demands on Corridor	41
2.15	Controlled Flow Demands on Corridor	42
3.1	Stability Region for Example 3.4a	56
3.2	Stability Regions for the One-Dimensional Problem 3.4b	59
3.3	Interaction of Stability Inequalities for the One-Dimensional Problem 3.4b	60
4.1	Structure of Decentralized Controller for General Freeway Corridor	75
4.2	Structure of Decentralized Controller for Example	78
4.3	Decentralized Control System Results for Example (Density) (Links 1 and 2)	82
4.4	Decentralized Control System Results for Example (Density) (Links 3 and 4)	83
4.5	Decentralized Control System Results for Example (Density) (Links 5 and 6)	84

FIGURE		PAGE
4.6	Decentralized Control System Results for Example (Velocity) (Links 1 and 2)	85
4.7	Decentralized Control System Results for Example (Velocity) (Links 3 and 4)	86
4.8	Decentralized Control System Results for Example (Velocity) (Links 5 and 6)	87
4.9	Decentralized Control System Results for Example (Controls)	88
4.10	Comparison of Flow Demands on Corridor	92

TABLES

TABLE		PAGE
2.1	Statistics for Main Freeway (A)	30
2.2	Statistics for Secondary Freeway (B)	31
3.1	Summary of Results for the One-Dimensional Problem 3.4a	57
3.2	Summary of Results for the One-Dimensional Problem 3.4b	61
3.3	Comparison of Resulting Solutions	63
4.1	Corridor Structure for Decentralized Control Example	76
4.2	Requirements for Solution of Static Optimization Problem	81
4.3	Comparison of Centralized and Decentralized Solutions for Sample Corridor	90

1. INTRODUCTION

Research in modern control theory has recently turned its attention from systems for which well defined and well understood models are available (such as the aerospace field) to socio-economic systems for which even the best models are only uncertain approximations to a real world that defies description. In addition, most socio-economic models are inherently infinite dimensional, and involve information accumulation from geographic areas large enough to make the cost of information transfer an important consideration. The problems presented by these systems are often dependent on the individual system with which one is working, and thus are difficult to solve generically.

Research is currently being done in the Electronic Systems Laboratory on the control of a freeway corridor. A freeway corridor is considered to be a system of parallel freeways and arterials connecting two locations. Freeway corridors typically connect suburban areas with a central business district in a nearby city. An individual motorist is assumed to be indifferent to the particular route used to travel between the two locations. Although most of the theory of modern control is applicable to this problem, the additional difficulties of a large dimensional system and information cost are presented and must be dealt with.

The advantages of an effective control system for a freeway corridor are numerous. Possibly, the most important inprovement may be the increase in effective capacity of existing freeway networks. In the past several years, new construction of freeways has not kept pace with the increase in demand for their use. This is especially true around large cities such as Los Angeles, Dallas, and New York. The result has been an increase in the number and duration of traffic jams on the main freeways, especially during rush-hour periods. Yet during the times that the main freeways are congested, there are often lower-capacity parallel arterials on which traffic is moving freely. The traffic control system may allow motorists to use the full capacity of the entire network, and not just that of the main freeway.

An effective control system may provide benefits to everyone using the

corridor. The average travel time for a motorist and the associated energy consumption may be reduced. Because the disruption of traffic flow as a result of accidents and normal rush-hour congestion may be minimized, the total gasoline consumption may be reduced, an important consideration today. Finally, the need for new roads may be reduced if the capacity of existing networks are fully used.

Models that have been developed for freeways can be placed in two categories: microscopic or macroscopic. Most of the microscopic models try to explain traffic phenomena by studying individual vehicles and their reactions to changes in speed of the vehicles ahead. This car-following literature has been well documented (Gazis et al. [1959] and Newell [1961]), but is difficult to use in the context of modern control theory.

More useful models for this purpose are the macroscopic models developed from an analogy to compressible gases. This analogy has been developed by Lighthill and Whitham [1955]. Greenberg [1959] has considered a specific form in which drivers accelerate proportional to the density gradient on the freeway. Isaksen and Payne [1972] have developed a similar model. The advantage of the macroscopic models is that these models use average flow rates, velocities, and densities, which are much easier to measure and track than the statistics of an individual vehicle.

Theoretically, once an appropriate state-space model has been developed for a freeway corridor, all the tools of modern control theory can be used to study and solve the problem. In particular, the Linear-Quadratic-Gaussian (LQG) regulator approach as summarized by Athans [1971] can be applied. Isaksen [1971] has presented an appropriate finite-dimensional model, and has used the model to derive traffic-responsive deterministic controls for a Los Angeles freeway. A complete non-deterministic control algorithm using the LQG regulator approach is given in Section 2.

Once the centralized control algorithm has been developed, consideration must be given to implementation problems associated with a large-scale system. These problems include numerical computation problems associated with finite-word length, and the cost of information transfer.

The numerical computation problems are a result of the large number of states needed to approximate an infinite-dimensional system for any reasonable freeway-network topology. For example, consider a 5-mile freeway-corridor system with the following topology:

a) ten, 1/2-mile freeway sections (links),

b) ten arterial links, and

c) six exit-and-entrance ramps.

With two state variables needed for each freeway and arterial link, and one state variable for each ramp, the total number of states for the system is 46. Solution of the noiseless centralized control problem with a linearized model involves a 46th-order Ricatti equation. If an estimator with identification of 1 parameter per link is included, the dimension of the estimator is 66, and the problem can quickly become intractable for on-line computation.

Assuming the computational difficulties can be solved, there is still the problem that measurements on the freeway-corridor system are made at points all along the length of the corridor. For a centralized controller to be effective, these measurements must be transmitted on the central processor, and the control must be transmitted back to the individual locations where they are to be implemented. To accomplish this information transfer, some form of communication channel (typically a rented telephone cable, or a private radio frequency) must be maintained. The cost of these channels can often be prohibitive.

The noise that is present in the communication channels will affect the performance of the controller. This imposes an additional cost on the control system since the control will not be as effective, and must be taken into account when designing the controller.

The usual approach to solving the problems stated above is to implement a decentralized suboptimal controller using the properties of the system in the design of the controller. Very little has been done in the way of research of the generic decentralized control problem. Witsenhausen [1968] and Chong [1970] have shown that controls for a decentralized system do not in general obey a separation theorem when the controllers have different information patterns. Carpenter [1972] has solved (in principle) the two controller

linear quadratic Gaussian problem with linear feedback and several noisy information patterns. Chong and Athans [1975] have demonstrated some sufficient conditions for the decomposition of a decentralized control problem into a two-level hierarchical minimization problem. A rather complete survey of decentralized methods can be found in Sandell, Varaiya and Athans [1975].

The problem of decentralized control of a freeway has hardly been considered. Thompson, Payne and Isaksen [1972] have used full-state feedback and a deterministic model to simulate decentralized control of a segment of the Hollywood freeway in Los Angeles. Houpt [1974] has developed a simplified finite-state model for a freeway corridor, and has demonstrated the difficulties associated with real-time decentralized feedback control. Except for the ad-hoc deterministic approach suggested by Isaksen and Payne [1972], there are virtually no stochastic decentralized control schemes which are both systematic in approach and practically feasible to implement.

This report will attempt to develop and apply a complete decentralized control algorithm for the freeway-corridor problem using the Isaksen-Payne model. The approach that will be taken is a parameterization of the infinite-time LQG regulator problem. The problem can be reformulated as a static minimization constrained by a Lyapunov matrix equation (see Appendix A).

Section 3 presents this approach and develops a method of solution for the static-minimization problem. Several problems are encountered in applying the solution. One of the most important is the difficulty of solving the Lyapunov equation for large systems (see Hagander [1972] for a survey of methods for the solution of this equation). Another important problem is the initial choice for the parameterization. Certain parameterizations admit non-unique solutions. This problem is closely related to the work done by Glover [1973] on identification.

The parameterization method for the design of decentralized control systems is then applied to a sample freeway-corridor system in Section 4. The results are compared with the results of the centralized control system which is developed in Section 2. It is found that the decentralized design works almost as well as the centralized control system.

The main contribution of this report is the development of a systematic method for the design of decentralized control systems which can be applied to practical problems.

2. CENTRALIZED CONTROLLER

2.1 Introduction

Although the ultimate objective of this report is to develop a decentralized control system, the design of a centralized controller is important for two reasons:

a) The centralized controller can give insights into the behavior and structure of the system. These insights will be invaluable when the design of the decentralized controller is attempted.

b) The centralized solution gives us a standard to which we can compare the decentralized controller.

This section will be concerned with the development of a centralized control system. The method of design is essentially the LQG regulator approac as summarized by Athans [1971]. Section 2.2 will present the model equations for the freeway corridor. Section 2.3 will discuss briefly the LQG regulator approach, and present the linearized equations. The final design of the centralized controller will be summarized and evaluated in section 2.4.

2.2 Freeway-Corridor Model

This section will present and briefly discuss the model equations that wi be used for the freeway corridor. A more detailed discussion can be found in Isaksen and Payne [1972].

The system to be controlled is a freeway corridor consisting of a freeway and several parallel arterials. The model for both the freeway and arterials will be the model developed by Isaksen and Payne [1972] with modifications to the beginning and ending links of the corridor.

Each roadway (freeway or arterial) is sectioned into links, with the length of the individual links determined by the topography of the corridor. The state variables are the spatial aggregate density (vehicles/hour) of the vehicles on each link (see figure 2.1 for the interpretation of aggregates). The equations for the ith link of the jth roadway are (see figure 2.2):

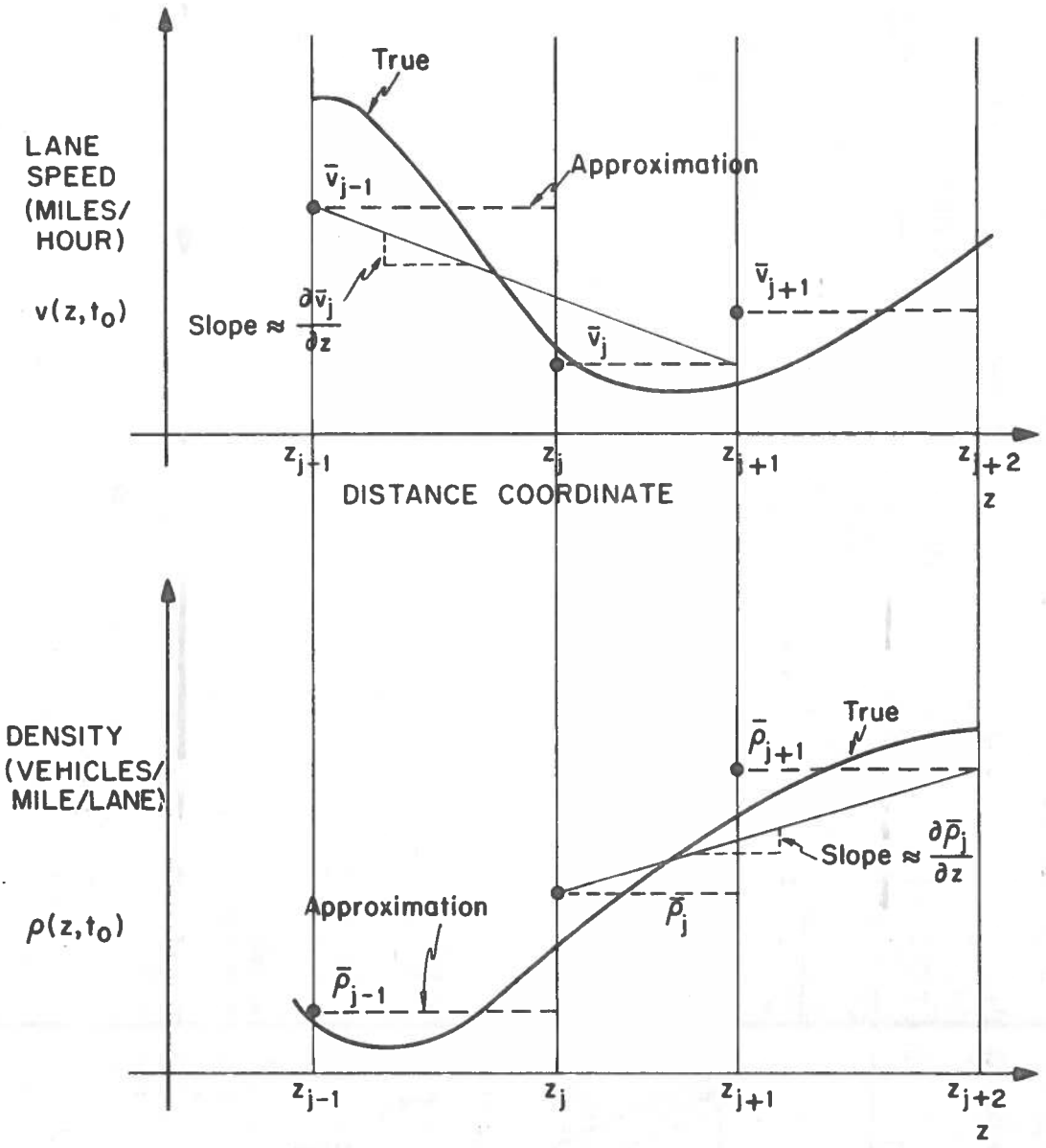

Figure 2.1 INTERPRETATION OF AGGREGATE VARIABLES

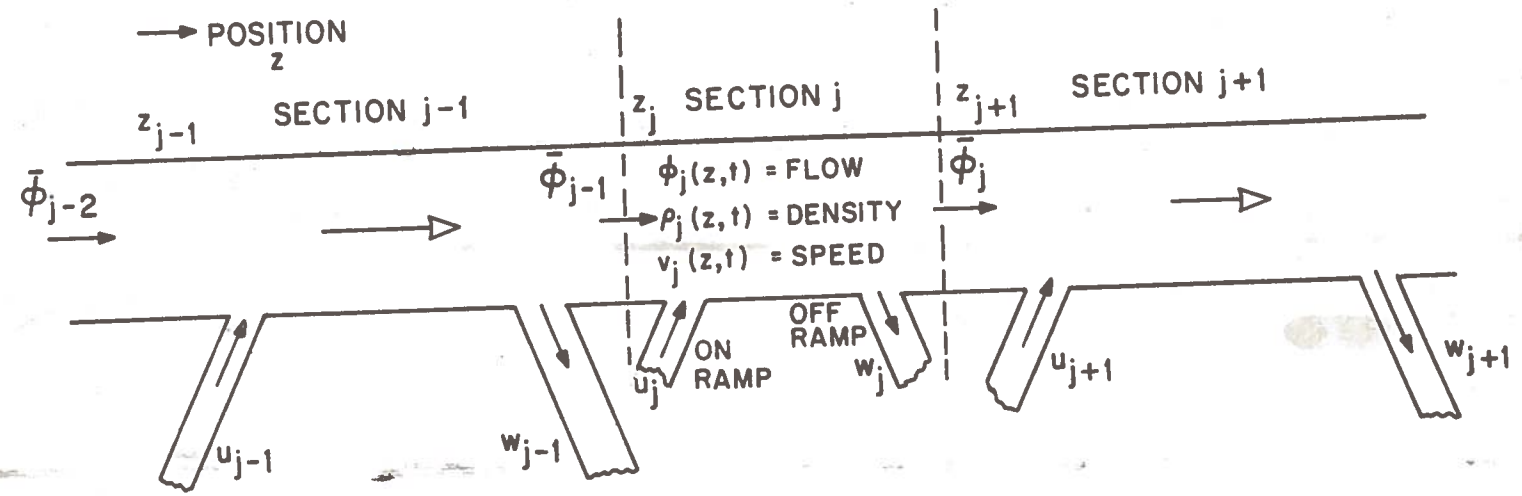

CONTINUUM VARIABLES:

$\phi_j(z,t)$ = veh flow (veh/hr) at pos z on section j

$\rho_j(z,t)$ = veh density (veh/mi) at pos z on section j

$v_j(z,t)$ = veh speed (mi/hr) at pos z on section j

$u_j(z,t)$ = entering (on ramp) flow (veh/hr) on link j

$w_j(z,t)$ = exiting (off ramp) flow (veh/hr)

SECTION "MEAN" VARIABLES: $t \in [t, t + \Delta T]$; $\Delta z_j = z_{j+1} - z_j$

$$\bar{\phi}_j(z) \triangleq \frac{1}{\Delta T} \int_t^{t+\Delta T} \phi_j(z,\tau)\, d\tau$$

$$\bar{\rho}_j(t) \triangleq \frac{1}{\Delta z_j} \int_{z_j}^{z_{j+1}} \rho_j(z,t)\, dz$$

$$\bar{v}_j(t) \triangleq \frac{1}{\Delta z_j} \int_{z_j}^{z_{j+1}} v_j(z,t)\, dz$$

Figure 2.2 DEFINITION OF FREEWAY VARIABLES

$$\frac{d}{dt}\rho_i^j = -\frac{\rho_i^j v_i^j - \rho_{i-1}^j v_{i-1}^j}{z_{i+1}^j - z_i^j} + \frac{r_i^j - w_i^j}{z_{i+1}^j - z_i^j} \quad ,$$

$$\frac{d}{dt}v_i^j = -v_i^j\left[\frac{v_i^j - v_{i-1}^j}{\frac{1}{2}\left(z_{i+1}^j - z_i^j\right)}\right] - \frac{1}{T}\left[v_i^j - v_{ei}^j\left(\rho_i^j\right)\right] - \frac{\nu}{T}\left(\frac{1}{\rho_i^j}\right)\left[\frac{\rho_{i+1}^j - \rho_i^j}{\frac{1}{2}\left(z_{i+2}^j - z_i^j\right)}\right] \qquad (2.2.1)$$

The equation for the initial links are:

$$\frac{d}{dt}\rho_i^j = -\frac{\rho_1^j v_1^j - f_{in}^j}{z_2^j - z_1^j} + \frac{r_1^j - w_1^j}{z_2^j - z_1^j} \quad ,$$

$$\frac{d}{dt}v_1^j = -\frac{1}{T}\left[v_1^j - v_{e1}^j\left(\rho_1^j\right)\right] - \frac{\nu}{T}\left[\frac{1}{\rho_1^j}\right]\left[\frac{\rho_2^j - \rho_1^j}{\frac{1}{2}\left(z_3^j - z_1^j\right)}\right] \qquad (2.2.2)$$

The equations for the last link are:

$$\frac{d}{dt}\rho_N^j = -\frac{\rho_N^j v_N^j - {}_{N-1}^{j} f_{N-1}^{j}}{z_{N+1}^j - z_N^j} + \frac{r_N^j - w_N^j}{z_{N+1}^j - z_N^j} \quad ,$$

$$\frac{d}{dt}v_N^j = -v_N^j\left[\frac{v_N^j - v_{N-1}^j}{\frac{1}{2}\left(z_{N+1}^j - z_{N-1}^j\right)}\right] - \frac{1}{T}\left[v_N^j - v_{eN}^j\left(\rho_N^j\right)\right] \qquad (2.2.3)$$

where:

$\rho_i^j \equiv$ spatial average density on the ith link of roadway j (veh/mi),

$v_i^j \equiv$ spatial average velocity on the ith link of roadway j (mi/hr),

$z_i^j \equiv$ distance to the beginning of link i of roadway j (miles),

$r_i^j \equiv$ on-ramp flow rate to link i of roadway j (veh/hr),

$w_i^j \equiv$ off-ramp flow rate from link i of roadway j (veh/hr),

$T \equiv$ driver reaction time constant (hours),

$\nu \equiv$ driver reaction sensitivity coefficient (mi^2/hr),

$f_{in}^j \equiv$ input flow to roadway j (veh/hr),

$v_{ei}^j \equiv$ desired velocity curve for link i of roadway j,

$N \equiv$ number of links of roadway j.

Remark 1: The model as stated above does not yet include noise. The effects of uncertainty will be considered later.

Remark 2: Both the freeway and the arterials will use this model. While this excludes corridors in which the arterials have many closely spaced signalized intersections, it appears to be a good approximation for situations in which the traffic signals are far apart, or when one lane of a freeway is used as a reversible link. The latter situation can occur, for example, when an outbound lane of a freeway is used for inbound traffic on the freeway during the morning rush hour.

Remark 3: The on-and-off ramp flow rates will be paired as the topography of the freeway corridor requires.

Remark 4: The density equations of (2.2.1) to (2.2.3) are derived from the "conservation of vehicles" principle; i.e., we assume all vehicles enter or leave a section either endogenously from other links or exogenously from on-and-off ramps.

Remark 5: The velocity equations of (2.2.1) to (2.2.3) are derived from several sources to approximate driver behavior. These are explain more fully in Isaksen and Payne [1972].

Remark 6: The differences in the equations for the first and last links aris from the fact that v_0^j is not available for the velocity equation for the first links, and ρ_{N+1}^j is not available for the velocity equation of the last links. Instead, it is assumed that:

$$v_0^j = v_1^j \ , \quad \rho_{N+1}^j = \rho_N^j$$

2.3 Centralized Solution

The main objective of a control system for a freeway corridor must be to move traffic through the corridor to minimize (or maximize) an appropriate performance index. The performance index is typically a measure of goodness, such as total average travel time through the corridor.

If we assume that the input flow is constant over a relatively long period of time, and that there are no noise sources, the dynamics of the corridor (equations (2.2.1) to (2.2.3)) reach a steady state in which the time derivatives are negligible. We first rewrite equations (2.2.1) to (2.2.3) using vector notation:

$$\dot{\underline{x}}(t) = \underline{\phi}[\underline{x}(t), \underline{u}(t), \underline{f}_{in}] \ , \tag{2.3.1}$$

where: $\underline{x}(t) \equiv [\rho_1^1(t) : v_1^1(t) : \rho_1^2(t) : \cdots : \rho_N^L(t) : v_N^L(t)]' \ ,$

$\underline{u}(t) \equiv [r_1^1(t) : w_1^1(t) : \cdots : r_N^L(t) : w_N^L(t)]' \ ,$

$\underline{f}_{in} \equiv [f_{in}^1 : \cdots : f_{in}^L]' \ ,$

$\underline{\phi}(\cdot,\cdot) \equiv$ vector of functions of the right-hand sides of equations (2.2.1) to (2.2.3),

$L \equiv$ number of roadways in the corridor.

The steady-state equations are then:

$$0 = \underline{\phi}\,[\underline{x},\underline{u},\underline{f}_{in}] \ . \tag{2.3.2}$$

We can now formulate that static optimization problem for the freeway corridor (see Gershwin [1975] for a more detailed presentation of the problem).

Static Optimization Problem:

$$\text{minimize } J(\underline{u}) = \mathscr{L}[\underline{x}, \underline{u}] \ ,$$
$$\text{subject to } 0 = \underline{\phi}[\underline{x}, \underline{u}, \underline{f}_{in}] \ ,$$

where $\mathscr{L}(\cdot,\cdot) \equiv$ performance index.

The solution of this problem gives a steady-state operating point $(\underline{x}_d, \underline{u}_d)$ for a particular value of $\underline{f}_{in}$. We now relax the assumption that the input flow is constant to the assumption that the time average of the input flow remains constant. We can still use the results of the static optimization problem, but the commanded input $\underline{u}_d$ must be modified to take into account the time variations of the system. Thus, we must choose a perturbational or corrective control $\underline{u}(t)$ to keep the system "near" the nominal static operatin point, defined by $\underline{x}_d$ and $\underline{u}_d$.

To help us choose the control law, we will use the LQG approach. First, expand equation (2.3.1) in an exact Taylor series:

$$\frac{d}{dt}(\underline{x}_0 + \delta\underline{x}(t)) = \underline{\phi}\Big|_0 + \frac{\partial\underline{\phi}}{\partial\underline{x}(t)}\Big|_0 \partial\underline{x}(t)$$

$$+ \frac{\partial\underline{\phi}}{\partial\underline{u}(t)}\Big|_0 \delta\underline{u}(t) + \underline{0}\left(||\delta\underline{x}(t)||\right) , \qquad (2.3.$$

where: $\underline{x}(t) = \underline{x}_d + \delta\underline{x}(t)$,

$\underline{u}(t) = \underline{u}_d + \delta\underline{u}(t)$,

$\underline{f}_{in}^0 \equiv$ time average of $\underline{f}_{in}(t)$,

$\underline{x}_d \equiv$ nominal state from static assignment algorithm,

$\underline{u}_d \equiv$ nominal control from static assignment algorithm,

$$\frac{\partial\underline{\phi}}{\partial\underline{x}(t)}\Big|_0 = \frac{\partial\underline{\phi}[\underline{x}(t),\underline{u}(t),\underline{f}_{in}^0]}{\partial\underline{x}(t)}\Bigg|_{\substack{\underline{x}(t)=\underline{x}_0 \\ \underline{u}(t)=\underline{u}_0}} ,$$

$\equiv$ the matrix of partial derivatives where the i, jth element is:

$$\left[\frac{\partial \underline{\phi}_i}{\partial \underline{x}_j(t)}\right] \quad ; \text{ evaluated at the nominal state and control } (\underline{x}_d, \underline{u}_d) \ ,$$

$$\left.\frac{\partial \underline{\phi}}{\underline{u}(t)}\right|_0 = \left.\frac{\partial \underline{\phi}[\underline{x}(t), \underline{u}(t), \underline{f}_{in}^0]}{\partial \underline{u}(t)}\right|_{\substack{\underline{x}(t) = \underline{x}_0 \\ \underline{u}(t) = \underline{u}_0}} ,$$

the matrix of partial derivative where the i, jth element is:

$$\left[\frac{\partial \underline{\phi}_i}{\partial \underline{u}_i(t)}\right] \quad ; \quad \text{evaluated at the nominal state and control.}$$

$\underline{0}\left(||\delta \underline{x}(t)||\right) \equiv$ vector function of $\underline{x}$ and $\underline{u}$ such that

$$\lim_{||\delta \underline{x}|| \to 0} \frac{\underline{0}\left(||\delta \underline{x}(t)||\right)}{||\delta \underline{x}(t)||} \to 0 \ .$$

Equation (2.2.3) is an exact expression for equation (2.3.1). If $||\delta \underline{x}||$ is small enough, equation (2.3.3), and hence, equation (2.3.1) can be very well approximated by the linear equation:

$$\delta \dot{\underline{x}}(t) = \underline{A}_0 \delta \underline{x}(t) + \underline{B}_0 \delta \underline{u}(t) \ , \qquad (2.3.4)$$

where:

$$\underline{A}_0 = \left.\frac{\partial \underline{\phi}}{\partial \underline{x}(t)}\right|_0 \qquad \text{(constant matrix)},$$

$$\underline{B}_0 = \left.\frac{\partial \underline{\phi}}{\partial \underline{u}(t)}\right|_0 \qquad \text{(constant matrix)},$$

since:

$$\frac{d}{dt}\underline{x}_d = \underline{0}\ ,$$

$$\underline{f}(\underline{x}_d,\ \underline{u}_d) = \underline{0} \quad \text{(from the constraint for choosing } \underline{x}_0,\ \underline{u}_0\text{)}, \tag{2.3.5}$$

$$0\left(||\delta\underline{x}||\right) << \underline{A}_0\delta\underline{x}(t) + \underline{B}_0\delta\underline{u}(t).$$

The last equation of (2.3.5) is actually a precise statement of what is meant by "small enough". One of the objectives of the LQG controller must be to insure that this relation holds. One way to accomplish this objective is to formulate the problem as a constrained minimization, i.e.:

Problem Statement 2.1:

minimize $\quad J = \ell(\delta\underline{x}(t),\ \delta\underline{u}(t))$,

subject to $\quad \delta\dot{\underline{x}}(t) - \underline{A}_0\delta\underline{x}(t) + \underline{B}_0\delta\underline{u}(t)$.

Here, the cost J is used to reflect the size of $0\left(||\delta\underline{x}(t)||\right)$. One possible cost which may be used is:

$$J = \lim_{T\to\infty}\int_0^T 0\left(||\delta\underline{x}(t)||\right)\,dt. \tag{2.3.6}$$

This, however, means that $0\left(||\delta\underline{x}(t)||\right)$ must be available. Again, we can resort to an approximation. The terms in $0\left(||\delta\underline{x}(t)||\right)$ are all quadratic or higher-order terms. If the quadratic terms can be made small (relative to the linear terms), the higher-order terms will be even smaller. Thus, it may seem appropriate to use a quadratic cost criterion of the form:

$$J = \lim_{T\to\infty}\int_0^T [\delta\underline{x}'(t)\underline{S}_1\delta\underline{x}(t) + \delta\underline{u}'(t)\underline{S}_2\underline{u}(t)]dt, \tag{2.3.7}$$

where the matrices $\underline{S}_1$ and $\underline{S}_2$ can be chosen to reflect the largest unexpected effect of the term $0\left(||\delta\underline{x}(t)||\right)$.

The problem can then be stated:

Deterministic Linear Regulator Problem:

$$\text{minimize} \quad J = \lim_{T\to\infty} \int_0^T [\delta\underline{x}'(t)\underline{S}_1\delta\underline{x}(t) + \delta\underline{u}'(t)\underline{S}_2\delta\underline{u}(t)]dt \ ,$$

$$\text{subject to} \quad \delta\dot{\underline{x}}(t) = \underline{A}_0\delta\underline{x}(t) + \underline{B}_0\delta\underline{u}(t) \ ,$$

where: $\underline{S}_1$ is positive semi-definite,

$\underline{S}_2$ is positive definite.

In the deterministic case when all the states are observed, the solution to the above problem is well known. The feedback law is linear:

$$\delta\underline{u}(t) = -\underline{G}_0\delta\underline{x}(t) \ , \tag{2.3.8}$$

where $\underline{G}_0$ is calculated from the matrix algebraic Ricatti equation:

$$\underline{0} = -\underline{A}_0'\underline{K} - \underline{K}\,\underline{A}_0 - \underline{S}_1 + \underline{K}\,\underline{B}_0\underline{S}_2^{-1}\underline{B}_0'\underline{K} \ ,$$

$$\underline{G}_0 = \underline{S}_2^{-1}\underline{B}_0'\underline{K} \ . \tag{2.3.9}$$

When the presence of uncertainty is admitted to the model, the problem becomes more difficult. The model then becomes:

$$\dot{\underline{x}}(t) - \underline{\phi}[\underline{x}(t), \underline{u}(t), \underline{f}_{in}(t), \underline{\xi}_c(t)] \ , \tag{2.3.10}$$

where: $\underline{\xi}_c(t) \equiv$ zero-mean stochastic process (generally non-white).

We also assume a non-linear observation equation:

$$\underline{y}(t) = \underline{c}[\underline{x}(t), \underline{\theta}_c(t)] \tag{2.3.11}$$

where: $\underline{\phi}[\cdot,\cdot,\cdot,\cdot] \equiv$ right-hand side of equations (2.2.1) to (2.2.3) appropriately modified to include noise disturbances,

$\underline{c}[\cdot,\cdot] \equiv$ appropriate measurement function to be specifically determined according to the type of sensor used,

$\underline{\theta}_c(t) \equiv$ zero-mean stochastic process (generally non-white).

Equations (2.3.10) and (2.3.11) provide a complex stochastic model for the freeway-corridor system. As in the deterministic case, we assume the time average of the input flow $\underline{f}_{in}^0$ remains constant for a sufficiently long time. The solution to the static assignment problem is computed, and deviations from the static solution are assumed to be small. Equations (2.3.10) and (2.3.11) are expanded in a Taylor series:

$$\frac{d}{dt}[\underline{x}_0 + \underline{x}(t)] = \underline{\phi}\Big|_0 + \frac{\partial \underline{\phi}}{\partial \underline{x}(t)}\Big|_0 \delta\underline{x}(t) + \frac{\partial \underline{\phi}}{\partial \underline{u}(t)}\Big|_0 \delta\underline{u}(t) + \frac{\partial \underline{\phi}}{\partial \underline{\xi}_c(t)}\Big|_{\substack{\underline{x}_0 \\ \underline{u}_0}} \overline{\underline{\xi}}(t) + \underline{O}\left[\,||\delta\underline{x}(t)||\,\right], \tag{2.3.12}$$

$$\underline{y}_0 + \delta\underline{y}(t) = \underline{c}\Big|_0 + \frac{\partial \underline{c}}{\partial \underline{x}(t)}\Big|_0 \partial\underline{x}(t) + \frac{\partial \underline{c}}{\partial \theta_c(t)}\Big|_0 \overline{\underline{\theta}}(t) + \underline{O}\left[\,||\delta\underline{x}(t)||\,\right], \tag{2.3.13}$$

where the notation is the same as for equation (2.3.3).

Again, the effects of the $\underline{O}\left[\,||\delta\underline{x}(t)||\,\right]$ terms are neglected, and the linearized system results:

$$\delta\dot{\underline{x}}(t) = \underline{A}_0\delta\underline{x}(t) + \underline{B}_0\delta\underline{u}(t) + \underline{\xi}(t) \ ,$$

$$\delta\underline{y}(t) = \underline{C}_0\delta\underline{x}(t) + \underline{\theta}(t) \ , \qquad (2.3.14)$$

where: $\underline{A}_0$, $\underline{B}_0$, $\underline{x}_d$, $\underline{u}_d$ as defined in equation (2.3.4),

$$\delta\underline{x}(t) = \underline{x}(t) - \underline{x}_d \ ,$$

$$\delta\underline{u}(t) = \underline{u}(t) - \underline{u}_d \ ,$$

$$\delta\underline{y}(t) = \underline{y}(t) - \underline{y}_0 \ ,$$

$$\underline{C}_0 = \left.\frac{\partial\underline{c}[\underline{x}(t),\underline{\theta}_c(t)]}{\partial\underline{x}(t)}\right|_{\substack{\underline{x}_d \\ \underline{u}_d}} \qquad \text{(constant matrix)},$$

$\underline{\xi}(t) \equiv$ normalized stochastic process from equation (2.3.12),

$\underline{\theta}(t) \equiv$ normalized stochastic process from equation (2.3.13).

We assume that $\underline{\xi}(t)$ and $\underline{\theta}(t)$ are zero-mean Gaussian white noise processes with covariances:

$$E\{\underline{\xi}(t)\underline{\xi}'(\tau)\} = \underline{Q}\delta(t-\tau) \quad ; \quad \underline{Q} \geq \underline{0} \ ,$$

$$E\{\underline{\theta}(t)\underline{\theta}'(\tau) = \underline{R}\delta(t-\ ) \quad ; \quad \underline{R} > 0 \ , \qquad (2.3.15)$$

$$E\{\underline{\theta}(t)\underline{\xi}'(\tau) = \underline{0} \ ,$$

such that $(\underline{A}, \sqrt{\underline{Q}})$* is controllable.

We can now state the LQG regulator problem.

---

* $\sqrt{\underline{Q}}$ is defined by the relation: $\sqrt{\underline{Q}}'\ \sqrt{\underline{Q}} \triangleq \underline{Q}$.

LQG Regulator Problem:

Consider the linear-time invariant system:

$$\delta\dot{\underline{x}}(t) = \underline{A}_0\delta\underline{x}(t) + \underline{B}_0\delta\underline{u}(t) + \underline{\xi}(t),$$

$$\delta\underline{y}(t) = \underline{C}_0\delta\underline{x}(t) + \underline{\theta}(t) \ , \qquad (2.3.16)$$

with $\underline{\xi}(t)$ and $\underline{\theta}(t)$ zero-mean gaussian white noise processes with covariances given by (2.3.15). Choose the control law:

$$\delta\underline{u}(t) = \underline{\gamma}[\delta\underline{y}(t)] \ ,$$

to minimize the quadratic cost criterion:

$$J(\delta\underline{u}(t)) = \lim_{T\to\infty} E \ \frac{1}{T}\int_0^T [\delta\underline{x}'(t)\underline{S}_1\delta\underline{x}(t) + \delta\underline{u}'(t)\underline{S}_2\delta\underline{u}(t)]dt \ .$$

The solution to the LQG regulator problem is well known, and can be divided into two parts (via the separation principle). The optimal control law is given by a linear feedback of the optimal estimate of the state:

$$\delta\underline{u}^*(t) = -\underline{G}_0\delta\underline{x}^*(t) \ , \qquad (2.3.17)$$

where: $\delta\underline{u}^*(t) \equiv$ optimal control,

$\delta\hat{\underline{x}}^*(t) \equiv$ optimal estimate of $\delta\underline{x}(t)$,

$\underline{G}_0 \equiv$ feedback control gain matrix.

The feedback gain $\underline{G}_0$ is the same as the gain in the deterministic case, and is calculated from the algebraic matrix Ricatti equation (2.3.9).

The optimal estimate is given by the linear Kalman filter:

$$\delta\dot{\hat{\underline{x}}}^*(t) = \underline{A}_0\delta\hat{\underline{x}}^*(t) + \underline{B}_0\delta\hat{\underline{u}}^*(t) + \underline{H}_0\left[\delta\underline{y}(t) - \underline{C}_0\delta\hat{\underline{x}}^*(t)\right] \ . \qquad (2.3.18)$$

The Kalman gain matrix $\underline{H}_0$ is also calculated from the algebraic matrix Ricatti

equation:

$$\underline{0} = \underline{A}_0\underline{\Sigma} + \underline{\Sigma}\,\underline{A}_0' + \underline{Q} - \underline{\Sigma}\,\underline{C}_0'\underline{R}^{-1}\underline{C}_0\,\underline{\Sigma}\ ,$$

$$\underline{H}_0 = \underline{\Sigma}\,\underline{C}_0'\underline{R}^{-1}\ . \qquad (2.3.19)$$

It is worthwhile to review the principles underlying the solution. We replaced the original non-linear problem with a simpler linear problem for which we knew the optimal solution. However, this solution is not optimal for the original problem. Yet, it may be close if the assumptions of "smallness" of the perturbations are accurate.

To hedge against the possibility that the assumption may not be entirely true, we will modify the estimator equations while still keeping their basic form. The result will be an extended Kalman filter (see Jazwinski [1970] for details).

We first note the structure of the linear Kalman filter (equations (2.3.18) and (2.3.19)). The right-hand side of equation (2.3.18) consists of two parts. The first part is the same as the linearized system dynamics (see equation (2.3.14)). Since the linearized system dynamics are used only to approximate the actual system behavior under small perturbation, propagating the actual non-linear system dynamics typically results in an improved filter.

The second part of the right-hand side is the optimal feedback of the difference between the actual observation and the expected observation. The feedback gain is chosen by letting the matrix Ricatti differential equation:

$$\frac{d}{dt}\underline{\Sigma}(t) - \underline{A}_0\underline{\Sigma}(t) + \underline{\Sigma}(t)\underline{A}_0' + \underline{Q} - \underline{\Sigma}(t)\underline{C}_0'\underline{R}^{-1}\underline{C}_0\underline{\Sigma}(t)\ , \qquad (2.3.20)$$

reach steady state. This Ricatti equation is actually the steady-state covariance of the linearized system (i.e., $\underline{\Sigma}(t) = E\{[\underline{x}(t) - \hat{\underline{x}}(t)][\underline{x}(t) - \hat{\underline{x}}(t)]'\}$).

Again, we will keep the same form (feedback of the difference between the observation and the expected observation) for the second part, by the gain will be chosen differently. Rather than using the initial linearized approximations

$\underline{A}_0$ and $\underline{C}_0$ for all time, one updates the linearization with each new estimate obtained. Assuming that the estimate $\hat{\underline{x}}$ is more likely to be close to the state than the static operating point $\underline{x}_d$, this relinearization procedure typically results in a smaller error covariance.

Implementing these two modifications, and assuming that the measurements are made at discrete times rather than continuously, the filter equations can be written: (see, e.g., Jazwinski [1970], p. 278)

$$\delta\hat{\underline{x}}(T) = \hat{\underline{x}}(T|T) - \underline{x}_d \ , \tag{2.3.21}$$

$$\dot{\hat{\underline{x}}}(t|T) = \underline{\phi}[\hat{\underline{x}}(t|T), \underline{u}(t), 0] \qquad T<t\leq T+\Delta \ , \tag{2.3.22}$$

$$\hat{\underline{x}}(T+\Delta|T+\Delta) = \hat{\underline{x}}(T+\Delta|T) + \underline{H}(T+\Delta)[\underline{y}(t) - \underline{c}(\hat{\underline{x}}(T+\Delta|T), 0)] \ , \tag{2.3.23}$$

$$\underline{H}(T+\Delta) = \underline{\Sigma}(T+\Delta|T)\hat{\underline{C}}'[\hat{\underline{C}}\ \underline{\Sigma}\ (T+\Delta|T)\hat{\underline{C}}' + \underline{R}]^{-1}, \tag{2.3.24}$$

$$\underline{\Sigma}(T+\Delta|T) = \underline{\Phi}(T+\Delta|T)\underline{\Sigma}(T|T)\underline{\Phi}'(T+\Delta|T) + \underline{Q} \ , \tag{2.3.25}$$

$$\underline{\Sigma}(T+\Delta|T+\Delta) = [\underline{I} - \underline{H}(T+\Delta)\hat{\underline{C}}]\underline{\Sigma}(T+\Delta|T) \ , \tag{2.3.26}$$

$$\frac{d}{dt}\underline{\Phi}(t|T) = \left.\frac{\partial\underline{\phi}[\underline{x}(t),\underline{u}(t)\underline{\xi}(t)]}{\partial\underline{x}(t)}\right|_{\substack{\underline{\Phi}(t\ T) \quad T<t\leq T+\Delta \\ \underline{\hat{x}}(t|T) \\ \underline{u}(t) \\ \underline{\xi}(t) = 0,}} \tag{2.3.27}$$

$$\underline{\Phi}(T\ T) = \underline{I} \ , \tag{2.3.28}$$

where: $\hat{\underline{x}}(t|s) \equiv$ estimate of state at time t given the observations up to time s,

$\Delta \equiv$ period between observations,

equation:

$$\underline{0} = \underline{A}_0\underline{\Sigma} + \underline{\Sigma}\,\underline{A}_0' + \underline{Q} - \underline{\Sigma}\,\underline{C}_0'\underline{R}^{-1}\underline{C}_0\,\underline{\Sigma}\ ,$$

$$\underline{H}_0 = \underline{\Sigma}\,\underline{C}_0'\underline{R}^{-1}\ . \qquad (2.3.19)$$

It is worthwhile to review the principles underlying the solution. We replaced the original non-linear problem with a simpler linear problem for which we knew the optimal solution. However, this solution is not optimal for the original problem. Yet, it may be close if the assumptions of "smallness" of the perturbations are accurate.

To hedge against the possibility that the assumption may not be entirely true, we will modify the estimator equations while still keeping their basic form. The result will be an extended Kalman filter (see Jazwinski [1970] for details).

We first note the structure of the linear Kalman filter (equations (2.3.18) and (2.3.19)). The right-hand side of equation (2.3.18) consists of two parts. The first part is the same as the linearized system dynamics (see equation (2.3.14)). Since the linearized system dynamics are used only to approximate the actual system behavior under small perturbation, propagating the actual non-linear system dynamics typically results in an improved filter.

The second part of the right-hand side is the optimal feedback of the difference between the actual observation and the expected observation. The feedback gain is chosen by letting the matrix Ricatti differential equation:

$$\frac{d}{dt}\underline{\Sigma}(t) - \underline{A}_0\underline{\Sigma}(t) + \underline{\Sigma}(t)\underline{A}_0' + \underline{Q} - \underline{\Sigma}(t)\underline{C}_0'\underline{R}^{-1}\underline{C}_0\underline{\Sigma}(t)\ , \qquad (2.3.20)$$

reach steady state. This Ricatti equation is actually the steady-state covariance of the linearized system (i.e., $\underline{\Sigma}(t) = E\{[\underline{x}(t) - \hat{\underline{x}}(t)][\underline{x}(t) - \hat{\underline{x}}(t)]'\}$).

Again, we will keep the same form (feedback of the difference between the observation and the expected observation) for the second part, by the gain will be chosen differently. Rather than using the initial linearized approximations

$\underline{A}_0$ and $\underline{C}_0$ for all time, one updates the linearization with each new estimate obtained. Assuming that the estimate $\hat{\underline{x}}$ is more likely to be close to the state than the static operating point $\underline{x}_d$, this relinearization procedure typically results in a smaller error covariance.

Implementing these two modifications, and assuming that the measurements are made at discrete times rather than continuously, the filter equations can be written: (see, e.g., Jazwinski [1970], p. 278)

$$\delta\hat{\underline{x}}(T) = \hat{\underline{x}}(T|T) - \underline{x}_d \ , \tag{2.3.21}$$

$$\dot{\hat{\underline{x}}}(t|T) = \underline{\phi}[\hat{\underline{x}}(t|T), \underline{u}(t), 0] \qquad T<t\leq T+\Delta \ , \tag{2.3.22}$$

$$\hat{\underline{x}}(T+\Delta|T+\Delta) = \hat{\underline{x}}(T+\Delta|T) + \underline{H}(T+\Delta)[\underline{y}(t) - \underline{c}(\hat{\underline{x}}(T+\Delta|T), 0)] \ , \tag{2.3.23}$$

$$\underline{H}(T+\Delta) = \underline{\Sigma}(T+\Delta|T)\hat{\underline{C}}'[\hat{\underline{C}}\ \underline{\Sigma}\ (T+\Delta|T)\hat{\underline{C}}' + \underline{R}]^{-1}, \tag{2.3.24}$$

$$\underline{\Sigma}(T+\Delta|T) = \underline{\Phi}(T+\Delta|T)\underline{\Sigma}(T|T)\underline{\Phi}'(T+\Delta|T) + \underline{Q} \ , \tag{2.3.25}$$

$$\underline{\Sigma}(T+\Delta|T+\Delta) = [\underline{I} - \underline{H}(T+\Delta)\hat{\underline{C}}]\underline{\Sigma}(T+\Delta|T), \tag{2.3.26}$$

$$\frac{d}{dt}\underline{\Phi}(t|T) = \left.\frac{\partial\underline{\phi}[\underline{x}(t),\underline{u}(t)\underline{\xi}(t)]}{\partial\underline{x}(t)}\right|_{\substack{\underline{\Phi}(t\ T) \quad T<t\leq T+\Delta \\ \underline{\hat{x}}(t|T) \\ \underline{u}(t) \\ \underline{\xi}(t) = 0,}} \tag{2.3.27}$$

$$\underline{\Phi}(T\ T) = \underline{I} \ , \tag{2.3.28}$$

where: $\hat{\underline{x}}(t|s) \equiv$ estimate of state at time t given the observations up to time s,

$\Delta \equiv$ period between observations,

$$\hat{\underline{C}} = \left.\frac{\partial \underline{c}[\underline{x}(t), \underline{\theta}(t)]}{\partial \underline{x}(t)}\right|_{\substack{\underline{x}(T+\Delta)\,|\,T) \\ \underline{\theta}(t) = 0}} .$$

Remark 1: Equation (2.3.22) is the non-linear propagation of the estimate.

Remark 2: Equation (2.3.23) is the update equation, and is used whenever a measurement is made. It takes the form of the feedback of the difference between the actual observation and the expected observation (the innovations process).

Remark 3: Equations (2.3.24) to (2.3.26) are the discrete version of the error covariance propagation using the approximation to the transition matrix. The discrete version is used because the measurements are now assumed to come at discrete intervals, the situation in actual practice.

Remark 4: The transition matrix is approximated by equations (2.3.27) and (2.3.28).

Remark 5: The input is still given by a linear feedback of the estimated perturbation $\delta\underline{x}(t)$ (as in equation (2.3.17)). The gain is the same as in the deterministic case.

The complete algorithm for the centralized controller is now given. Figure (2.3) gives a flow-chart description of the algorithm, while Figure (2.4) is a block diagram of the controller.

Centralized Control Algorithm:

(a) Solve the static optimization problem for the static operating point $(\underline{x}_d, \underline{u}_d)$.

(b) Solve the matrix algebraic Ricatti equation (2.3.9) for the feedback gain $\underline{G}_0$.

(c) Start the extended Kalman filter (by integrating equations (2.3.22) and (2.3.27) from either:

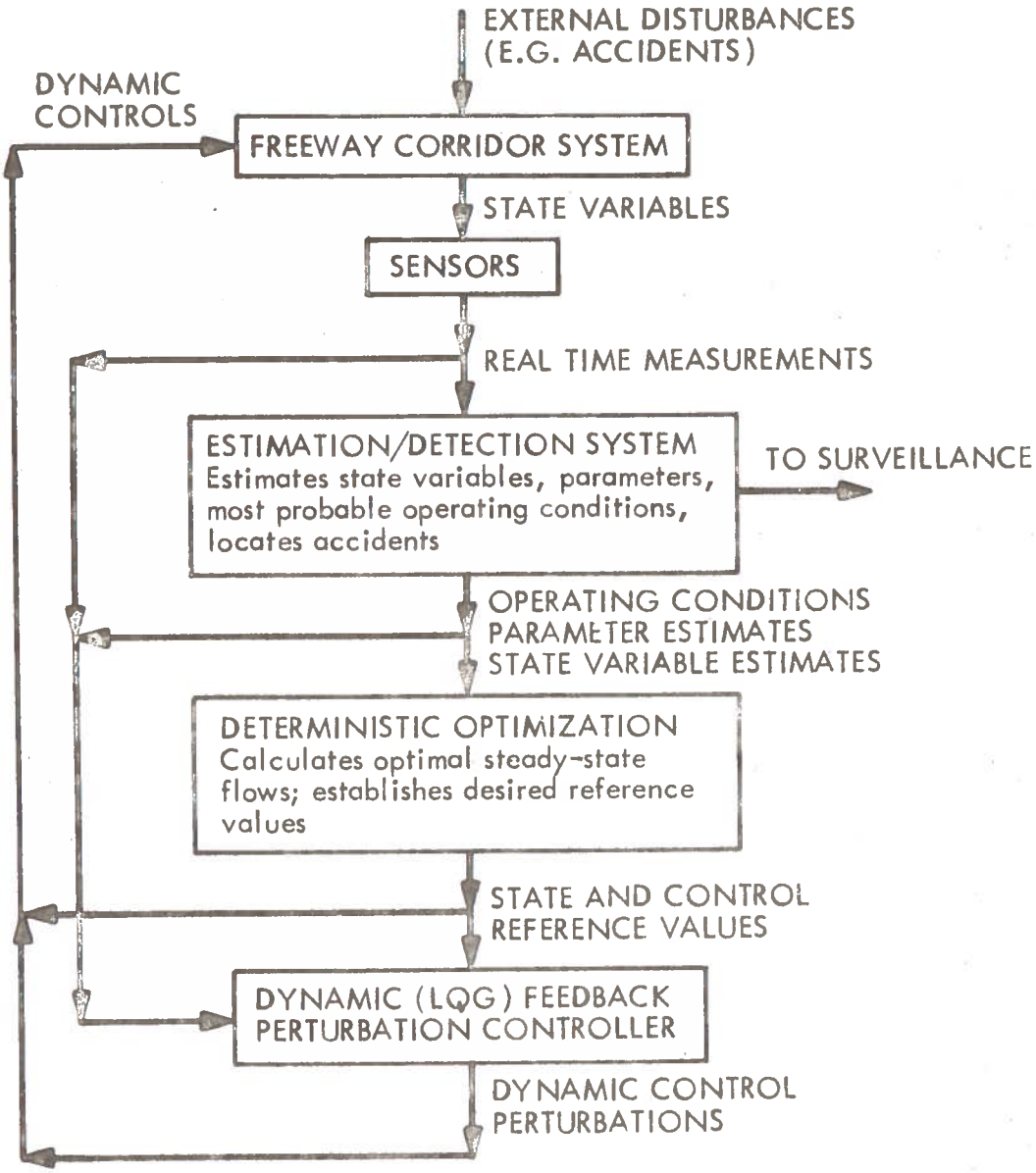

Figure 2.3 CONTROL ALGORITHM FLOW CHART

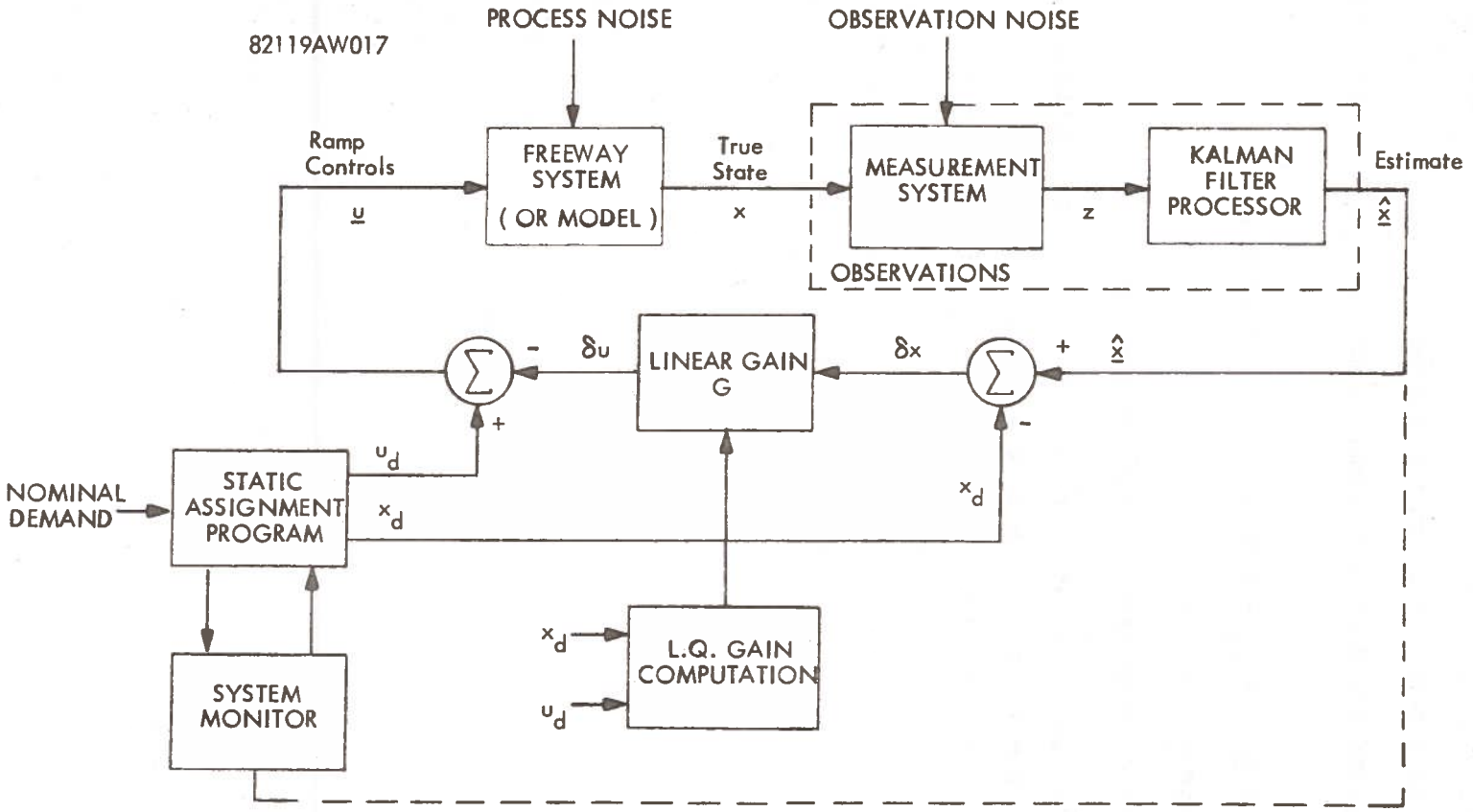

Figure 2.4 BLOCK DIAGRAM OF CENTRALIZED CONTROL SYSTEM

1) The last updated estimate,

2) some initial guess if this is the first time through the step.

(d) Take a measurement of the system.

(e) Update the extended Kalman filter by equations (2.3.23) through (2.3.26).

(f) Set $\underline{u}(t) = \underline{u}_d - \underline{G}_0 \delta\hat{\underline{x}}(T)$, $\quad T<t\leq T+\Delta$,

(g) Repeat step (c).

We conclude this section with two comments:

(a) Throughout the section we have made the assumptions that the perturbations are "small", in the sense that the second-order effects of the nonlinear system are negligible compared with the linear terms. We shall see in the next section that the controller works well even when the second-order effects are not small. The reasons will be discussed in section 2.4.

(b) The material in this section has been superficially discussed. Some references have been given throughout the section for more detailed derivations. For convenience, these are repeated below:

1) LINEAR QUADRATIC GAUSSIAN PROBLEM: Athans [1971].

2) STATIC ASSIGNMENT: Gershwin [1975].

3) EXTENDED KALMAN FILTERING: Jazwinski [1970], Orlhac et al [1975] (application to freeway corridor.

2.4 Centralized Control Example

Now that the centralized control system for the freeway corridor has been designed, it must be tested on a practical problem. We will use a simple but reasonable nontrivial freeway corridor example to observe the behavior of the system. In most cases throughout this example, the effect of the behavior of the extended Kalman filter is minimized since it is covered in great detail by Orlhac et al [1975].

The actual corridor that we will use is shown in figure (2.5). The corridor consists of two freeways, each divided into three homogeneous links. Each

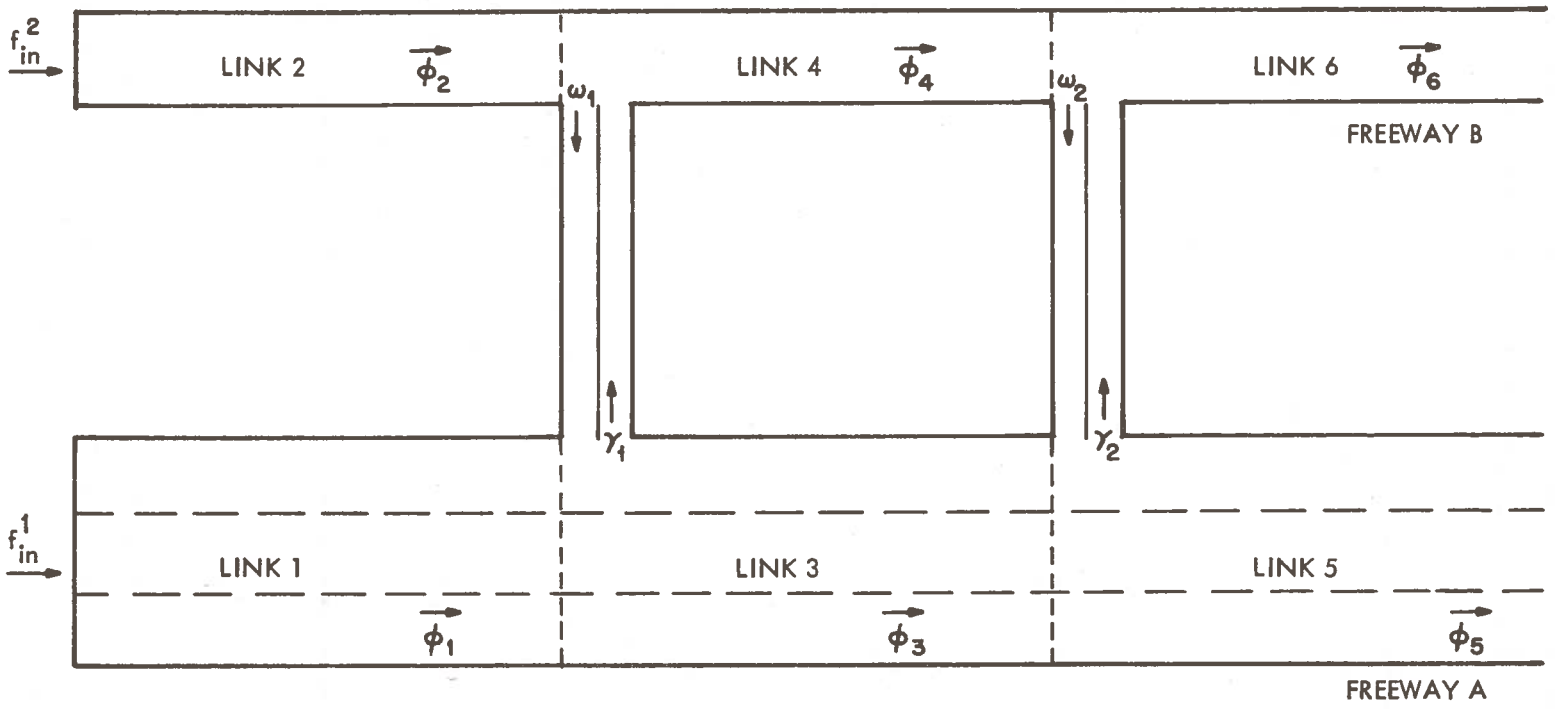

Figure 2.5 FREEWAY CORRIDOR STRUCTURE FOR EXAMPLE

link is 1/2-mile long. The main freeway (freeway A in figure 2.5) has a maximum flow capacity of approximately 6220 vehicles/hour. The secondary freeway (freeway B in figure 2.5) has a maximum flow capacity of approximately 2075 vehicles/hour.

The available controls are two on-and-off ramp pairs connecting the beginning of links 3 and 4, and links 5 and 6. The commanded control is the percentage of flow that remains on each freeway past these points. Let:

$\phi_i \equiv$ flow on link i,

$\gamma_1 \equiv$ ramp flow from link 3 to link 4,

$\omega_1 \equiv$ ramp flow from link 4 to link 3.

Then, if $\gamma_1 > \omega_1$:

$$u_1 = \frac{\gamma_1 - \omega_1}{\phi_1} \quad . \tag{2.4.1}$$

However, if $\omega_1 > \gamma_1$:

$$u_1 = \frac{\gamma_1 - \omega_1}{\phi_2} \quad . \tag{2.4.2}$$

The second control is defined analogously with ϕ_1 and ϕ_2 replaced by ϕ_3 and ϕ_4, respectively.

The models used for each freeway are the models presented in section 2.2. The variable T and ν are taken to be:

$$T = 5.0 \text{ sec} \ , \qquad \nu = 9.375 \text{ mi}^2/\text{hr}. \tag{2.4.3}$$

These values produce a faster driver-reaction time and faster disturbance propagation than actually is observed, but the qualitative behavior remains the same. The desired velocity curve is a modified exponential as in figure (2.6).

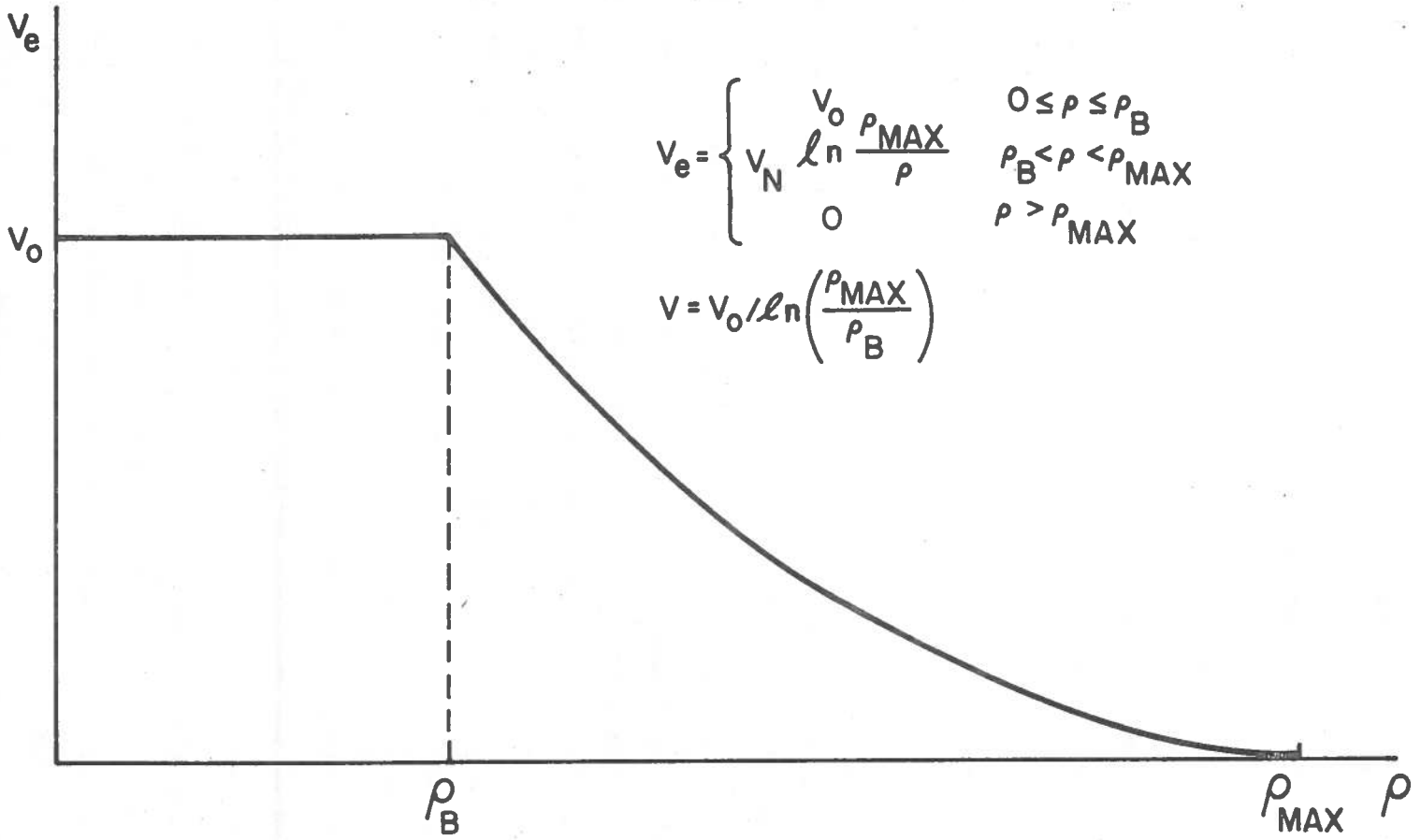

Figure 2.6 DRIVER-DESIRED VELOCITY CURVE

The values ρ_{max}, ρ_B, and v_0 for the main freeway are:

$$\rho_{max} = 675 \text{ vehicles/mile},$$

$$\rho_B = 75 \text{ vehicles/mile}, \qquad (2.4.4)$$

$$v_0 = 55 \text{ miles/hour}.$$

The values for the secondary freeway are:

$$\rho_{max} = 225 \text{ vehicles/mile},$$

$$\rho_B = 25 \text{ vehicles/mile}, \qquad (2.4.5)$$

$$v_0 = 55 \text{ miles/hour}.$$

These values correspond approximately to a 3-lane road for the main freeway and a 1-lane road for the secondary freeway.

The input flow to the corridor is modeled as a colored poisson process; i.e., a process with independent arrivals that is filtered to make the second moment independent from the mean. In this manner, we can control the level of "noise" in the input flow. The other noise sources are introduced through the controls. The controls are taken to be uniformly distributed with the commanded value as the mean. The limits of the distribution are $\pm$ 10 percent of the commanded value. Thus, all the system-noise sources are additive, and affect only the density equations.

The measurements available from the system are assumed to be linear measurements of the densities on all six links. The measurements are corrupted by zero-mean Gaussian white noise processes.

To choose the appropriate weighting matrices $\underline{S}_1$ and $\underline{S}_2$ for the feedback gain computation, we will use a method proposed by Bryson and Ho [1969]. The idea is to select the quadratic performance index by establishing the maximum desired deviations of the state variables and controls from their nominal value, and using the maximum deviations to scale the corresponding values in

the weighting matrices. Since we will be using diagonal matrices for $\underline{S}_1$ and $\underline{S}_2$, the cost functional can be written:

$$J = \lim_{T\to\infty} E \frac{1}{T} \int_0^T \left[\sum_{i=1}^{2n} \delta x_i^2(t) S_{1(ii)} + \sum_{i=1}^{M} \delta u_i^2(t) S_{2(ii)} \right] dt \quad . \qquad (2.4.6)$$

We like to make the terms $\delta x_i^2(t) S_{1(ii)}$ and $\delta u_j^2(t) S_{2(ii)}$ about the same order of magnitude when $\delta x_i(t)$ and $\delta u_j(t)$ take on their maximum values. If we let:

$$\delta x_i(t)_{max} = 70 \text{ veh/mi} \qquad i \text{ odd},$$

or (2.4.7)

$$\delta x_i(t)_{max} = 30 \text{ mi/hr} \qquad i \text{ even},$$

and

$$\delta u_i(t)_{max} = 1. \qquad (2.4.8)$$

Then, the values,

$$S_{1(ii)} = 1,$$

$$S_{2(ii)} = 5000, \qquad (2.4.9)$$

satisfy the above requirement.

The choice of constants described in the last few paragraphs are summarized in table 2.1 for the main freeway and table 2.2 for the secondary freeway. The initial conditions for each freeway are also given in these tables. Appendix B contains the linearized system matrix $\underline{A}_0$, the linearized input matrix $\underline{B}_0$, and the linear feedback gain $\underline{G}_0$.

The level of the noise sources for this example are relatively low. The reason is that we are not trying to test the extended Kalman filter as much as we are trying to test the control algorithm as a whole. The results will

TABLE 2.1

STATISTICS FOR MAIN FREEWAY (A)

Driver Behavior Constants:	v_0 = 55 mi/hr T = 5 sec	ρ_{max} = 675 veh/mi ρ_B = 75 veh/mi ν = 9.375 mi^2/hr
Initial State:	ρ = 74 veh/mi v = 55 mi/hr	each link each link
Initial Estimate:	$\hat{\rho}$ = 74 veh/mi $\hat{v}$ = 55 mi/hr	each link each link
Static Operating Point:	ρ_d = 74 veh/mi v_d = 55 mi/hr	each link each link
Input Flow: Colored poisson process with: Mean = 4077 veh/hr Std. deviation = 1211 veh/hr (Normal poisson std. dev. = 64 veh/hr) 40-sec pulse from t=12 to t=52 with: Mean = 14270 veh/hr Std. deviation = 2266 veh/hr		
Observations: Density measurement on each link corrupted by zero mean Gaussian white noise process with: Variance = 16 veh^2/hr^2		

TABLE 2.2

STATISTICS FOR SECONDARY FREEWAY (B)

Driver Behavior Constants:	v_0 = 55 mi/hr T = 5 sec	ρ_{max} = 225 veh/mi ρ_B = 25 veh/mi ν = 9.375 mi^2/hr
Initial State:	ρ = 18 veh/mi v = 55 mi/hr	each link each link
Initial Estimate:	$\hat{\rho}$ = 18 veh/mi $\hat{v}$ = 55 mi/hr	each link each link
Static Operating Point:	ρ_d = 18 veh/mi v_d = 55 mi/hr	each link each link
Input Flow: Colored poisson process with: Mean = 1000 veh/hr Std. deviation = 600 veh/hr (Normal poisson Std. dev. = 31.6 veh/hr)		
Observations: Density measurement on each link corrupted by zero mean Gaussian white noise process with: Variance = 16 veh^2/hr^2		
Weighting matrices (both freeways): $\underline{S}_1 = \underline{I}$ $S_2 = \begin{bmatrix} 5000 & 0 \\ 0 & 5000 \end{bmatrix}$		

deteriorate to some extent if the level of noise is raised, but the filter still works reasonably well (see orlhac et al [1975]). Thus, we may expect that the control system will work reasonably well under higher-noise levels also. For these same reasons, the measurements are taken to be linear, and the initial conditions for the filter are the same as the initial conditions for the states.

The results from the example are shown in figures 2.7 through 2.13. The graphs are paired corresponding to their physical location on the freeways. The density graphs for the first links (links 1 and 2) of each freeway are in figure 2.7, the second links (links 3 and 4) in figure 2.8, and the last links (links 5 and 6) in figure 2.9. The velocity graphs are similarly organized in figures 2.10 through 2.12. The graphs of the controls are in figure 2.13. The length of the experiment is 200 seconds, or 3-1/3 minutes. If the constants ν and T are chosen to correspond to their typical physical values, the time span may be longer (approximately 10 to 15 minutes), but the qualitative behavior remains the same.

To analyze the behavior of the controller, we will first consider the open-loop (uncontrolled) state. On the secondary freeway (links 2,4, and 6), the density and velocity remain approximately at their nominal values. The reasons for this behavior are that the system is stable near this operating point, the level of the driving noise is low, and there is not input to secondary freeway from the ramps. Thus, the traffic which is initially in a steady-state condition continues to flow smoothly.

The conditions on the main freeway are not nearly as satisfactory. When the flow pulse enters the system, the density on link 1 of the main freeway increases rapidly because the capacity of the link is exceeded. This effect peaks at t=52 seconds, and the density starts to decline on the first link until it has almost returned to the nominal by t=200 seconds. The pulse of flow continues to propagate downstream increasing the density and decreasing the velocity successively on links 3 and 5.

The situation is that there are a lot of vehicles slowed on the main freeway while there is much unused capacity on the secondary freeway. This

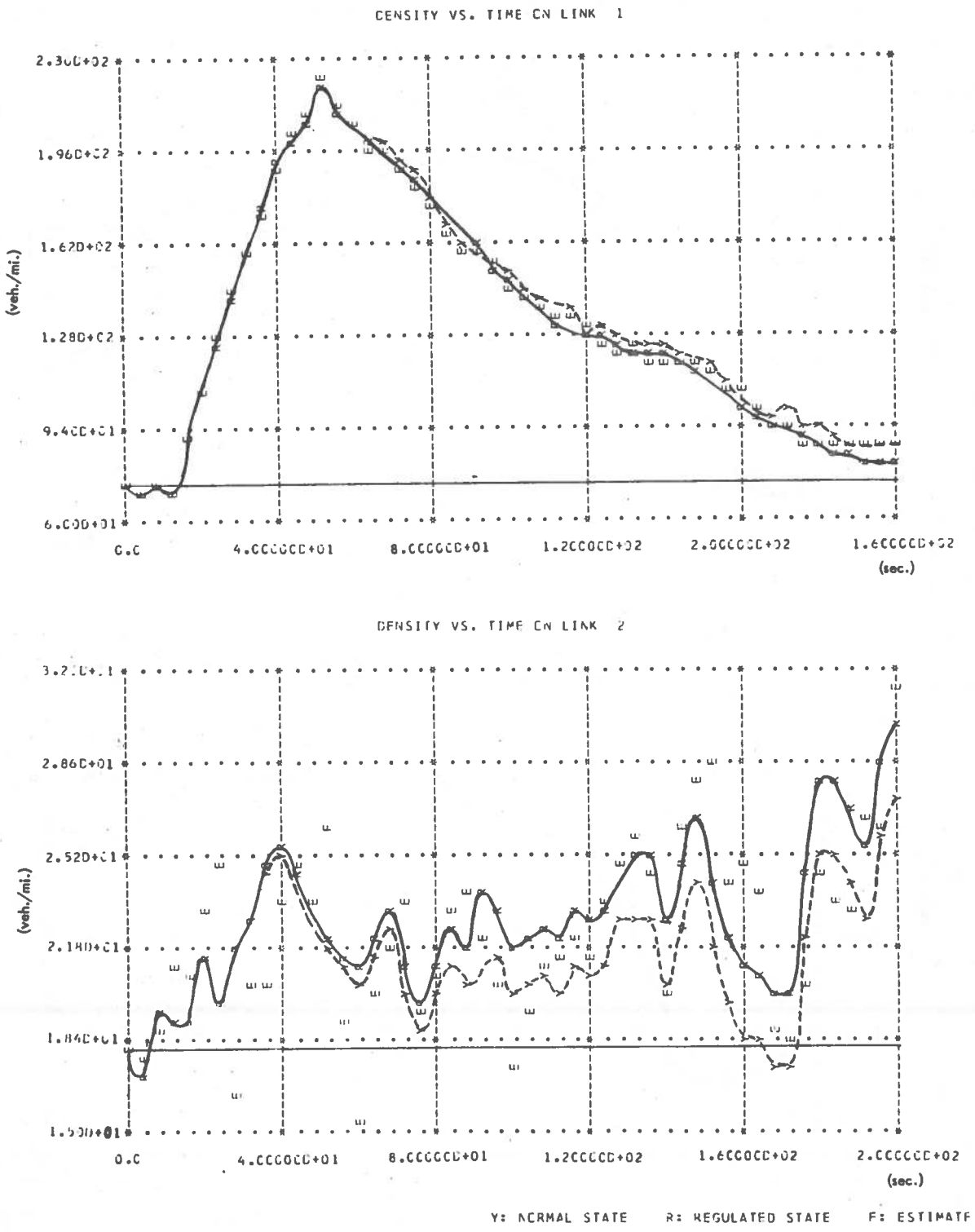

Figure 2.7 CENTRALIZED CONTROL SYSTEM RESULTS FOR EXAMPLE (DENSITY) (LINKS 1 and 2)

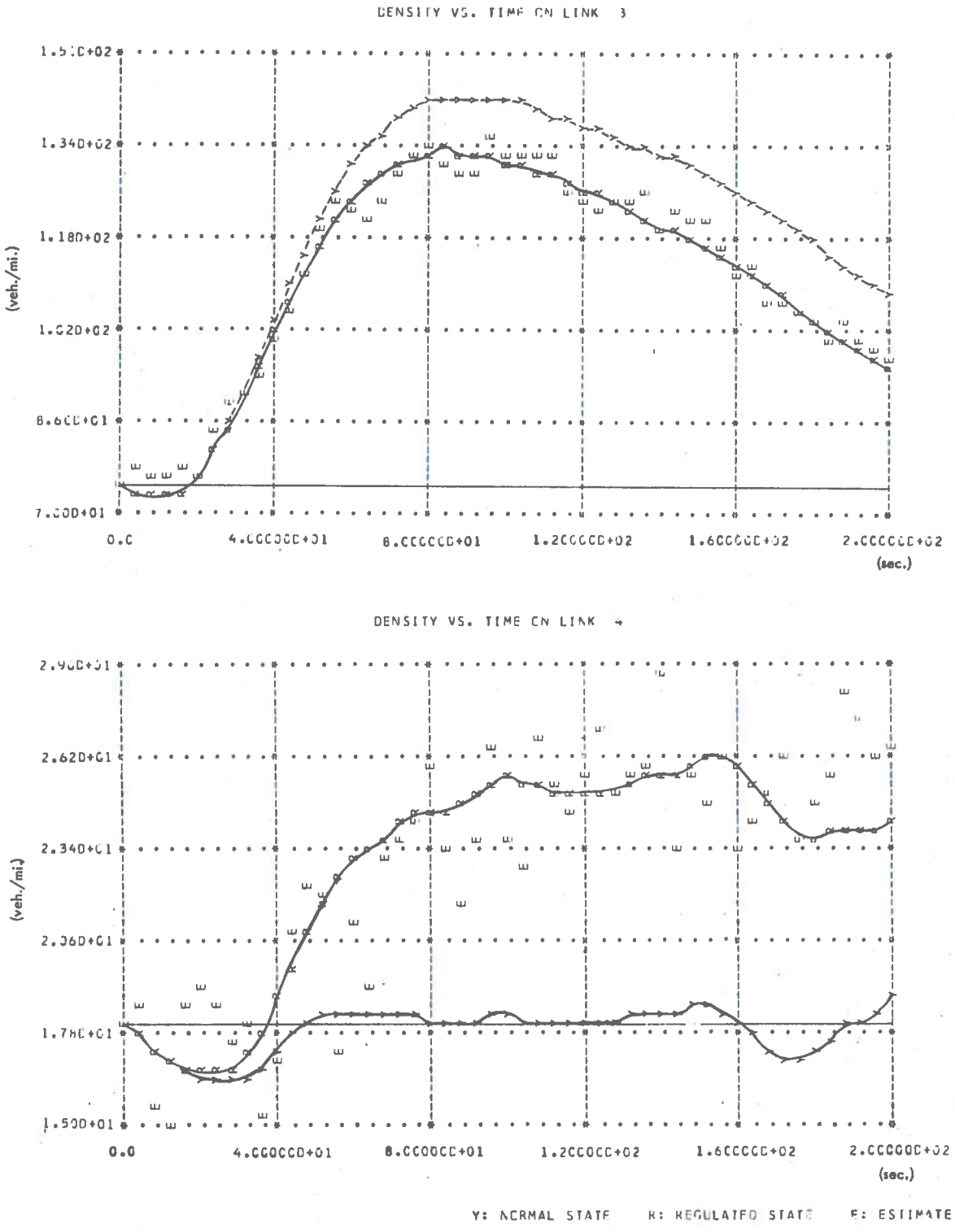

Figure 2.8 CENTRALIZED CONTROL SYSTEM RESULTS FOR EXAMPLE (DENSITY) (LINKS 3 and 4)

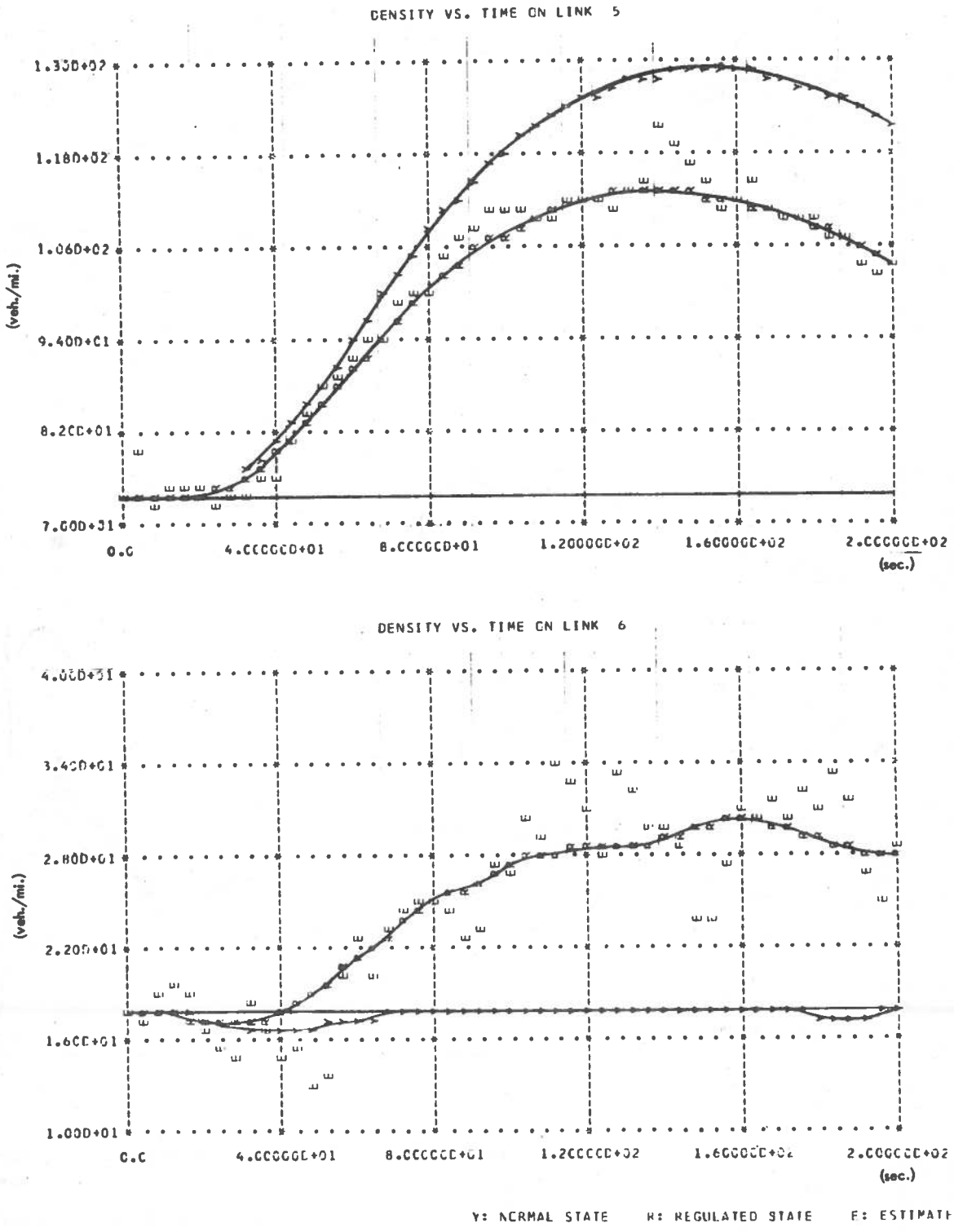

Figure 2.9 CENTRALIZED CONTROL SYSTEM RESULTS FOR EXAMPLE (DENSITY) (LINKS 5 and 6)

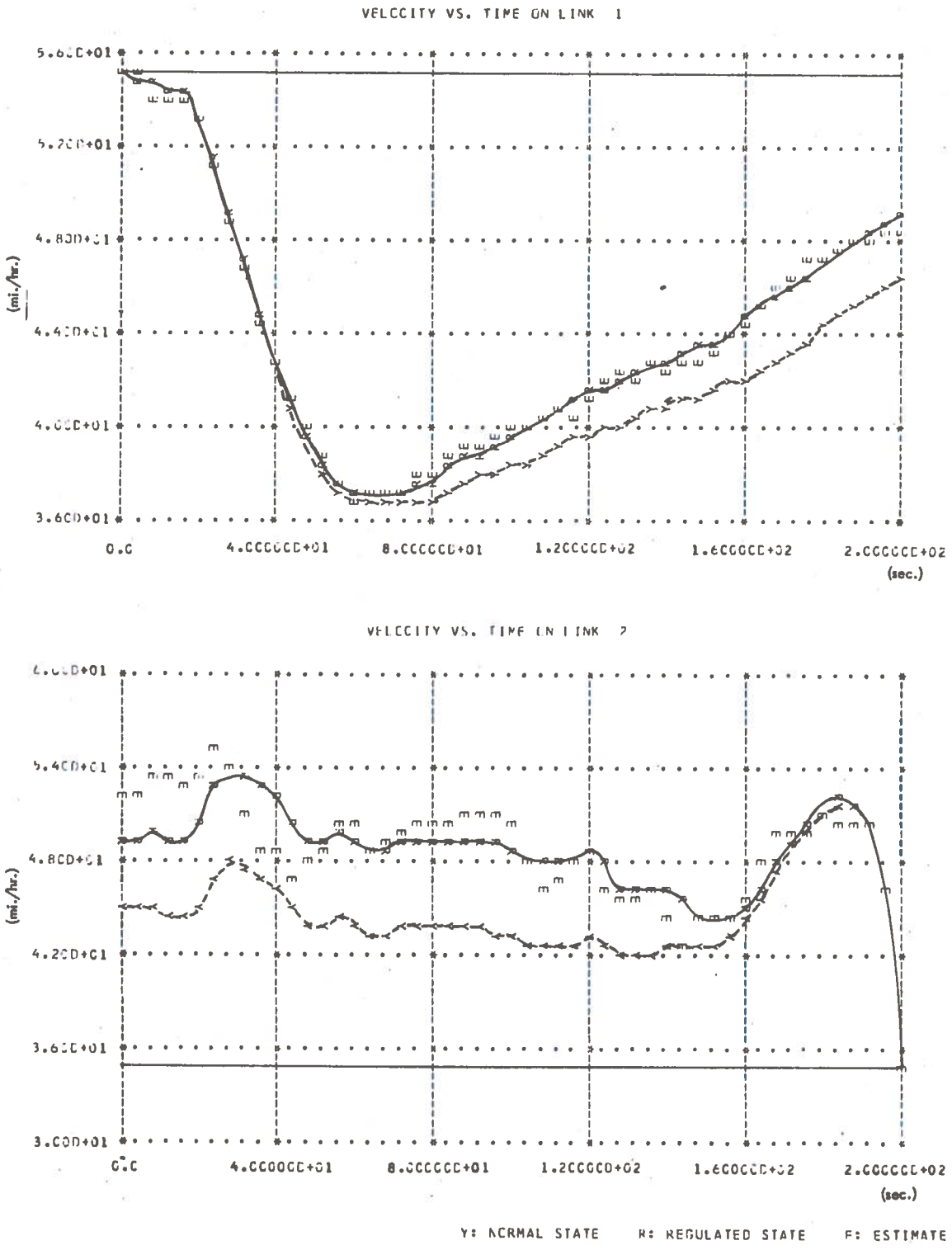

Figure 2.10 CENTRALIZED CONTROL SYSTEM RESULTS FOR EXAMPLE (VELOCITY) (LINKS 1 and 2)

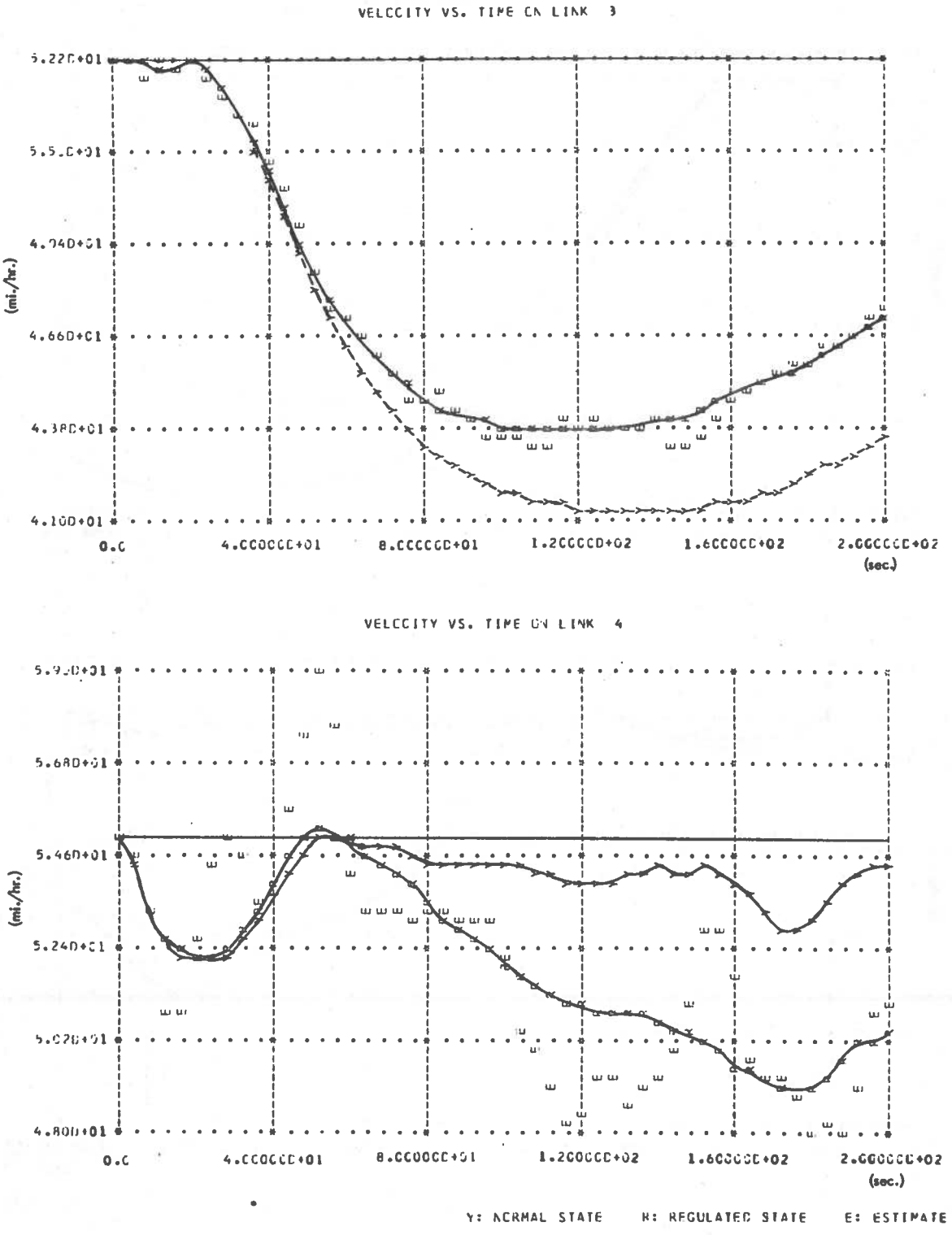

Figure 2.11 CENTRALIZED CONTROL SYSTEM RESULTS FOR EXAMPLE (VELOCITY) (LINKS 3 and 4)

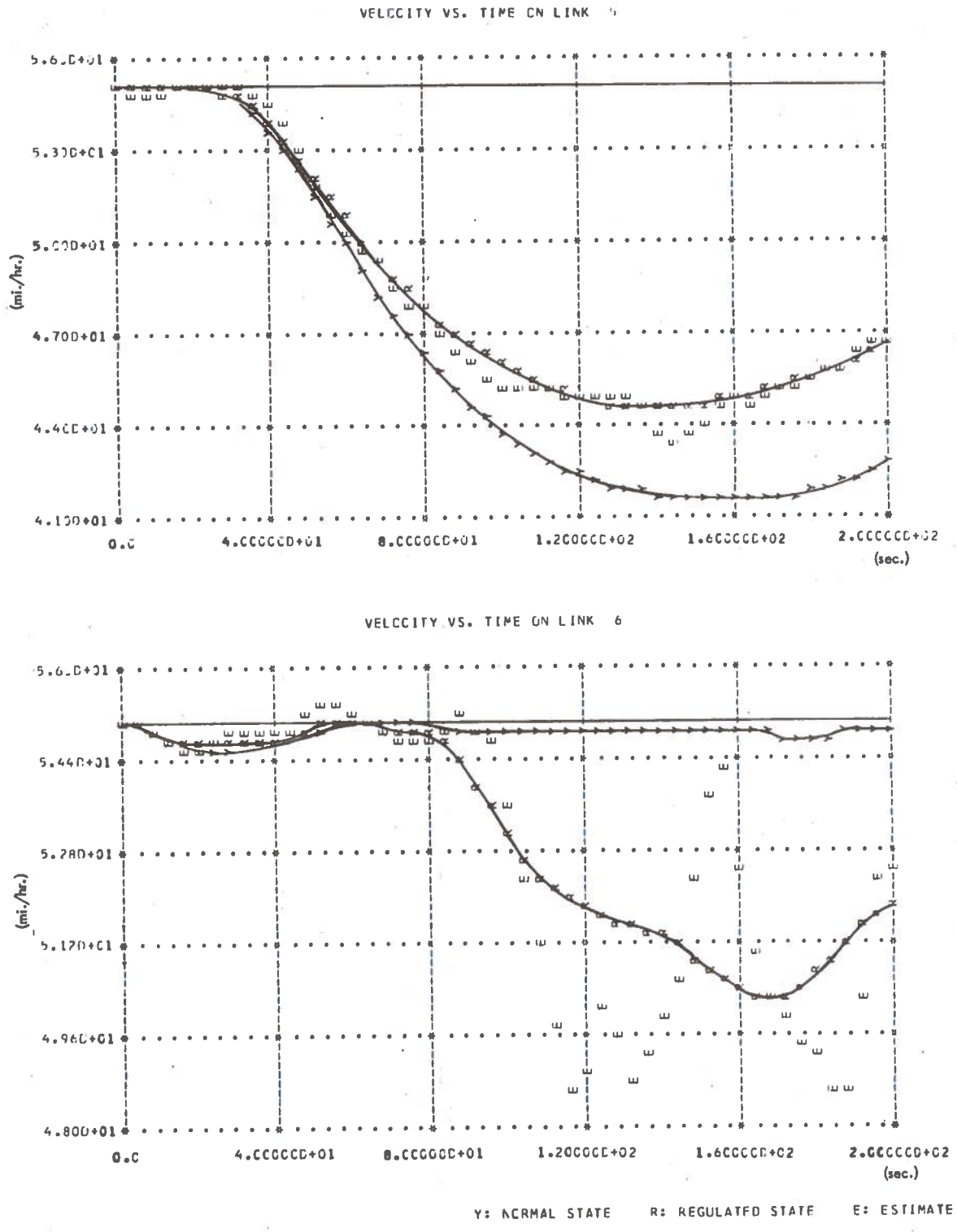

Figure 2.12 CENTRALIZED CONTROL SYSTEM RESULTS FOR EXAMPLE (VELOCITY) (LINKS 5 and 6)

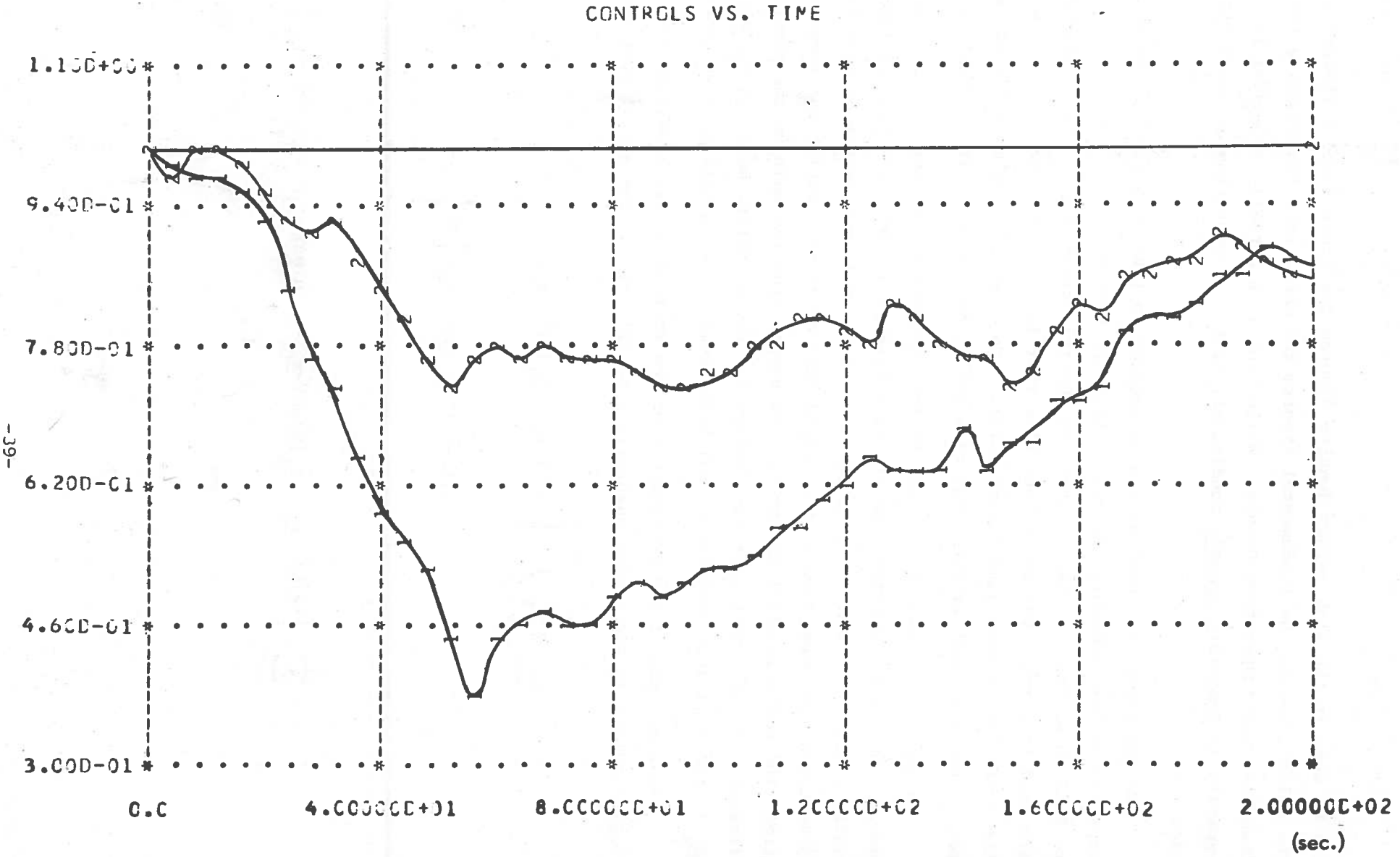

Figure 2.13 CENTRALIZED CONTROL SYSTEM RESULTS FOR EXAMPLE (CONTROLS)

can be seen in the flow versus density diagram for links 3 and 4 (figure 2.14). The solid curve is the fundamental diagram for each link, representing the feasible static operating points. While link 3 is actually exceeding its capacity (a temporary dynamic condition), link 4 is operating at about half-capacity.

We may expect the centralized controller to take advantage of the unused capacity of the secondary freeway to help the system recover. As figures 2.7 to 2.12 show, this is exactly what the control system does. Links 2,4, and 6 are used to carry a portion of the flow that is carried on the main freeway in the controller system (see figure 2.15). Consequently, the main freeway is not affected as much by the input-flow pulse, and can recover more quickly.

Figure 2.13 shows the actions of the controller. We see that a large amount of flow is diverted from the main freeway at the first pair of ramps during, and for a short time after, the pulse. A lesser amount of flow is diverted at the same time at the second pair of ramps. During the remaining time, the controls still divert flow as needed from the main to the secondary freeway. We also note that our choices for the weighting matrices $\underline{S}_1$ and $\underline{S}_2$ in the quadratic cost functional have seemed to work well in this case.

As a measure of the performance of the controller, we have used an approximation to the actual quadratic cost criterion. The actual cost is:

$$J = \lim_{T\to\infty} E\left\{\frac{1}{T}\int_0^T \left[(\underline{x}(t)-\underline{x}_0)'\ \underline{S}_1(\underline{x}(t)-\underline{x}_0) + (\underline{u}(t)-\underline{u}_0)'\ \underline{S}_2(\underline{u}(t)-\underline{u}_0)\right] dt\right\}. \qquad (2.4.10)$$

We approximate this by a finite sum over the interval of the experiment:

$$\hat{J} = \sum_{k=0}^{50} \left\{[\underline{x}(k\Delta)-\underline{x}_0]'\ \underline{S}_1[\underline{x}(k\Delta)-\underline{x}_0] + [\underline{u}(k\Delta)-\underline{u}_0]'\ \underline{S}_2[\underline{u}(k\Delta)-\underline{u}_0]\right\},$$

$$\Delta=4. \qquad (2.4.11)$$

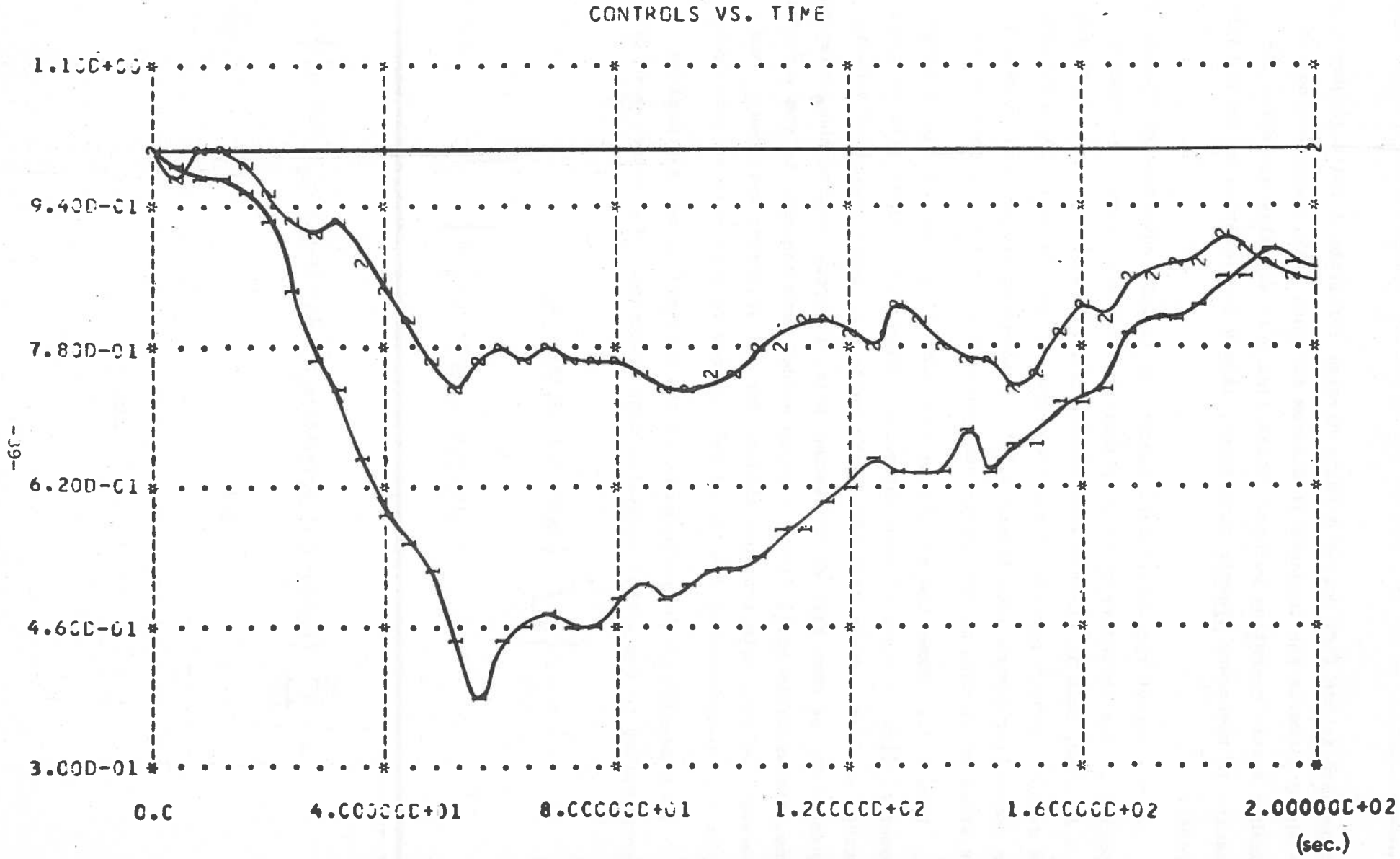

Figure 2.13 CENTRALIZED CONTROL SYSTEM RESULTS FOR EXAMPLE (CONTROLS)

can be seen in the flow versus density diagram for links 3 and 4 (figure 2.14). The solid curve is the fundamental diagram for each link, representing the feasible static operating points. While link 3 is actually exceeding its capacity (a temporary dynamic condition), link 4 is operating at about half-capacity.

We may expect the centralized controller to take advantage of the unused capacity of the secondary freeway to help the system recover. As figures 2.7 to 2.12 show, this is exactly what the control system does. Links 2,4, and 6 are used to carry a portion of the flow that is carried on the main freeway in the controller system (see figure 2.15). Consequently, the main freeway is not affected as much by the input-flow pulse, and can recover more quickly.

Figure 2.13 shows the actions of the controller. We see that a large amount of flow is diverted from the main freeway at the first pair of ramps during, and for a short time after, the pulse. A lesser amount of flow is diverted at the same time at the second pair of ramps. During the remaining time, the controls still divert flow as needed from the main to the secondary freeway. We also note that our choices for the weighting matrices $\underline{S}_1$ and $\underline{S}_2$ in the quadratic cost functional have seemed to work well in this case.

As a measure of the performance of the controller, we have used an approximation to the actual quadratic cost criterion. The actual cost is:

$$J = \lim_{T\to\infty} E\left\{\frac{1}{T}\int_0^T \left[(\underline{x}(t)-\underline{x}_0)'\ \underline{S}_1(\underline{x}(t)-\underline{x}_0) + (\underline{u}(t)-\underline{u}_0)'\ \underline{S}_2(\underline{u}(t)-\underline{u}_0)\right] dt\right\}. \qquad (2.4.10)$$

We approximate this by a finite sum over the interval of the experiment:

$$\hat{J} = \sum_{k=0}^{50} \left\{[\underline{x}(k\Delta)-\underline{x}_0]'\ \underline{S}_1[\underline{x}(k\Delta)-\underline{x}_0] + [\underline{u}(k\Delta)-\underline{u}_0]'\ \underline{S}_2[\underline{u}(k\Delta)-\underline{u}_0]\right\},$$

$$\Delta=4. \qquad (2.4.11)$$

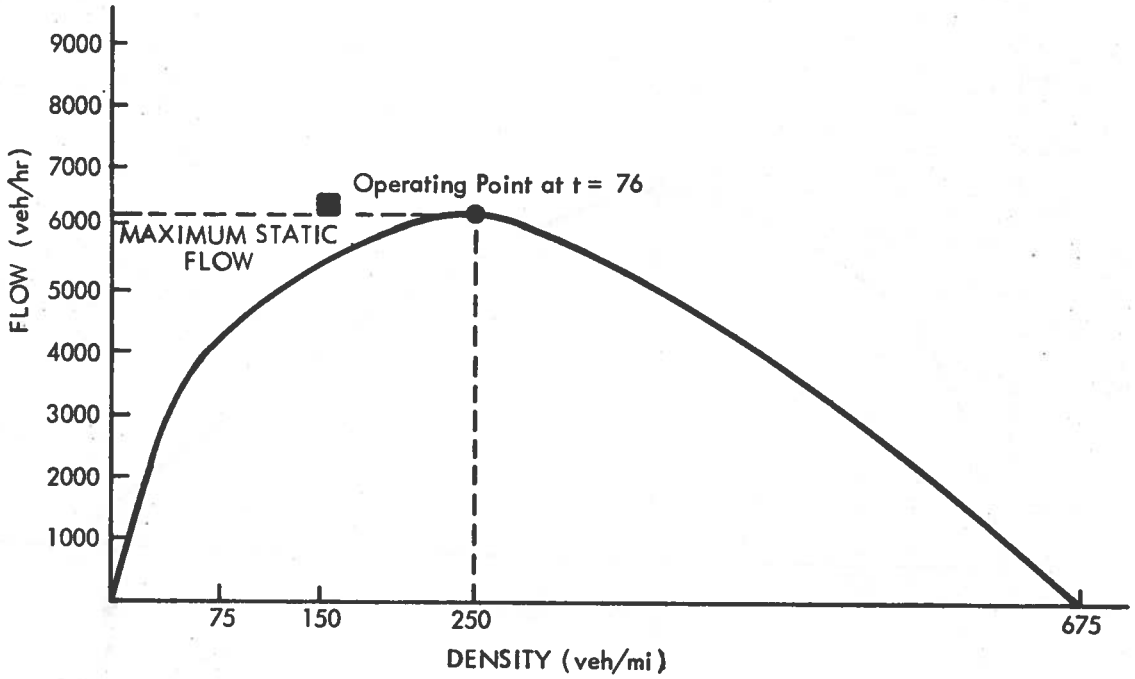

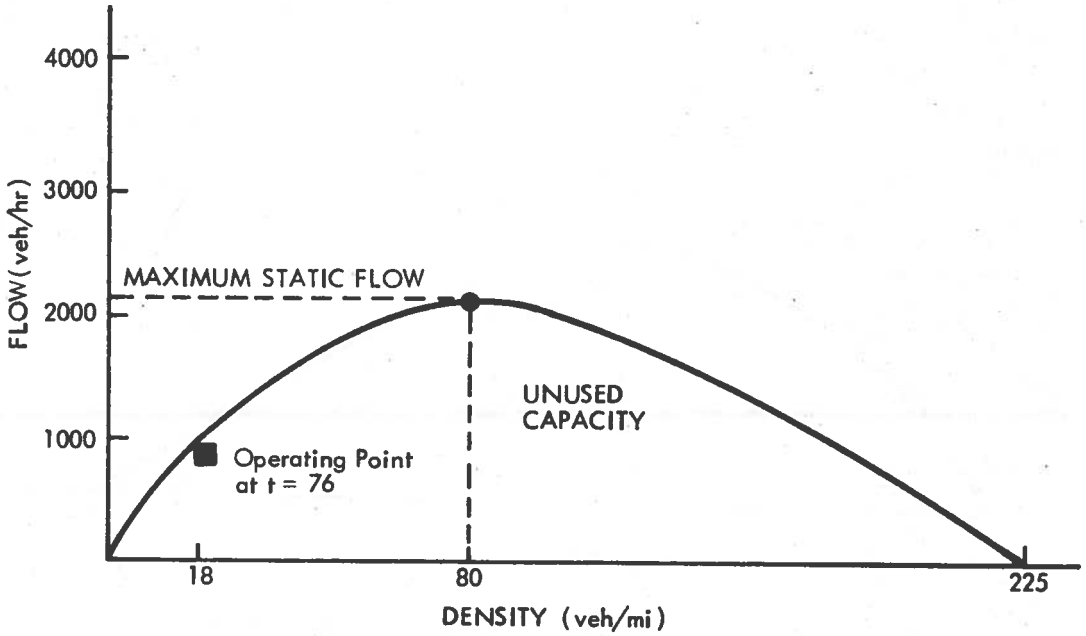

Figure 2.14 UNCONTROLLED FLOW DEMANDS ON CORRIDOR

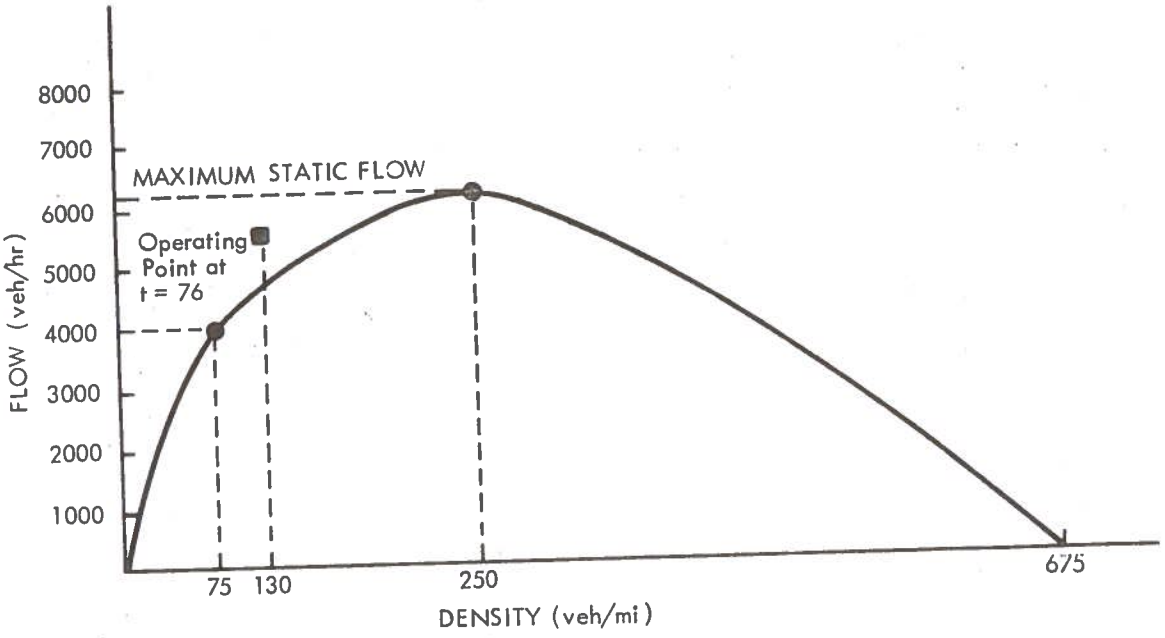

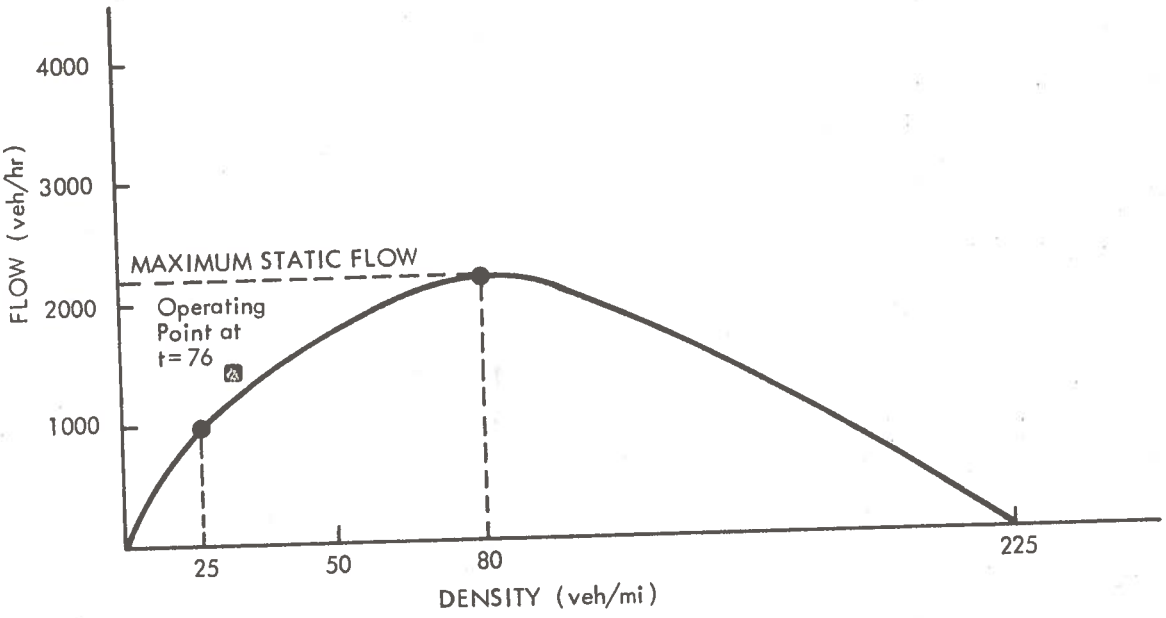

Figure 2.15 CONTROLLED FLOW DEMANDS ON CORRIDOR

The results from this type of approximation must be viewed with caution. Since the statistic is evaluated one time for only on case, the statistical validity is questionable. Taken in this context however, it can given an indication of the improvement in the system performance. The resulting open-and-closed loop statistical costs are:

$$\hat{J}_{\text{open loop}} = 5.15 \times 10^5 ,$$

$$\hat{J}_{\text{closed loop}} = 4.74 \times 10^5 , \qquad (2.4.12)$$

$$\% \text{ improvement} = 8.$$

2.5 Conclusion

In this section, we have given a brief development of the LQG regulator approach to control-system design. The LQG design philosophy has been applied to the freeway corridor problem, and the resulting design to a small problem. Although more testing is needed, the results from the problem indicate that the centralized controller represents a workable design.

3. AN APPROACH TO DECENTRALIZED CONTROL

3.1 Introduction

As has been shown in section 2, a working centralized stochastic control system can be designed for a freeway corridor. The control system has two majc drawbacks however. The first is that a large amount of computation is requirec and this requirement grows rapidly with the number of sections in the corridor. The second is that the amount of communication required quickly becomes prohibi tive as the length of the corridor increases.

These two problems impose a serious limitation on the effectiveness of the centralized controller. To reduce the computational and communication require- ments, some type of decentralized control algorithm must be implemented. In de signing the decentralized controller, it is desirable to avoid an ad-hoc approa as much as possible. Instead, we may rather rely on theory and mathematical techniques subject to the computation and communication constraints.

To accomplish this objective, we will step back from the specifics of the freeway corridor, and concentrate on a more general class of decentralized con trol problems. The remainder of this section presents the decentralized contr problem, and develops a sub-optimal strategy for its solution.

3.2 The Decentralized Control Problem

Consider the stationary linear (or linearized) system:

$$\dot{\underline{x}}(t) = \underline{A}\,\underline{x}(t) + \underline{B}\,\underline{u}(t) + \underline{\xi}(t),$$

$$\underline{y}(t) = \underline{C}\,\underline{x}(t) + \underline{\theta}(t), \tag{3.2.1}$$

where $\underline{\xi}$ and $\underline{\theta}$ are Gaussian white noise processes with:

$$E\{\underline{\xi}(t)\ \underline{\xi}'(\tau)\} = \underline{Q}\,\delta(t-\tau),$$

$$E\{\underline{\theta}(t)\ \underline{\theta}'(\tau)\} = \underline{R}\ \ (t-\tau), \tag{3.2.2}$$

$$E\{\underline{\xi}(t)\ \underline{\theta}'(T)\} = E\{\underline{\xi}(t)\ \underline{x}'(0)\} = E\{\underline{\theta}(t)\ \underline{x}'(0)\} = 0.$$

As in section (2.3), we wish to choose a feedback law

$$\underline{u}(t) = \underline{f}(\hat{\underline{x}}(t)), \tag{3.2.3a}$$

$$\dot{\hat{\underline{x}}}(t) = \underline{h}(\hat{\underline{x}}(t), \underline{u}(t), \underline{y}(t)), \tag{3.2.3b}$$

to minimize the cost functional:

$$J = \underset{T\to\infty}{\text{LIM}} \; E\left\{\frac{1}{T}\int_0^T \left[\underline{x}'(t)\ \underline{S}_1\ \underline{x}(t) = \underline{u}'(t)\ \underline{S}_2\ \underline{u}(t)\right] dt\right\}. \tag{3.2.4}$$

If the estimator (3.2.3b) is the same dimension as the system (3.2.1) and all the observations are available, the optimal estimate is given by the linear Kalman filter (see section 2.3). The optimal feedback law is also linear:

$$\underline{u}^*(t) = -\underline{G}\ \hat{\underline{x}}(t). \tag{3.2.5}$$

The feedback gain matrix $\underline{G}$ and the Kalman gain matrix $\underline{H}$ can be readily found off-line.

In the case we will consider, we will assume that there are M controllers. Each controller has a subset of the system states, $\underline{x}_i$, and a subset of the control variables, $\underline{u}_i$. The individual controller's objective is to choose its input variables as a function of its estimate of its states to minimize the cost function (3.2.4). The controller is allowed to use only a subset of the measurements, $\underline{y}_i$, and certain communicated estimates from other controllers to form its own estimates $\underline{x}_i$.

Mathematically,

$$\underline{u}_i(t) = \underline{f}_i(\hat{\underline{x}}_i(t)),$$

$$\dot{\hat{\underline{x}}}_i(t) = \underline{h}_i(\hat{\underline{x}}_i(t), \underline{y}_i(t), \underline{D}_i\hat{\underline{x}}(t), \underline{u}(t)), \tag{3.2.6}$$

where

$$\hat{\underline{x}}(t) = \begin{bmatrix} \hat{\underline{x}}_1(t) \\ \vdots \\ \hat{\underline{x}}_M(t) \end{bmatrix},$$

$$\underline{u}(t) = \begin{bmatrix} \underline{u}_1(t) \\ \vdots \\ \underline{u}_M(t) \end{bmatrix},$$

$\underline{D}_i \equiv$ matrix fixing the structure of the communicated estimates and $\underline{f}_i$ and $\underline{h}_i$, i = 1, M are chosen to minimize the cost function (3.2.4).

Unlike the centralized control problem with classical information pattern, the solution to this problem is in general non-linear, and the problem is impossible to solve optimally in most cases. What is needed is a suboptimal design that:

(a) is not too difficult to solve;

(b) is practical to implement from a computation and communication standpoint;

(c) works reasonably well; and

(d) avoids being ad-hoc as much as possible.

Although these conditions are loosely stated, they give us guidelines for choosing a method of suboptimal design which is applicable to a wide range of problems. To satisfy these conditions, a parameterization approach suggested earlier will be used. First, we will choose the filter structure $\underline{h}_i$ and the feedback law $\underline{g}_i$ to be linear. It will be seen later in this section that condition (a) is satisfied. The linearity and structure of the filter satisfy condition (b) as well as any method can, and the only part of the method that is ad-hoc is the restriction to linearity.

The only condition that remains to be satisfied is the performance of the resulting controller. This condition will not be satisfied for every type of system. However, if the system is stabilizable through the decentralized linear feedback, it will be possible in many cases to find a "reasonable" linear solution. This will be verified for the freeway corridor in section 4.

We first fix the structure of the estimator and feedback law for the ith

controller to be linear:

$$\underline{u}_i(t) = -\underline{G}_i\, \hat{\underline{x}}_i(t), \tag{3.2.7}$$

$$\dot{\hat{\underline{x}}}_i(t) = \underline{F}_{ii}\, \hat{\underline{x}}_i(t) + \sum_{\substack{j=1 \\ j\neq i}}^{M} \underline{F}_{ij}\, \hat{\underline{x}}_j(t) + \underline{H}_i(\underline{y}_i(t) - \underline{C}_i \hat{\underline{x}}_i(t)) + \underline{B}_i\, \underline{u}(t).$$

Where the elements (or some of the elements, the others begin prespecified) of the matrices $\underline{F}_{ii}$, $\underline{F}_{ij}$, $\underline{H}_i$, and $\underline{G}_i$ are chosen to minimize the cost functional (3.2.4).

By defining the matrices:

$$\underline{F} = \left[\underline{F}_{ij}\right],$$

$$\underline{H} = \text{diag}\left[\underline{H}_i\right],$$

$$\underline{G} = \text{diag}\left[\underline{G}_i\right], \tag{3.2.8}$$

we can rewrite equations (3.2.7) as:

$$\underline{u}(t) = -\underline{G}\, \hat{\underline{x}}(t), \tag{3.2.9a}$$

$$\dot{\hat{\underline{x}}}(t) = \underline{F}\, \hat{\underline{x}}(t) + \underline{H}(\underline{y}(t) - \underline{C}\, \hat{\underline{x}}(t)) + \underline{B}\, \underline{u}(t). \tag{3.2.9b}$$

Recalling the original system equations:

$$\dot{\underline{x}}(t) = \underline{A}\, \underline{x}(t) + \underline{B}\, \underline{u}(t) + \underline{\xi}(t),$$

$$\underline{y}(t) = \underline{C}\, \underline{x}(t) + \underline{\theta}(t), \tag{3.2.10}$$

we can combine equations (3.2.9) and (3.2.10) to form the overall system equation:

$$\begin{bmatrix} \dot{\underline{x}}(t) \\ \dot{\hat{\underline{x}}}(t) \end{bmatrix} = \begin{bmatrix} \underline{A} & -\underline{B}\underline{G} \\ \underline{H}\,\underline{C} & \underline{F} - \underline{B}\,\underline{G} - \underline{H}\,\underline{C} \end{bmatrix} \begin{bmatrix} \underline{x}(t) \\ \hat{\underline{x}}(t) \end{bmatrix} + \begin{bmatrix} \underline{I} & \underline{0} \\ \underline{0} & \underline{H} \end{bmatrix} \begin{bmatrix} \underline{\xi}(t) \\ \underline{\theta}(t) \end{bmatrix}. \tag{3.2.11}$$

We can now state the problem:

PROBLEM STATEMENT A:

Choose the elements of $\underline{F}$, $\underline{G}$, and $\underline{H}$ which are not prespecified to minimize the cost functional:

$$J = \lim_{T\to\infty} E\left\{\frac{1}{T}\int_0^T \left[\underline{x}'(t)\ \underline{S}_1\ \underline{x}(t) + \underline{u}'(t)\ \underline{S}_2\ \underline{u}(t)\right]dt\right\}, \tag{3.2.12}$$

subject to equation (3.2.11).

Although problem statement A is a precise statement of the problem, it offers no insight to the solution of the problem. To obtain the insight, we try to reformulate the problem. Substituting (3.2.9a) in (3.2.12) we get:

$$J = \lim_{T\to\infty} E\left\{\frac{1}{T}\int_0^T \left[\underline{x}'(t)\ \underline{S}_1\ \underline{x}(t) + \hat{\underline{x}}'(t)\ \underline{G}'\ \underline{S}_2\ \underline{G}\ \hat{\underline{x}}(t)\right]dt\right\}. \tag{3.2.13}$$

Wonham [1969] has justified the interchange of the expectation and integration operations in (3.7.13). Interchanging these operations gives:

$$J = \lim_{T\to\infty} \frac{1}{T}\int_0^T E\{\underline{x}'(t)\ \underline{S}_1\ \underline{x}(t) + \underline{x}'(t)\ \underline{G}'\ \underline{S}_2\ \underline{G}\ \hat{\underline{x}}(t)\}\ dt\ . \tag{3.2.14}$$

We now use the basic trace identity

$$\mathrm{tr}\left[\underline{A}'\underline{B}\right] = \mathrm{tr}\left[\underline{B}\underline{A}'\right], \tag{3.2.15}$$

and the linearity of the trace and expectation operators to get:

$$J = \lim_{T\to\infty} \frac{1}{T}\int_0^T \left[\mathrm{tr}\ \underline{S}_1\ E\ \{\underline{x}(t)\ \underline{x}'(t)\} + \mathrm{tr}\ \underline{G}'\ \underline{S}_2\ \underline{G}\ E\ \{\hat{\underline{x}}(t)\ \hat{\underline{x}}'(t)\}\right]dt. \tag{3.2.16}$$

Using the linearity of the integral and making the identifications:

$$\underline{\Sigma}_{11}(t) = E\{\underline{x}(t)\ \underline{x}'(t)\},$$

$$\underline{\Sigma}_{22}(t) = E\{\hat{\underline{x}}(t)\ \hat{\underline{x}}'(t)\}, \tag{3.2.17}$$

we get:

$$J = \underset{T\to\infty}{\text{Lim}}\ \text{tr}\left\{\underline{S}_1\left[\frac{1}{T}\int_0^T \underline{\Sigma}_{11}(t)\ dt\right] + \underline{G}'\ \underline{S}_2\ \underline{G}\left[\frac{1}{T}\int_0^T \underline{\Sigma}_{22}(t)\ dt\right]\right\} . \tag{3.2.18}$$

Now define:

$$\underline{S}(\alpha) = \begin{bmatrix} \underline{S}_1 & \underline{0} \\ \underline{0} & \underline{G}'(\underline{\alpha})\ \underline{S}_2\ \underline{G}(\underline{\alpha}) \end{bmatrix}$$

$$\underline{\Sigma}(t) = \begin{bmatrix} \underline{\Sigma}_{11}(t) & \underline{\Sigma}_{12}(t) \\ \underline{\Sigma}_{21}(t) & \underline{\Sigma}_{22}(t) \end{bmatrix} = E\left\{\begin{bmatrix} \underline{x}(t) \\ \hat{\underline{x}}(t) \end{bmatrix}\begin{bmatrix} \underline{x}(t) \\ \hat{\underline{x}}(t) \end{bmatrix}'\right\} , \tag{3.2.19}$$

$$\underline{A}(\alpha) = \begin{bmatrix} \underline{A} & -\underline{B}\ \underline{G}(\underline{\alpha}) \\ \underline{H}(\underline{\alpha})\underline{C} & \underline{F}(\underline{\alpha}) - \underline{B}\ \underline{G}(\underline{\alpha}) - \underline{H}(\underline{\alpha})\underline{C} \end{bmatrix},$$

$$\underline{L}(\alpha) = \begin{bmatrix} \underline{I} & 0 \\ 0 & \underline{H}(\underline{\alpha}) \end{bmatrix} \qquad \underline{\Xi} = \begin{bmatrix} \underline{Q} & 0 \\ 0 & \underline{R} \end{bmatrix},$$

where: $\underline{\alpha} \equiv$ vector of the elements of the matrices F, G, and H that are not prespecified.

Then (3.2.18) can be rewritten as:

$$J = \underset{T\to\infty}{\text{Lim}}\ \text{tr}\left\{\underline{S}(\alpha)\left[\frac{1}{T}\int_0^T \underline{\Sigma}(t)\ dt\right]\right\} , \tag{3.2.20}$$

and $$\dot{\underline{\Sigma}}(t) = \underline{A}(\alpha)\ \underline{\Sigma}(t) + \underline{\Sigma}(t)\ \underline{A}'(\alpha) + \underline{L}(\alpha)\underline{\Xi}\ \underline{L}'(\alpha) . \tag{3.2.21}$$

If $\underline{A}(\alpha)$ is stable, $\underline{\Sigma}(t)$ approaches the limit $\underline{\Sigma}_{ss}$ given by:

$$0 = \underline{A}(\alpha)\ \underline{\Sigma}_{ss} + \underline{\Sigma}_{ss}\underline{A}'(\alpha) + \underline{L}(\alpha)\underline{\Xi}\ \underline{L}'(\alpha) . \tag{3.2.22}$$

Where:

$$\underset{T\to\infty}{\text{Lim}}\ \frac{1}{T}\int_0^T \underline{\Sigma}(t)\ dt \triangleq \underline{\Sigma}_{ss} . \tag{3.2.23}$$

Combining (3.2.22), (3.2.23), and (3.2.20) produces the following problem, equivalent to problem statement A:

PROBLEM STATEMENT B:

$$\min_{\underline{\alpha}} J(\underline{\alpha}) = \text{tr } \underline{S}(\underline{\alpha})\ \underline{\Sigma}_{ss} \ , \tag{3.2.24}$$

$$\text{subject to } 0 = \underline{A}(\underline{\alpha})\ \underline{\Sigma}_{ss} + \underline{\Sigma}_{ss}\ \underline{A}'(\underline{\alpha}) + \underline{L}(\underline{\alpha})\ \underline{\Xi}\ \underline{L}'(\underline{\alpha}) \ . \tag{3.2.25}$$

In concluding this section we make several remarks about the problem:

(a) The design of the decentralized control system has been reduced to a static minimization problem which can be solved off-line. Thus, the condition that the problem be fairly easily solved is satisfied.

(b) The structure of $\underline{A}(\underline{\alpha})$ and $\underline{L}(\underline{\alpha})$ is fixed by equations (3.2.19). In turn, the structure of $\underline{F}(\underline{\alpha})$, $\underline{G}(\underline{\alpha})$, and $\underline{H}(\underline{\alpha})$ are fixed by (3.2.8). By using the special properties of the system that this method is being applied to, the F_{ij}, $\underline{H}_i$, and $\underline{G}_i$ matrices of (3.2.8) can often be fixed before the static minimization is begun. This further reduces the complexity of the problem.

(c) It should be emphasized that problem statements A and B are entirely equivalent.

3.3 Method of Solution

In section 3.2, the problem of designing a decentralized controller is reduced to a constrained static minimization problem. There are several efficient methods available (see, for example Fletcher and Powell [1963] or Powell [1964]) for the minimization of a multivariable function. The method that will be used for this report is the Davidon-Fletcher-Powell (DFP) algorithm.

The DFP method requires the calculation of the gradient of the cost function. Define:

$$\frac{\partial}{\partial \underline{\alpha}} J(\underline{\alpha}) = \begin{bmatrix} \frac{\partial}{\partial \alpha_1} J(\underline{\alpha}) \\ \vdots \\ \frac{\partial}{\partial \alpha_q} J(\underline{\alpha}) \end{bmatrix} \equiv \text{gradient of } J(\underline{\alpha}). \tag{3.3.1}$$

Computing the derivative with respect to α_i:

$$\frac{\partial}{\partial \alpha_i} J(\underline{\alpha}) = \mathrm{tr}\left\{\frac{\partial}{\partial \alpha_i} \underline{Q}(\underline{\alpha})\ \underline{\Sigma}_{ss} + \underline{Q}(\underline{\alpha})\ \frac{\partial}{\partial \alpha_i} \underline{\Sigma}_{ss}\right\}. \tag{3.3.2}$$

The first term of the right-hand side is easy to compute since $\underline{\Sigma}_{ss}$ is already available from the calculation of $J(\underline{\alpha})$. To compute the second term, we first differentiate the constraint equation (3.2.22):

$$0 = \underline{A}(\underline{\alpha})\ \frac{\partial}{\partial \alpha_i} \underline{\Sigma}_{ss} + \frac{\partial}{\partial \alpha_i} \underline{\Sigma}_{ss}\ \underline{A}'(\underline{\alpha})$$

$$+ \left\{\frac{\partial}{\partial \alpha_i} A(\underline{\alpha})\underline{\Sigma}_{ss} + \underline{\Sigma}_{ss}\ \frac{\partial}{\partial \alpha_i} A(\underline{\alpha})' + \frac{\partial}{\partial \alpha_i}\left[\underline{L}(\alpha)\ \underline{\Xi}\ \underline{L}'(\underline{\alpha})\right]\right\} \tag{3.3.3}$$

which can be solved for $\frac{\partial}{\partial \alpha_i} \underline{\Sigma}_{ss}$. This suggests the following algorithm to compute the cost and its gradient.

(a) Solve equation (3.2.22) for $\underline{\Sigma}_{ss}$,

(b) Evaluate $J(\underline{\alpha})$,

(c) Compute the driving term (the term in brackets) for equation (3.3.3) for $i = 1,\ldots q$,

(d) Compute $\frac{\partial}{\partial \alpha_i} J(\alpha_i)$ from equation (3.3.2).

Although the concept of the algorithm is simple, solving the matrix equations as required by steps (a) and (c) can be difficult. A total of $q + 1$ Lyapunov equations must be solved for each gradient evaluation.

A considerable amount of research concerning the efficient solution of the matrix Lyapunov equation has been done. The methods of solution fall into four categories (for a survey of methods see Hagander [1972]); direct or linear-equation methods, eigenvalue methods, companion-form methods, and iterative methods. Of these classes, the eigenvalue and companion-form methods suffer from accuracy problems.

The method of solution of the Lyapunov equation must come from the remaining two classes. Of these classes, the iterative methods at first appear computationally faster. The drawback is that there is no way for these methods to take advantage of the sparsity of $\underline{A}(\underline{\alpha})$. The iterative methods require 2

matrix multiplications for each iteration of the Lyapunov solution, and approximately 10 iterations for convergence. For each gradient evaluation, this means approximately 20 qn^3 multiplications (where q is the number of parameters and n is the dimension of $\underline{A}(\underline{\alpha})$). For n = 30, q = 30, and a single multiplication time of 10^{-5} seconds, the time for one gradient evaluation is over 2-1/2 minutes. Obviously, we must make use of direct methods.

To use a direct method, we must take advantage of the sparsity of $\underline{A}(\underline{\alpha})$ and the structure of the problem. For a non-sparse $\underline{A}(\underline{\alpha})$, the most accurate and efficient method, the L-U decomposition (see Moler and Forsythe [1967], and Appendix A) requires approximately n^6 multiplications for the factorization. The matrix $\underline{A}(\underline{\alpha})$ will contain relatively few non-zero elements for most large-dimensional problems. This property can be used to eliminate all multiplications involving zeroes, and thus reduce the computational requirements considerably.

Another property of the static-minimization problem can be used efficiently by the direct methods. The equations for $\underline{\Sigma}_{ss}$ and for $\frac{\partial}{\partial \alpha_i} \underline{\Sigma}_{ss}$ differ only in the driving term; the system matrices are the same. This means that the L-U decomposition need only be done once per gradient evaluation. The solutions of the (q + 1) Lyapunov equations can be accomplished by forward and backward substitution. This normally requires approximately n^4 multiplications per equation, but this again can be considerably reduced by taking advantage of the sparsity of $\underline{A}(\underline{\alpha})$.

In summary, the method used to solve the constrained static-optimization problem of section 3.2 will be to use the DFP gradient method. The gradients will be computed using the following algorithm (slightly modified from the earlier algorithm to save computation time and storage):

(a) Expand $\underline{A}(\underline{\alpha})$ (and denote the expanded version $\overline{\underline{A}}(\alpha)$) to write the upper-half of $\underline{\Sigma}_{ss}$ as a column vector (denoted $\overline{\underline{\Sigma}}_{ss}$) and thus transform the n-dimemsional equations into a $\frac{n(n+1)}{2}$ dimensional linear equation of the form:

$$\overline{\underline{A}}(\underline{\alpha})\overline{\underline{\Sigma}}_{ss} = \overline{\underline{\Theta}}_{ss} \ , \qquad (3.3.4)$$

(b) Factor $\bar{A}(\alpha)$ into lower and upper triangular form (L-U decomposition).

(c) Use forward and backward substitution to solve for $\bar{\Sigma}_{ss}$.

(d) Compute $J(\underline{\alpha})$.

(e) Let i = 1.

(f) Solve for $\frac{\partial}{\partial \alpha_i} \Sigma(\underline{\alpha})$ by using forward and backward substitution.

(g) Compute $\frac{\partial}{\partial \alpha_i} J(\underline{\alpha})$.

(h) i = i + 1; If $i \leq q$, to to (e) and repeat steps (e) through (h). Otherwise return to DFP algorithm.

3.4 An Example

To give some insight into the method of design of decentralized controllers presented in sections 3.2 and 3.3, we will examine a simple 2-dimensional problem.

Problem 3.4a: Given the 1-dimensional system:

$$\dot{x}(t0 = x(t) + u(t) + \xi(t),$$

$$y(t) = x(t) + \theta(t),$$

$$E\{\xi(t)\xi(\tau)\} = \delta(t-\tau),$$

$$E\{\theta(t)\theta(\tau)\} = \delta(t-\tau),$$

$$E\{\theta(t)\xi(\tau)\} = 0. \qquad (3.4.1)$$

Choose h and g in the following control system:

$$u(t) = -g\hat{x}(t),$$

$$\dot{\hat{x}}(t) = \hat{x}(t) + h(y(t)-\hat{x}(t)) + u(t). \qquad (3.4.2)$$

To minimize the cost functional:

$$J = E\left\{\lim_{T\to\infty} \frac{1}{T} \int_0^T (x^2(t) + u^2(t))dt\right\}. \qquad (3.4.3)$$

Solution 1: We note that this is simply a 1-dimensional LQG problem. The gains

g and h can be found by solving the scalar algebraic Ricatti equations:

$$0 = 2\sigma + 1 - \sigma^2$$

$$h = \sigma \tag{3.4.4}$$

$$0 = -2k - 1 + \sigma^2$$

$$g = k. \tag{3.4.5}$$

These equations give the solutions:

$$h = 1 + \sqrt{2},$$

$$g = 1 + \sqrt{2}. \tag{3.4.6}$$

Solution 2: We now apply the method discussed in section 3.3. Formulating the problem as in problem statement B, we have the closed-loop system:

$$\begin{bmatrix} \dot{x}(t) \\ \dot{\hat{x}}(t) \end{bmatrix} = \begin{bmatrix} 1 & -g \\ h & 1-g-h \end{bmatrix} \begin{bmatrix} x(t) \\ \hat{x}(t) \end{bmatrix} + \begin{bmatrix} 1 & 0 \\ 0 & h \end{bmatrix} \begin{bmatrix} \xi(t) \\ \theta(t) \end{bmatrix}, \tag{3.4.7}$$

which gives the problem:

$$\text{minimize } J(\underline{\alpha}) = \text{tr} \begin{bmatrix} 1 & 0 \\ 0 & g^2 \end{bmatrix} \underline{\Sigma}\ (\underline{\alpha}). \tag{3.4.8}$$

Subject to:

$$0 = \begin{bmatrix} 1 & -g \\ h & 1-g-h \end{bmatrix} \underline{\Sigma}\ (\underline{\alpha}) + \underline{\Sigma}\ (\underline{\alpha}) \begin{bmatrix} 1 & h \\ -g & 1-g-h \end{bmatrix} + \begin{bmatrix} 1 & 0 \\ 0 & h^2 \end{bmatrix}, \tag{3.4.9}$$

where:

$$\underline{\alpha} = \begin{bmatrix} g \\ h \end{bmatrix}.$$

The first problem encountered is that the open-loop system is unstable. To solve the problem, we need a stabilizing initial guess. Consider the closed loop system (3.4.7). The characteristic polynomial of this system is:

$$s^2 + (g+h-2)s + (1-g-h+gh) = 0, \tag{3.4.10}$$

Which gives the requirements:

$$g + h > 2,$$
$$(g-1)(h-1) > 0. \tag{3.4.11}$$

The stability region is drawn in figure 3.1.

A total of seven stabilizing initial guesses have been tried. The location of the initial guesses are shown in figure 3.1, and the results summarized in table 3.1. For the best initial guess (g = 1.5, h = 1.5), the convergence is rapid and accurate. Several of the initial conditions have problems when the DFP algorithm takes a step out of the region of stability. This, however, is avoided in subsequent runs for all but one case by adjusting the stepsize in the DFP algorithm. Otherwise, the algorithm has worked well for this problem.

Problem 3.4b: Given the 1-dimensional system (3.4.1), choose g,h, and f in the following control system:

$$u(t) = -g\hat{x}(t),$$
$$\dot{\hat{x}}(t) = f\hat{x}(t) + h(y(t)-\hat{x}(t)) + u(t). \tag{3.4.12}$$

To minimize the cost functional:

$$J = E\{\lim_{T\to\infty} \frac{1}{T}\int_0^T (x^2(t) + u^2(t))dt\}. \tag{3.4.13}$$

Solution 1: Again this is simply a 1-dimensional LQG problem. The solution is:

$$f = 1.0,$$
$$g = 1 + \sqrt{2}, \tag{3.4.14}$$
$$h = 1 + \sqrt{2}.$$

Solution 2: We apply the static minimization method as in the solution to problem (3.4.1). The closed-loop system with f, g and h arbitrary is:

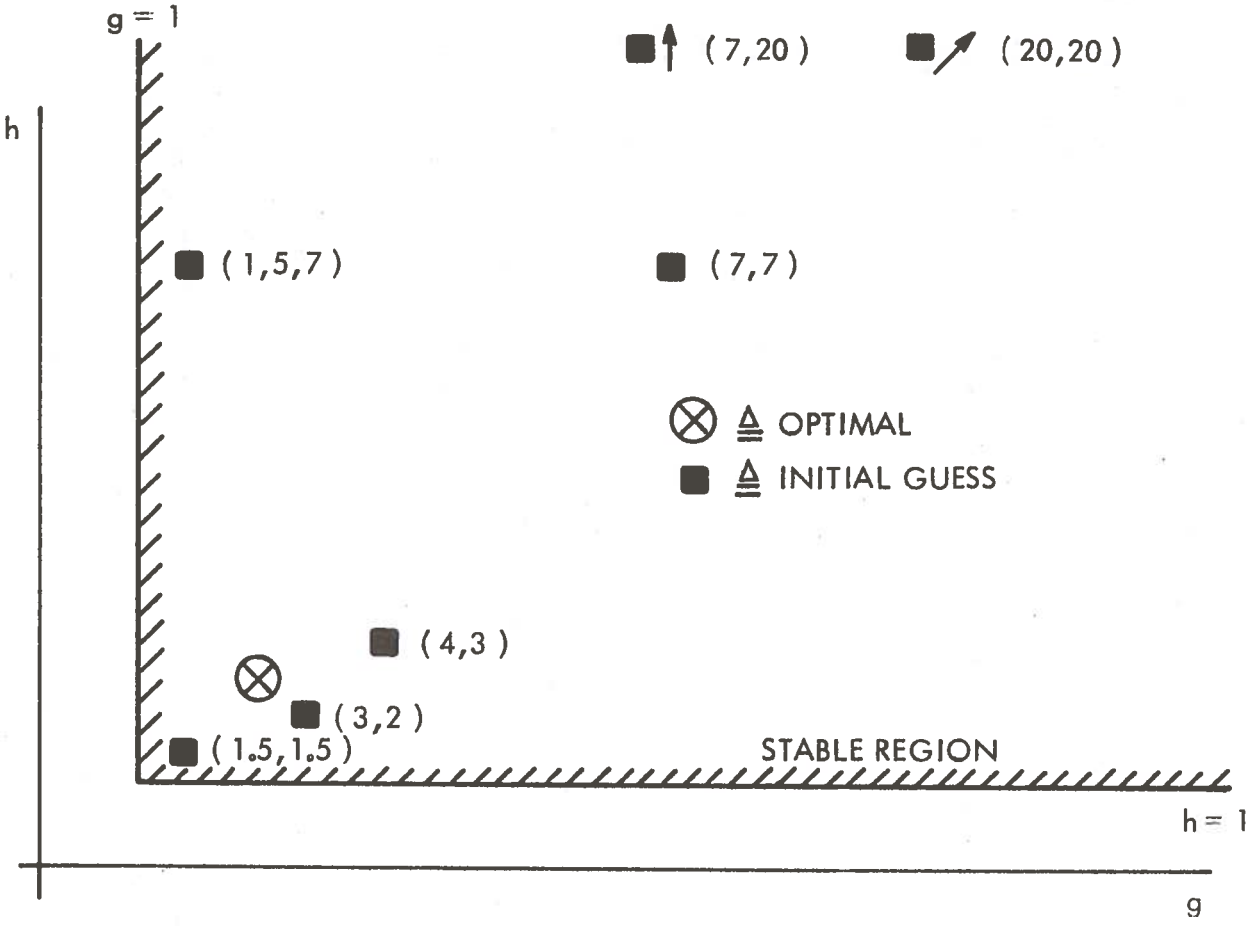

Figure 3.1 STABILITY REGION FOR EXAMPLE 3.4a

TABLE 3.1

SUMMARY OF RESULTS FOR THE ONE-DIMENSIONAL PROBLEM 3.4a

Initial Guess		Resulting Value		Cost	Iteration
g	h	g	h		
1.5	1.5	2.414232	2.414230	16.484241	4
3.0	2.0	2.4913101	2.3411570	16.485260	10*
4.0	3.0	2.550866	2.288164	16.485345	13
1.5	7.0	2.343572	2.489523	16.485266	15*
7.0	7.0	2.414219	2.414235	16.485254	4
7.0	20.0	D I D N O T C O N V E R G E			**
20.0	20.0	2.413993	2.414135	16.485271	4
OPTIMAL		2.414214	2.414214		

$$\begin{bmatrix} \dot{x}(t) \\ \dot{\hat{x}}(t) \end{bmatrix} = \begin{bmatrix} 1 & -g \\ h & f-g-h \end{bmatrix} \begin{bmatrix} x(t) \\ \hat{x}(t) \end{bmatrix} + \begin{bmatrix} 1 & 0 \\ 0 & h \end{bmatrix} \begin{bmatrix} \xi(t) \\ \theta(t) \end{bmatrix} . \tag{3.4.15}$$

Again, we restate the problem in the form of problem statement B:

$$\text{minimize} \quad J(\underline{\alpha}) = \text{tr} \begin{bmatrix} 1 & 0 \\ 0 & g^2 \end{bmatrix} \underline{\Sigma}\ (\underline{\alpha}), \tag{3.4.16}$$

subject to:

$$0 = \begin{bmatrix} 1 & -g \\ h & f-g-h \end{bmatrix} \underline{\Sigma}\ (\alpha) + \underline{\Sigma}\ (\alpha) \begin{bmatrix} 1 & h \\ -g & f-g-h \end{bmatrix} + \begin{bmatrix} 1 & 0 \\ 0 & h^2 \end{bmatrix}. \tag{3.4.17}$$

To solve the problem, we again need a stabilizing initial guess. Proceed as in problem (3.4.1), we find that the system (3.4.15) has the characteristic polynomial:

$$s^2 + (g+h-f-1)s + (f-g-h+gh) = 0, \tag{3.4.18}$$

which gives the requirements:

$$\begin{aligned} &g + h > f + 1, \\ &(g-1)(h-1) > 1-f, \end{aligned} \tag{3.4.19}$$

for system (3.4.15) to be stable. The stability regions for f=2, f=-1, and f=-4 are shown in figure 3.2. The stability region for f=1 is the same as in figure 3.1.

The interesting feature that can be observed from figure 3.2 is that there are two stable regions for f=-4. The second equation of (3.4.19) divide the g-h plane into three regions, two of which satisfy the inequality if f < 1 (see figure 3.3a). For f > -3, the line generated by the first equation of (3.4.19) does not intersect region (B) (see figure 3.3b). However, if f < -3, the line intersects region (B), and forms a second stable region (figure 3.3c)

The results for eight initial guesses are summarized in table 3.2. Two interesting problems have occurred. For the initial guess g = 20.0, h = 20.0, and f = 1.5, the DFP has stepped from one stable region to the other, then has interpolated between the two regions.

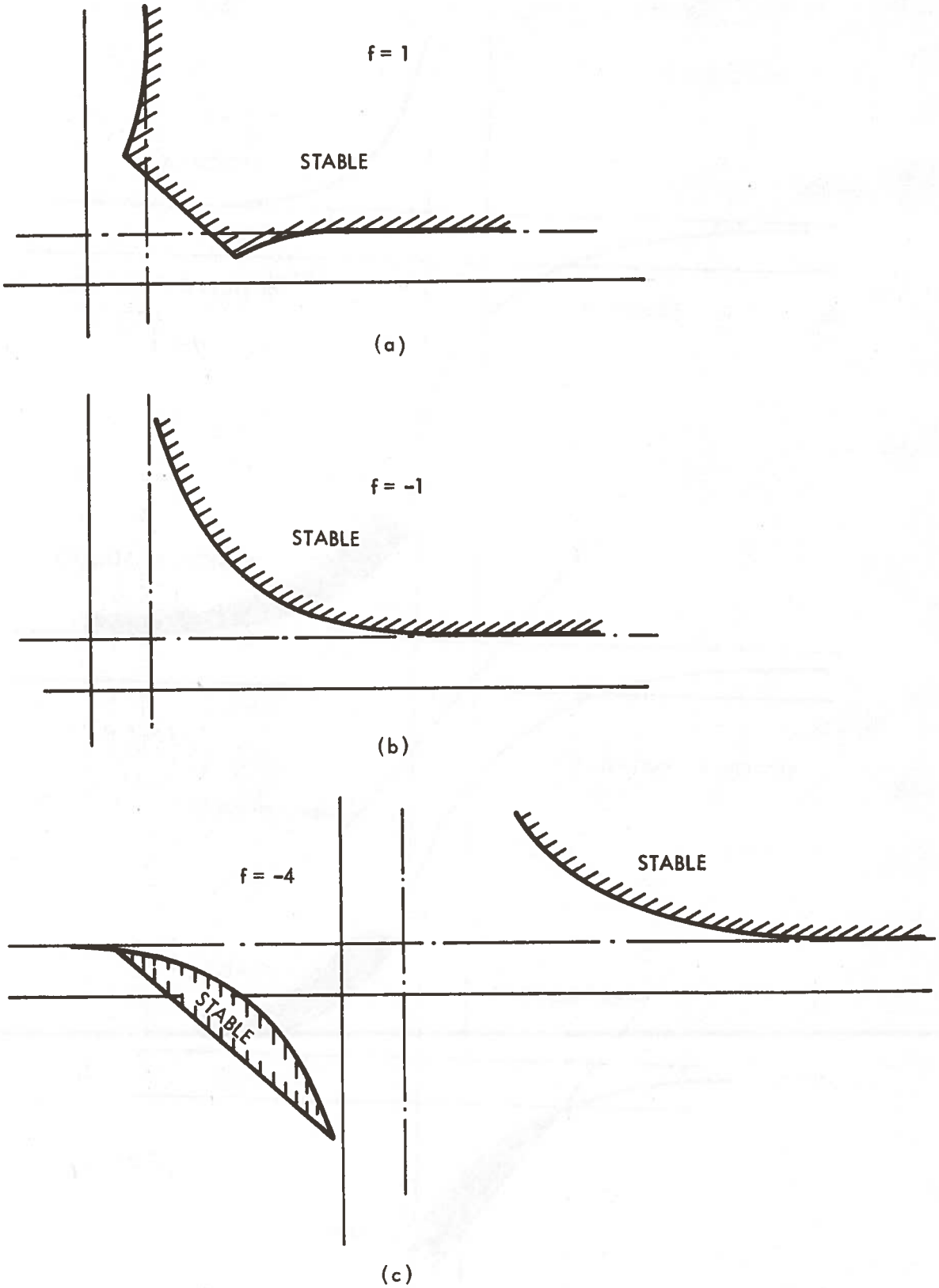

Figure 3.2 STABILITY REGIONS FOR THE ONE-DIMENSIONAL PROBLEM 3.4b

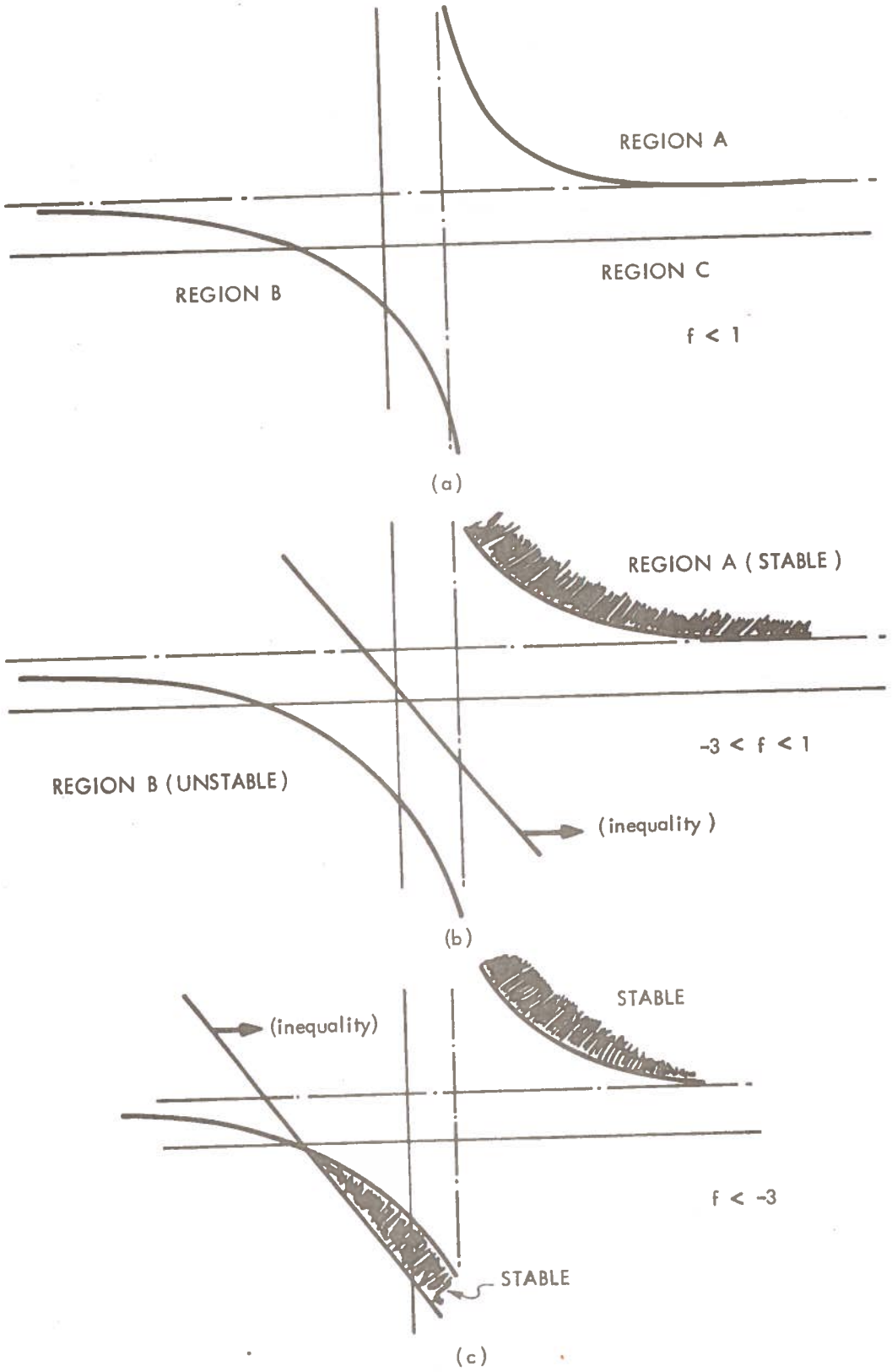

Figure 3.3 INTERACTION OF STABILITY INEQUALITIES FOR THE ONE-DIMENSIONAL PROBLEM 3.4b

TABLE 3.2

SUMMARY OF RESULTS FOR THE ONE-DIMENSIONAL PROBLEM 3.4b

Initial Guess			Resulting Value			Cost	Iteration
g	h	f	g	h	f		
..5	1.5	1.5	2.415746	2.415755	1.002979	16.485341	5
..5	2.5	1.5	2.139196	3.002152	.9610236	16.544185	3
:.0	3.0	1.5	3.192386	1.868619	1.173455	16.491242	3
).0	7.0	1.5	13.607823	.4283597	10.207073	16.485272	7
'.0	7.0	1.5	2.414417	2.414443	.999611	16.485271	6
).0	20.0	1.5	D I D N O T C O N V E R G E			*	
:.0	3.0	0.0	3.169702	1.838773	1.180188	16.485283	7
'.0	7.0	0.0	2.48561	2.485624	0.971772	16.514650	5
OPTIMAL			2.414214	2.414214	1.0		

The second problem is that there seems to be several points with the same minimum cost. To explain this, we rewrite the system as:

$$\begin{bmatrix} \dot{x}(t) \\ \dot{\hat{x}}(t) \end{bmatrix} = \begin{bmatrix} 1 & -g \\ h & f-g-h \end{bmatrix} \begin{bmatrix} x(t) \\ \hat{x}(t) \end{bmatrix} + \begin{bmatrix} 1 & 0 \\ 0 & h \end{bmatrix} \begin{bmatrix} \xi(t) \\ \theta(t) \end{bmatrix},$$

$$\underline{y}(t) = \begin{bmatrix} 1 & 0 \\ 0 & g \end{bmatrix} \begin{bmatrix} x(t) \\ \hat{x}(t) \end{bmatrix}, \qquad (3.4.20)$$

with the cost function:

$$J = E\{\lim_{T\to\infty} \frac{1}{T} \int_0^T \underline{y}(t')\underline{y}(t)\,dt\}. \qquad (3.4.21)$$

This problem is equivalent to problem (3.4.2).

The transfer function of system (3.4.20) is:

$$\underline{Y}(s) = \left[\begin{array}{cc|c} \frac{s-(f-g-h)}{(s-1)[s-(f-g-h)]+gh} & \frac{-gh}{(s-1)[s-(f-g-h)]+gh} & \Xi(s) \\ \hline \frac{gh}{(s-1)[s-(f-g-h)]+gh} & \frac{gh(s-1)}{(s-1)[s-(f-g-h)]+gh} & \Theta(s) \end{array}\right]. \qquad (3.4.22)$$

Examining (3.4.22), we find that the parameters appear in only two expressions (f-g-h) and (gh). Thus, any parameter combination which satisfies:

$$f - g - h = \gamma,$$
$$gh = \beta, \qquad (3.4.23)$$

will have the same input-output behavior, and hence, from equation (3.4.21) th same cost. Equations (3.4.23) describe a continuous curve in parameter space for each (β,γ) pair. Thus, there is not a unique solution, even locally, to problem (3.4.2). Table 3.3 compares the optimal β and γ with the results fron equation (3.4.2).

The two problems described above are problems that are likely to occur ir

TABLE 3.3

COMPARISON OF RESULTING SOLUTIONS

Resulting Value			Cost	$\gamma=f-g-h$	$\beta=gh$	Percent Deviation	
g	h	f				γ	β
2.414214*	2.414214*	1.0*		-3.828427	5.828427	0	0
2.415746	2.415755	1.002974	16.485341	-3.828527	5.835850	0.0026	0.127
2.139196	3.002152	0.9610236	16.544185	-4.180329	6.422192	9.19	10.2
3.192386	1.868619	1.173455	16.491242	-3.88755	5.965353	1.54	2.35
3.607823	0.4283597	10.207073	16.485272	-3.829110	5.829043	0.018	0.011
2.414417	2.414443	0.999611	16.485271	-3.829249	5.829472	0.021	0.018
3.169702	1.838773	1.180188	16.485283	-3.828287	5.828362	0.0037	0.0011
2.48561	2.485624	0.971772	16.51465	-3.999462	6.178292	4.47	6.0

* Optimal.

many situations. For this reason, they are discussed more generally in the following two sections.

3.5 Choosing the Parameters

Problem (3.4b) indicates that the solution of the decentralized design problem depends crucially on the choice of parameters. If a poor parameterization is made, the solution may not be unique. However, if the parameterization is made too cautiously, the controller may not behave as well as possible. Some guidelines for choosing parameters are needed.

The first problem is to define a "good" parameterization.

Definition 3.5.1:

The static-optimization problem (problem statement B) is identifiable from the cost if for every $\hat{\underline{\alpha}}$ which locally minimizes $J(\underline{\alpha})$, there exists an $\varepsilon > 0$, such that

$$\text{(i)} \quad ||\underline{\alpha} - \hat{\underline{\alpha}}|| < \varepsilon,$$

$$\text{(ii)} \quad J(\underline{\alpha}) = J(\underline{\alpha}),$$

imply $\alpha = \hat{\alpha}$.

It can be seen in the 2-dimensional example (3.4.2) that when the transfer function is not uniquely determined by the parameters, the static optimization problem is not identifiable from the cost. Identification of system parameters from the transfer function has been examined extensively by Glover [1973]. Using his definition:

Definition 3.5.2:

Let $(\underline{A},\underline{B},\underline{C})(\underline{\alpha})$*: $\Omega \subset R^q \to R^N$ $(N = n(n+m+p))$ be a parameterization of the system matrices (A,B,C) of a linear dynamical system. This parameterization is said to be locally identifiable (from the transfer function) at $\underline{\alpha} = \hat{\underline{\alpha}} \in \Omega$ if there exists an $\varepsilon > 0$, such that

$$\text{(i)} \quad ||\underline{\alpha} - \hat{\underline{\alpha}}|| < \varepsilon \quad ||\underline{\beta} - \hat{\underline{\alpha}}|| < \varepsilon, \ \underline{\alpha}, \underline{\beta} \in \Omega,$$

---

* A is nxn; B is nxm; C is pxn.

and

$$\text{(ii)}\quad \underline{C}(\alpha)\underline{A}^{k}(\alpha)\underline{B}(\alpha) = \underline{C}(\beta)\underline{A}^{k}(\beta)\underline{B}(\beta);\ k=0,1,2,\ldots,$$

imply $\underline{\alpha} = \underline{\beta}$.

We state the following proposition:

Proposition 3.5.1: Problem statement B of section (3.2) is identifiable with respect to cost only if the system $(\underline{A}(\alpha), \underline{L}(\alpha), \underline{C}(\alpha)$ where:

$$\underline{C}'(\alpha)\underline{C}(\alpha) = \underline{S}(\alpha),$$

$\underline{A}(\alpha)$ and $\underline{L}(\alpha)$ as given by equation (3.2.19),

is locally identifiable from the transfer function at every $\hat{\underline{\alpha}}$ which locally minimizes $J(\underline{\alpha})$.

Proof: Suppose $\underline{\alpha}$ is a local minimum of $J(\underline{\alpha})$.
Assume the system $(\underline{A}(\alpha), \underline{L}(\alpha), \underline{C}(\alpha))$ is not locally identifiable at $\hat{\underline{\alpha}}$. Then there exists a nonsingular matrix $\underline{P}$ and $\underline{\beta} \neq \hat{\underline{\alpha}}$, such that

$$\underline{A}(\hat{\underline{\alpha}}) = \underline{P}^{-1}\underline{A}(\beta)\underline{P}, \tag{3.5.1}$$

$$\underline{L}(\hat{\underline{\alpha}}) = \underline{P}^{-1}\underline{L}(\beta), \tag{3.5.2}$$

$$\underline{C}(\hat{\underline{\alpha}}) = \underline{C}(\beta)\underline{P} \quad \text{for all } \varepsilon > 0. \tag{3.5.3}$$

This implies (using (3.5.3) in (3.2.24)):

$$J(\hat{\underline{\alpha}}) = \mathrm{tr}\{\underline{S}(\hat{\underline{\alpha}})\ \underline{\Sigma}\ (\hat{\underline{\alpha}})\} = \mathrm{tr}\{\underline{P}'\underline{C}'(\beta)\underline{C}(\beta)\underline{P}\ \underline{\Sigma}\ (\hat{\underline{\alpha}})\}$$

$$= \mathrm{tr}\{\underline{C}'(\beta)\underline{C}(\beta)\underline{P}\ \underline{\Sigma}\ (\hat{\underline{\alpha}})\underline{P}'\}. \tag{3.5.4}$$

Now:

$$\underline{A}(\hat{\underline{\alpha}})\ \underline{\Sigma}\ (\hat{\underline{\alpha}}) + \underline{\Sigma}\ (\hat{\underline{\alpha}})\underline{A}'(\hat{\underline{\alpha}}) + \underline{L}(\hat{\underline{\alpha}})\ \underline{\Xi}\ \underline{L}'(\hat{\underline{\alpha}}) = 0. \tag{3.5.5}$$

Premultiplying by $\underline{P}$ and past-multiplying by $\underline{P}'$ we obtain

$$\underline{P}\ \underline{A}(\hat{\underline{\alpha}})\underline{P}^{-1}\underline{P}\ \underline{\Sigma}\ (\hat{\underline{\alpha}})\underline{P}' + \underline{P}\ \underline{\Sigma}\ (\hat{\underline{\alpha}})\underline{P}'(\underline{P}')^{-1}\underline{A}'(\hat{\underline{\alpha}})\underline{P}' + \underline{P}\ \underline{L}(\underline{\alpha})\ \underline{\Xi}\ \underline{L}'(\underline{\alpha})\underline{P}' = 0 \tag{3.5.6}$$

$$\Rightarrow \underline{A}(\underline{\beta})[\underline{P}\ \underline{\Sigma}\ (\hat{\underline{\alpha}})\underline{P}'] + [\underline{P}\ \underline{\Sigma}\ (\hat{\underline{\alpha}})\underline{P}']\underline{A}'(\underline{B}) + \underline{L}(\beta)\ \underline{\Xi}\ \underline{L}'(\beta) = 0. \tag{3.5.7}$$

Denoting:

$$\underline{\Sigma}\ (\underline{\beta}) = \underline{P}\ \underline{\Sigma}\ (\hat{\underline{\alpha}})\underline{P}'. \tag{3.5.8}$$

Hence:

$$J(\hat{\underline{\alpha}}) = tr\{\underline{C}'(\underline{\beta})\underline{C}(\underline{\beta})\ \underline{\Sigma}\ (\underline{\beta})\} = J(\underline{\beta}), \tag{3.5.9}$$

=> the problem is not identifiable with respect to cost.

This result however is not sufficient, as the following counterexample demonstrates:

Example 3.5.1: Consider the 1-dimensional 1-parameter system:

$$\left.\begin{aligned} &\dot{x}(t) = \alpha x(t) + \xi(t), \\ &E\{\xi(t)\,\xi(\tau)\} = \delta(t-\tau), \\ &\text{with: } J(\alpha) = E\{\lim_{T\to\infty} \frac{1}{T} \int_0^T \alpha x^2(t)\,dt\}. \end{aligned}\right\} \tag{3.5.10}$$

Reformulating in terms of problem statement B:

We obtain

$$J(\underline{\alpha}) = tr\{\underline{Q}(\underline{\alpha})\ \underline{\Sigma}\} = \alpha\,\sigma. \tag{3.5.11}$$

Thus,

$$-2\alpha\sigma + 1 = 0. \tag{3.5.12}$$

Which implies

$$\sigma = \frac{1}{2\alpha}. \tag{3.5.13}$$

Which results in

$$J(\alpha) = \alpha\,\frac{1}{2\alpha} = \frac{1}{2}, \tag{3.5.14}$$

for all α. Thus, the problem is not identifiable with respect to the cost alth it is identifiable from the transfer function:

$$X(s) = \frac{\alpha}{s+\alpha}\ \Xi(s). \tag{3.5.15}$$

If identifiability from the transfer function is a sufficient condition fo a parameterization to be identifiable from the cost, we may have several system

tests for the latter. Glover [1973] has developed two such tests for identifiability from the transfer function in terms of the determinant of a large matrix being non-zero. As we have seen in example 3.5.1, a parameterization satisfying these tests will not necessarily be identifiable from the cost. These tests can, however, give us some guideline for the initial parameterization. When used with physical reasoning and intuition, the tests can provide a reasonable choice of parameters.

3.6 Existence of Solutions

One of the problems encountered in section 3.4 is that the DFP algorithm stepped out of one stable region into an unstable region or another stable region. In this section, we will present a local existence result which will allow us to draw several conclusions concerning the behavior of the DFP algorithm.

The following theorem guarantees the existence of a local minimum to problem statement B with some slight restrictions. Then, the proposition shows that the restrictions are satisfied for a general class of problems.

Theorem 3.6.1: Consider the problem:

$$\text{minimize} \quad J(\underline{\alpha}) = \text{tr}\{\underline{S}(\underline{\alpha})\ \underline{\Sigma}\ (\underline{\alpha})\}, \tag{3.6.1}$$

$$\text{subject to} \quad \underline{A}(\underline{\alpha})\ \underline{\Sigma}\ (\underline{\alpha}) + \underline{\Sigma}\ (\underline{\alpha})\underline{A}'(\underline{\alpha}) + \underline{\Xi}(\underline{\alpha}) = \underline{0}.$$

Assume:

(a) $\lim_{||\underline{\alpha}||\to\infty} J(\underline{\alpha}) \to \infty$,

(b) $\text{Re}\{\lambda_i[\underline{A}(\underline{\alpha})]\} < 0 \quad \underline{\alpha} \in \mathcal{A} \subset R^q,\ i = 1,\ldots,n,$

(c) $\underline{A}(\underline{\alpha})$ is continuous and differentiable (i.e., C'), $\underline{\alpha} \in \mathcal{A}$,

(d) $\underline{\Xi}(\underline{\alpha})$ is C' $\underline{\alpha} \in \mathcal{A}$,

(e) $\underline{S}(\underline{\alpha})$ is C' $\underline{\alpha} \in \mathcal{A}$,

(f) $(\underline{A}(\underline{\alpha}), \sqrt{\underline{S}(\underline{\alpha})})$ is observable (where $\sqrt{\underline{S}(\underline{\alpha})}\ \sqrt{\underline{S}(\underline{\alpha})} \triangleq \underline{S}(\underline{\alpha})$),

(g) $(\underline{A}(\underline{\alpha}), \sqrt{\underline{\Xi}(\underline{\alpha})})$ is controllable.

Then, there exists a local minimum of $J(\underline{\alpha})$ on $\mathcal{A}$. Moreover,

$$\frac{\partial J(\underline{\alpha})}{\delta \underline{\alpha}} \text{ exists } \forall\, \underline{\alpha} \in \mathcal{A}. \tag{3.6.2}$$

Outline of Proof: The proof is in 3 steps. In step 1, we use a result by Mather [1973] to show that $J(\underline{\alpha})$ is C' on $\mathcal{A}$. Step 2 demonstrates that as $\underline{\alpha}$ leaves $\mathcal{A}$ the cost must go to infinity. Step 3 then summarizes the conclusions and completes the proof.

Proof: Step 1. Rewrite equation (3.6.2) as a linear equation parameterized by $\underline{\alpha}$.

$$\bar{\underline{A}}(\underline{\alpha})\ \underline{\Sigma}_v\ (\underline{\alpha}) = -\underline{\Xi}_v(\underline{\alpha}), \tag{3.6.3}$$

where:

$\bar{\underline{A}}(\underline{\alpha})$ ≡ expanded version of $\underline{A}(\underline{\alpha})$,

$\underline{\Sigma}_v(\underline{\alpha})$ row-wise vector of $\underline{\Sigma}\ (\underline{\alpha})$,

$\underline{\Xi}_v(\underline{\alpha})$ ≡ row-wise vector of $\underline{\Xi}(\underline{\alpha})$.

We can now apply an extended version of a theorem by Mather [1973]. The theorem states that if $M(\underline{\alpha})$ and $\underline{f}(\underline{\alpha})$ of the linear equation:

$$\underline{M}(\underline{\alpha})\underline{x}(\underline{\alpha}) = \underline{f}(\underline{\alpha}), \tag{3.6.4}$$

are continuous and differentiable for all $\underline{\alpha} \in \mathcal{A} \subset R^q$, then $\underline{x}(\underline{\alpha})$ is continuou and differentiable for all $\underline{\alpha} \in \mathcal{A} \subset R^q$. Since $\underline{A}(\underline{\alpha})$ and $\underline{\Xi}(\underline{\alpha})$ are C' for all $\underline{\alpha} \in \mathcal{A}$ (assumptions (c) and (d)), so are $\bar{\underline{A}}(\underline{\alpha})$ and $\underline{\Xi}_v\ (\underline{\alpha})$. Thus, by Mather's theorem, $\underline{\Sigma}_v(\underline{\alpha})$ and therefore $\underline{\Sigma}(\underline{\alpha})$ are C' for all $\alpha \in \mathcal{A}$. Since $\underline{S}\ (\underline{\alpha})$ is C' on $\mathcal{A}$ (assumption (e)) we can conclude that $J(\underline{\alpha})$ is C' on $\mathcal{A}$.

Step 2. Define $\partial\mathcal{A}$ to be the closure of $\mathcal{A}$; i.e.:

$$\partial\mathcal{A} = \{\underline{\alpha} \mid \text{Re}\,\lambda_i[A(\underline{\alpha})] = 0 \text{ for some } i \in [1,n]\}. \tag{3.6.5}$$

We now show that as $\underline{\alpha} \to \partial\mathcal{A}$ from within $\mathcal{A}$ the cost $J(\underline{\alpha})$ blows up; i.e., goes to infinity. Let $\underline{T}(\underline{\alpha})$ be such that:

$$\underline{T}(\underline{\alpha})\ \underline{A}(\underline{\alpha})\ \underline{T}^{-1}(\underline{\alpha}) = \begin{bmatrix} \underline{D}_1 & & 0 \\ & \ddots & \\ 0 & & \underline{D}_n \end{bmatrix},$$

where

$$\underline{D}_i = \begin{bmatrix} \lambda_i & 1 & & \\ 0 & \lambda_i & & 0 \\ & & \ddots & 1 \\ 0 & & & \lambda_i \end{bmatrix}.$$

Then (3.6.2) becomes:

$$(\underline{T}\underline{A}\underline{T}^{-1})(\underline{T}\underline{\Sigma}\underline{T}') + (\underline{T}\underline{\Sigma}\underline{T}')(TAT^{-1})' + \underline{T}\,\underline{\Xi}\,\underline{T}' = 0, \tag{3.6.6}$$

and (3.6.1) becomes:

$$J(\underline{\alpha}) = \mathrm{tr}\{(\underline{T}^{-1})'\underline{S}\,\underline{T}^{-1}(\underline{T}\underline{\Sigma}\underline{T}')\}, \tag{3.6.7}$$

where the explicit dependence on $\underline{\alpha}$ has been suppressed. To simplify (3.6.6) and (3.6.7), let us define,

$$\begin{aligned} \underline{A}_J &\triangleq TAT^{-1}, \\ \underline{\Sigma}_J &\triangleq \underline{T}\,\underline{\Sigma}\,\underline{T}' = [\sigma_{ij}], \\ S_J &\triangleq (\underline{T}^{-1})'\underline{S}\,\underline{T}^{-1}, \\ \underline{\Xi}_J &\triangleq \underline{T}\,\underline{\Xi}\,\underline{T}' \triangleq [\xi_{ij}]. \end{aligned} \tag{3.6.8}$$

We then obtain

$$\underline{A}_J\underline{\Sigma}_J + \underline{\Sigma}_J\underline{A}'_J + \underline{\Xi}_J = 0, \tag{3.6.9}$$

$$J(\underline{\alpha}) = \mathrm{tr}\,\{\underline{S}_J\,\underline{\Sigma}_J\}. \tag{3.6.10}$$

The solution to (3.6.7) if $\underline{A}_J$ is diagonal is:

$$\sigma_{ij} = \frac{-\xi_{ij}}{\lambda_i + \lambda_j}. \tag{3.6.11}$$

If $\underline{A}_J$ is not diagonal (the dimension of the largest Jordan block D_i is greater than 1), the solution σ_{ij} is still a linear function, L, of $\sigma_{(i-1)j}$, $\tau_{i(j-1)}$, and ξ_{ij}:

$$\sigma_{ij} = \frac{L(\sigma_{(i-1)j}, \sigma_{i(i-1)}) - \xi_{ij}}{\lambda_i + \lambda_j} . \qquad (3.6.12)$$

(For a more detailed derivation of (3.6.11) and (3.6.12), see Heinen [1971].

Consider now the behavior of the solutions as $\underline{\alpha}$ approaches $\delta\mathscr{A}$ from within $\mathscr{A}$. As $\underline{\alpha}$ approaches $\delta\mathscr{A}$, at least one eigenvalue, or one pair of eigenvalues (since $\underline{A}$ is real) must approach the imaginary axis in the left-half plane. Suppose λ_i is real, and $\lambda_i \to 0$. Since $(\underline{A}, \sqrt{\underline{\Xi}}$ is controllable with $\underline{\Xi} \geq \underline{0}$, the numerator of equation (3.6.11) (or (3.6.1a) if $\underline{A}_J$ is not diagonal) is non-zero. Thus, we see that

$$\lim_{\mathrm{Re}[\lambda_i]\to 0} \sigma_{ii} \to \infty. \qquad (3.6.13)$$

If λ_i and λ_j are conjugate pairs:

$$\lim_{\mathrm{Re}[\lambda_i,\lambda_j] \to 0} \sigma_{ij} \to \infty. \qquad (3.6.14)$$

Because $(\underline{A}, \sqrt{\underline{Q}})$ is observable with $\underline{Q} \geq \underline{0}$, equations (3.6.13) and (3.6.14) impl

$$\lim_{\underline{\alpha}\to\delta\mathscr{A}} J(\underline{\alpha}) \to \infty. \qquad (3.6.15)$$

Step 3. In step 1, we have shown that $J(\underline{\alpha})$ is C' on S. Step 2 has shown that $J(\underline{\alpha})$ approaches infinity as $\underline{\alpha}$ approaches the boundary of $\mathscr{A}$. By assumption (a we have that the cost approaches infinity as $||\underline{\alpha}||$ approaches infinity. Since the cost $J(\underline{\alpha})$ approaches infinity as $\underline{\alpha}$ approaches any possible edge of $\mathscr{A}$, and since $J(\underline{\alpha})$ is C' on $\mathscr{A}$, $J(\underline{\alpha})$ must attain a minimum (although not necessarily a unique minimum) on $\mathscr{A}$.

Proposition 3.6.1: Problem statement B with $\underline{G}$ and $\underline{H}$ as parameters (not $\underline{F}$) satisfies the assumptions (a) through (e) of theorem (3.6.1) if assumptions (f) and (g) hold.

Proof: (b)-(e) are trivial.

Consider the equivalent problem statement A:

$$\left.\begin{aligned} J(\underline{\alpha}) &= \lim_{T\to\infty} E\left\{\frac{1}{T}\int_0^T [\underline{x}(t)'\ \underline{Q}\ \underline{x}(t) + \underline{u}(t)'\ \underline{R}\ \underline{u}(t)]dt\right\}, \\ u(t) &= -G(\underline{\alpha})\ \hat{\underline{x}}(t). \end{aligned}\right\} \tag{3.6.16}$$

Since $\underline{R}$ is positive definite and of full rank, and because $E\{\hat{\underline{x}}(t)\ \hat{x}(t)\} > 0$, then

$$\lim_{||\underline{\alpha}_G||\to\infty} J(\underline{\alpha}) \to \infty,$$

where $\underline{\alpha}_G \equiv$ parameters associated with $\underline{G}$. Similarly, applying the triangular inequality to (3.6.2):

$$2||\underline{A}(\underline{\alpha})\ \underline{\Sigma}(\underline{\alpha})|| \geq ||\ \underline{\Xi}(\underline{\alpha})||,$$

and therefore:

$$||\underline{\Sigma}(\underline{\alpha})|| > \frac{||\underline{\Xi}\ (\underline{\alpha})||}{2||\underline{A}\ (\underline{\alpha})||}. \tag{3.6.17}$$

Taking the limit:

$$\lim_{||\underline{\alpha}_H||\to\infty} ||\underline{\Sigma}(\underline{\alpha})|| \to \infty. \tag{3.6.18}$$

Since $(\underline{A}(\underline{\alpha}), \sqrt{\underline{Q}(\underline{\alpha})})$ is observable:

$$\lim_{||\underline{\alpha}_H||\to\infty} J(\underline{\alpha}) \to \infty, \tag{3.6.19}$$

From (3.6.19) and (3.6.16), we can conclude that assumption (a) holds.

From the theorem and proposition presented in this section, we can conclude that the reason the DFP has left the region of stability is that the stepsize is too large. The problem is not caused by a low cost along the border of the region. Therefore, we can hope to remedy the problem by reducing the stepsize. However, this solution must be used cautiously since the convergence of the algorithm slows down as the stepsize is reduced.

4. IMPLEMENTATION OF THE DECENTRALIZED CONTROL ALGORITHM

4.1 Introduction

Section 3 has developed a promising algorithm for the decentralized control of large-scale systems. This section evaluates the algorithm for the freeway-corridor control problem which is presented and solved for the centralized case in section 2.

Section 4.2 discusses the corridor structure and philosophy for choosing the structure of the decentralized controller. Section 4.3 contains the actual corridor to which the algorithm is applied. The results are presented and discussed in section 4.4.

4.2 Corridor and Controller Structure

The freeway-corridor structure is the same as in section 2.2. The corridor consists of a main freeway and one or more parallel arterials. All roadways (freeway or arterial) are sectioned into links according to the topography of the corridor. The dynamics of the corridor are governed by equations (2.2.1) to (2.2.3) with the state variables being the spatial aggregate density and velocity on each link. The controls that are available for the corridor are the flows on the ramps which connect the roadways.

Since we are interested in applying the decentralized control algorithm developed in section 3, we must separate the states, controls, and observations into subgroups which will define subsystems, each of which will be controlled by a different controller. Then, it must be decided which variables each controller will be allowed to communicate to other controllers.

One way of choosing the subsystems is to use the centralized feedback and Kalman gains as guidelines. The gains can be used to determine which states are important to the controls and estimates of the other states. Suppose that the (i,j)th element of the feedback gain $\underline{G}_0$ is several orders of magnitude smaller than the other elements of the ith row of $\underline{G}_0$, and that the standard deviations of the states are approximately the same size. Then, it is reasonable to assume that the elimination of state j would have little effect o

input i. In this manner, we can decide which states are most important in determining the individual controls. The extended Kalman gain matrix $\underline{H}$ can be used in a similar manner to determine which outputs are important to the individual state estimates.

Since the inputs and outputs are distributed along the freeway corridor, they can easily be associated with states of the corridor. The states are grouped according to their mutual importance, and the separation of the subsystems can be chosen to coincide with any natural points of weak coupling that may occur.

Often, the natural points of weak coupling will not occur as close together as we like. In these cases, there may be too many states for one controller to handle, or the physical distance over which the controller must communicate will be too large. The system then must be separated at points where the filter and feedback gain matrices are smallest even though the effects of the interconnections are not necessarily small. Thus, a tradeoff must be made between the size of subsystems and the performance of the decentralized controllers. If no points of weak coupling occur within a subsystem which is too large, dividing the subsystem into two or more smaller controllers may degrade the decentralized control system performance. The two designs must be evaluated, and a judgment made as to whether smaller controller size (and hence, less communication) or better system performance is more important.

Once the system has been decomposed into its individually controlled subsystems, the structure of the communicated variables must be fixed. We recall the linearized decentralized filter equation:

$$\dot{\underline{\hat{x}}}_i(t) = \underline{F}_{ii}\underline{\hat{x}}_i(t) + \sum_{j\neq i} \underline{F}_{ij}\underline{\hat{x}}_j(t) + \underline{B}_i\underline{u}_i(t) + \underline{H}_i[\underline{y}_i(t) - \underline{C}_i\underline{\hat{x}}_i(t)]. \tag{4.2.1}$$

We note that for this particular filter structure (on which the analysis of section 3 is based) allows only communication of estimates of the controllers. This communication can be restricted by specifying the structure of the $\underline{F}_{ij}$ matrices.

One way to choose the structure of the $\underline{F}_{ij}$'s is to note which state variables are "communicated" internally through the system dynamics; i.e., which states are naturally coupled across the borders of the subsystems. The $\underline{F}_{ij}$ matrices can be chosen to duplicate the internal coupling of the system, and thus, closely approximate the dynamics.

The manner in which the subsystems are fixed, and the communication structure is chosen is closely analogous to the reasoning (see section 2.3) behind the use of the extended Kalman filter. The communication structure is picked to duplicate (as closely as possible) the linearized dynamics in the propagation portion of the filter equation (4.2.1). The system is separated into subsystems in such a way so that as little information as possible is lost through the elimination of the off-diagonal terms in the filter gain matrix $\underline{H}$ and the feedback gain matrix $\underline{G}$.

A schematic diagram of the implementation of the decentralized control system is shown in figure 4.1. The measurements are made on each subsystem and are communicated to the respective controller. Each controller updates its estimates from its observations and communicates its estimate to the appropriate set of the other controllers. At the same time, it is receiving estimates from other controllers, and using these to propagate its own state estimates and construct its own controls.

4.3 A Specific Corridor Structure

In this section, we will consider a specific freeway-corridor structure to which we will apply the methods described in section 3. Since our ultimate goal is to compare the centralized and decentralized controller designs, we will use the same corridor and experiment as are used in section 2.4.

The corridor consists of a main freeway with a static capacity of 6220 vehicles/hour and a secondary parallel freeway with a capacity of 2075 vehicles/hour (see figure 2.3). The driver-behavior constants, noise statistics, and the penalty matrices $\underline{S}_1$ and $\underline{S}_2$ are repeated in table 4.1 for convenience.

The first problem to be faced is how to choose the decentralized structur[illegible] Following the discussion of section 4.2, we examine the feedback gain [illegible]

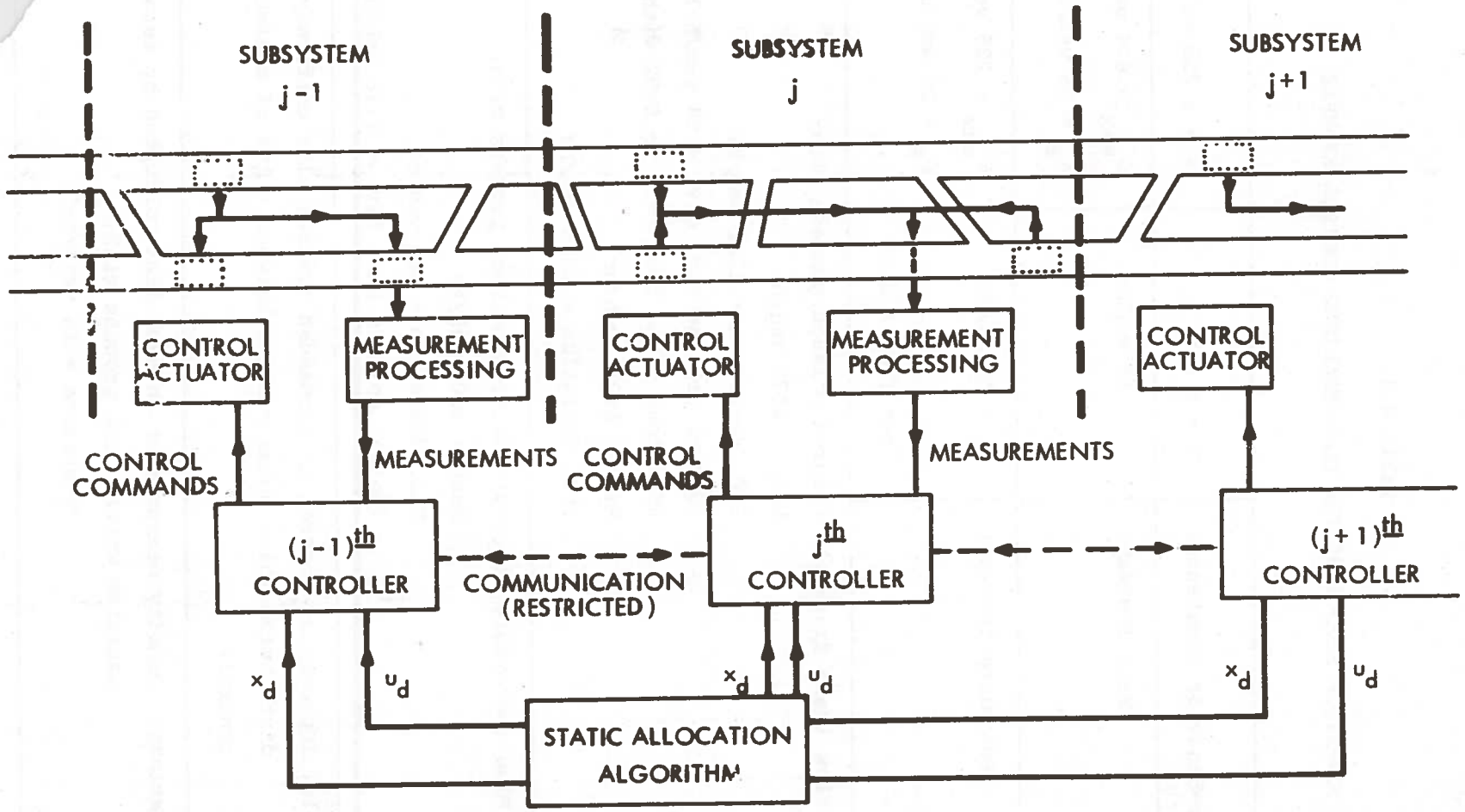

Figure 4.1 STRUCTURE OF DECENTRALIZED CONTROLLER FOR GENERAL FREEWAY CORRIDOR

Table 4.1

CORRIDOR STRUCTURE FOR DECENTRALIZED CONTROL EXAMPLE

Driver-Behavior Constants:	T = 5 sec	$\nu = 9.735\ mi^2/hr$
Main freeway:	$v_0 = 55$ mi/hr	$\rho_{max} = 674$ veh/mi $\rho_B = 75$ veh/mi
Secondary freeway:	$v_0 = 55$ mi/hr (see figure 2.4)	$\rho_{max} = 225$ veh/mi $\rho_B = 25$ veh/mi
Input Flow (Main freeway):	Colored poisson process with: Mean = 4077 veh/hr Std. deviation = 1211 veh/hr (Normal poisson std. dev. = 64 veh/hr) 40 second pulse from t=12 to t=52 with: Mean = 14270 veh/hr Std. deviation = 2266 veh/hr	
Input Flow (secondary freeway):	Colored poisson process with: Mean = 1000 veh/hr Std. deviation = 600 veh/hr (Normal poisson std. dev. = 3.16 veh/hr)	
Controls:	Implemented control is commanded control plus uniformly distributed white noise process between $\pm$ 10% of maximum control.	
Observations:	Density measurement on each link corrupted by zero mean Gaussian white noise process with: Covariance = 16 veh^2/hr^2	

the extended Kalman filter gain $\underline{H}$ that are found in the centralized solution[1] (see Appendix B).

We can see by examining $\underline{G}_0$ and $\underline{H}$ that all the couplings are approximately the same strength. By examining the relative magnitudes of the gain matrices, we note that observations and controls from adjacent links have a decreasing weighting by about one order of magnitude per link of spatial separation. Thus, it appears that all reasonable partitions will be approximately equivalent from the analysis of the gain matrix.

Since the gain matrices do not give much insight into the choice of a decentralized structure, we must use the topography of the corridor as a guide. Because we are trying to design a decentralized control system, we obviously want the two controls that are available to be generated from separate control "stations". Therefore, we will separate the system into two subsystems (see figure 4.2), with links 1 and 4 being assigned to controller A, and links 5 and 6 assigned to controller B.

The next step is to decide which state estimates to allow the controller to communicate. By examining the matrix $\underline{A}_0$ (Appendix B), we notice that the only coupling between subsystems A and B are:

(a) density on link 3 to density equation for link 5,

(b) velocity on link 3 to density equation and velocity equation for link 5,

(c) density on link 4 to density equation for link 6,

(d) velocity on link 4 to density-and-velocity equations for link 6,

(e) density on link 5 to velocity equation for link 3,

(f) density on link 6 to velocity equation for link 4.

If we allow the communication (see figure 4.2),

(1) Controller A transmits its estimates of density and velocity on

---

[1] If the linear Kalman filter is used, the appropriate gain is obviously the linear Kalman gain matrix $\underline{H}_0$. Also, if the extended Kalman gain matrix $\underline{H}$ has not reached a steady-state condition, the linear gain $\underline{H}_0$ can be used in place of $\underline{H}$.

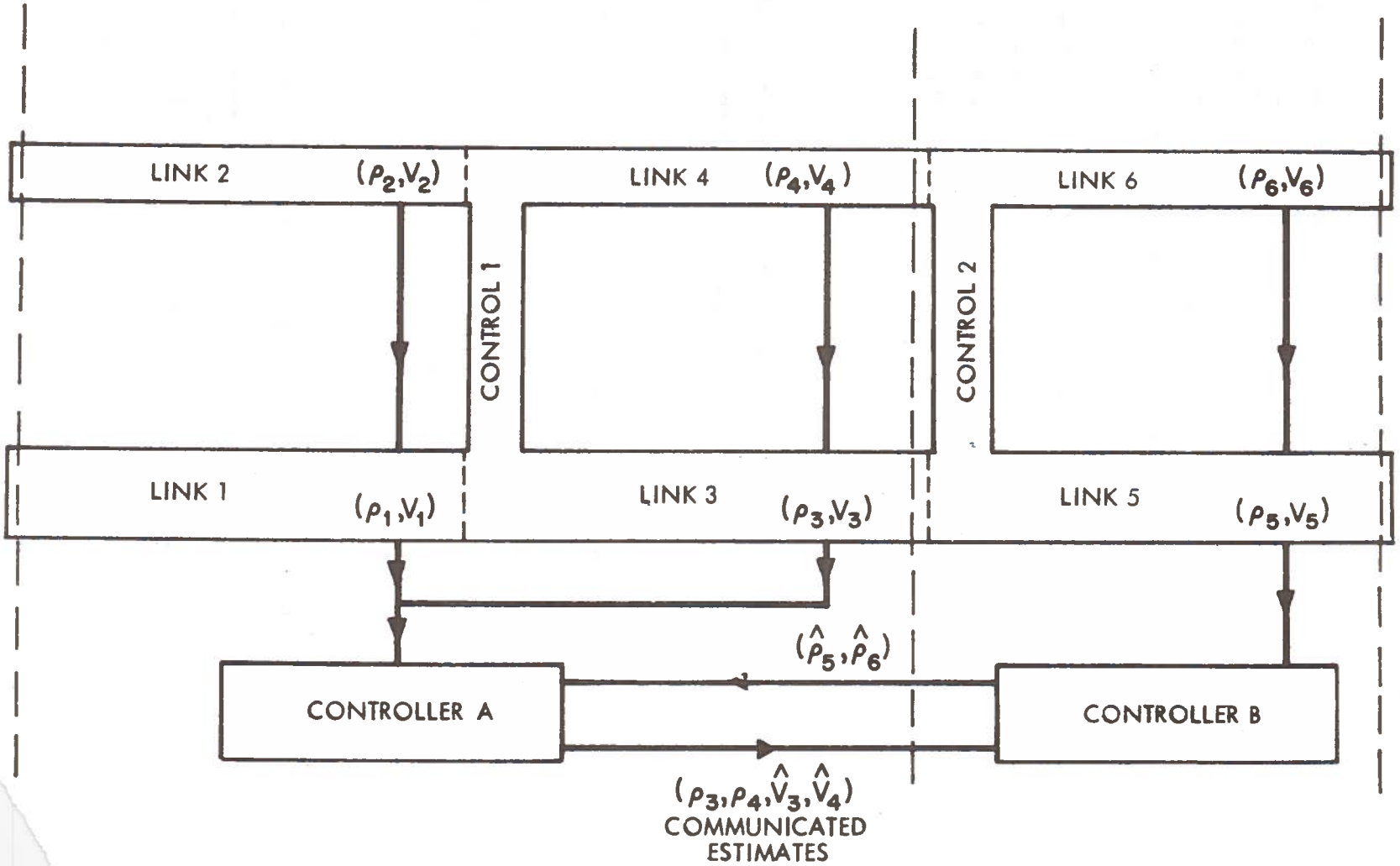

Figure 4.2 STRUCTURE OF DECENTRALIZED CONTROLLER FOR EXAMPLE

link 3 ($\hat{\rho}_3$,$\hat{v}_3$) and its estimates of density and velocity on link 4 ($\hat{\rho}_4$,$\hat{v}_4$) to controller B,

(2) Controller B transmits its estimates of density on link 5 ($\hat{\rho}_5$) and density on link 6 ($\hat{\rho}_6$) to controller A,

we can choose $\underline{F} = \underline{A}_0$, and thus, propagate the exact linearized dynamics of the system in the estimates for each controller.

By restricting the information transmitted between controllers to the communications described in (1) and (2) (the estimates of the variables (a) to (f) which couple the two controllers), the need to communicate the other six state variables (especially the states associated with links 1 and 2) over longer distances is eliminated. The advantage to this restriction is not very dramatic for this small example. However, the communication requirements will only grow linearly with the number of controllers in the system (assuming the controllers remain about the same size). When compared with the much more rapid growth in communication requirements for a centralized controller, the advantage becomes much more apparent.

We can now formulate the problem in terms of problem statement B of section 3.2:

$$\text{minimize: } J(\underline{\alpha}) = \text{tr}\{\underline{S}(\underline{\alpha})\underline{\Sigma}(\underline{\alpha})\},$$

$$\text{subject to: } 0 = \underline{A}(\underline{\alpha})\underline{\Sigma}(\underline{\alpha}) + \underline{\Sigma}(\underline{\alpha})\underline{A}(\underline{\alpha}) + \underline{\Xi}(\underline{\alpha}), \qquad (4.3.1)$$

where:

$$\underline{S}(\underline{\alpha}) = \begin{bmatrix} \underline{S}_1 & \underline{0} \\ \underline{0} & \underline{G}_D'\underline{S}_2\underline{G}_D \end{bmatrix},$$

$$\underline{A}(\underline{\alpha}) = \begin{bmatrix} \underline{A}_0 & -\underline{B}_0\underline{G}_D \\ \underline{H}_D\underline{C}_0 & \underline{F}-\underline{B}_0\underline{G}_D-\underline{H}_D\underline{C}_0 \end{bmatrix},$$

$$\underline{\Xi}(\underline{\alpha}) = \begin{bmatrix} \underline{Q} & \underline{0} \\ \underline{0} & \underline{H}_D\underline{R}\underline{H}_D' \end{bmatrix},$$

Ξ linearized system matrix given in Appendix B,

$\underline{B}_0 \equiv$ linearized input matrix given in Appendix B,

$C_0 \equiv$ observation matrix given in Appendix B,

$\underline{S}_1 \equiv$ state penalty matrix (table 4.1),

$\underline{S}_2 \equiv$ input penalty matrix (table 4.1),

$R \equiv$ observation noise spectral density (table 4.1),

$Q \equiv$ process noise spectral density derived from the input noise sources (table 4.1),

$\underline{F}=\underline{A}_0$ since the communication structure as fixed above allow this choice,

$\underline{G}_D \equiv$ decentralized feedback gain matrix (locations of non-zero elements fixed),

$\underline{H}_D \equiv$ decentralized filter gain matrix (locations of non-zero elements fixed),

$\underline{\alpha} \equiv$ vector of non-zero elements of $\underline{G}_D$ and $\underline{H}_D$.

With this formulation, we can apply the method described in section 3.3 to solve for the decentralized feedback gain $\underline{G}_D$ and decentralized filter gain $\underline{H}_D$. The resulting matrices can be found in Appendix C. Table 4.2 gives the requirements of the algorithm for this problem along with a comparison of the initial and final costs to the optimal costs $J^*(\underline{\alpha})$ using the full feedback and Kalman gains.

4.4 Decentralized Control Example

This section will use the gains developed in section 4.3 (Appendix C) to implement the decentralized control structure shown in figure 4.2 The same experiment that is performed in section 2.4 (see tables 2.1 and 2.2) with the centralized controller is performed in this section with the decentralized controller.

The resulting graphs for the freeway can be found in figures 4.3 to

Table 4.2

REQUIREMENTS FOR SOLUTION OF STATIC OPTIMIZATION PROBLEM

Dimension of system:	12 states
Dimension of filter:	12 states
Number of controls:	2
Number of observations:	6
Number of controllers:	2*
Parameterization:	Gain and filter matrices for both controllers: 12 control gain parameters 20 filter gain parameters
Total	32 parameters
Computer storage:	325 kilobytes
Iteration:	3**
Gradient evaluation:	7**
CPU Time:	0.5-0.75 minutes**
Optimal cost:	1952.9661
Cost of initial guess:	2332.6114
Percent increase over optimal:	19.4
Cost of results:	2159.7843
Percent increase over optimal:	10.6

* See Figure 4.2.

** The program has continued for 5 more iterations (25 total gradient evaluations). The reduction in cost over thse 5 iterations is less than 0.0025 percent.

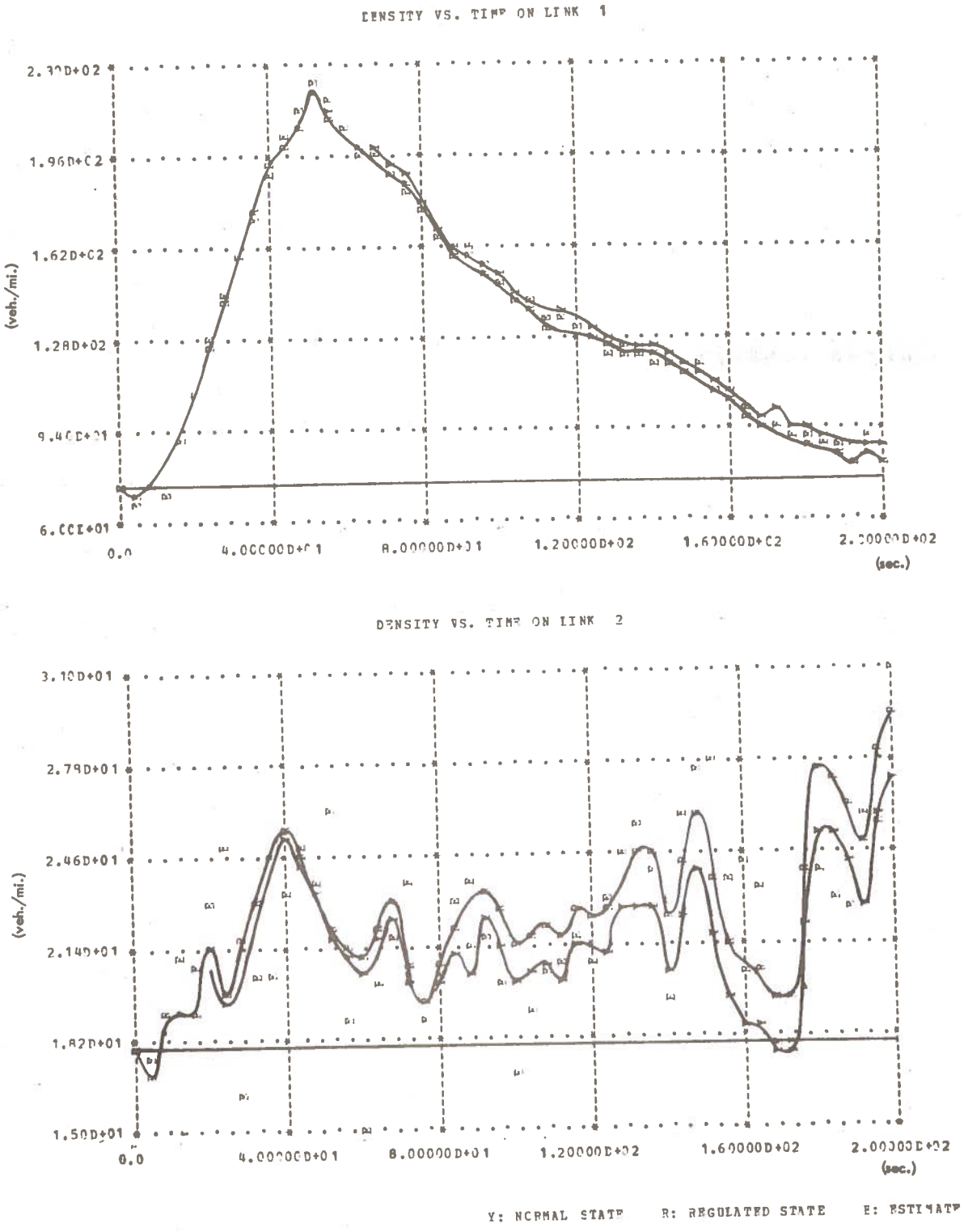

Figure 4.3 DECENTRALIZED CONTROL SYSTEM RESULTS FOR EXAMPLE (DENSITY) (LINKS 1 and 2)

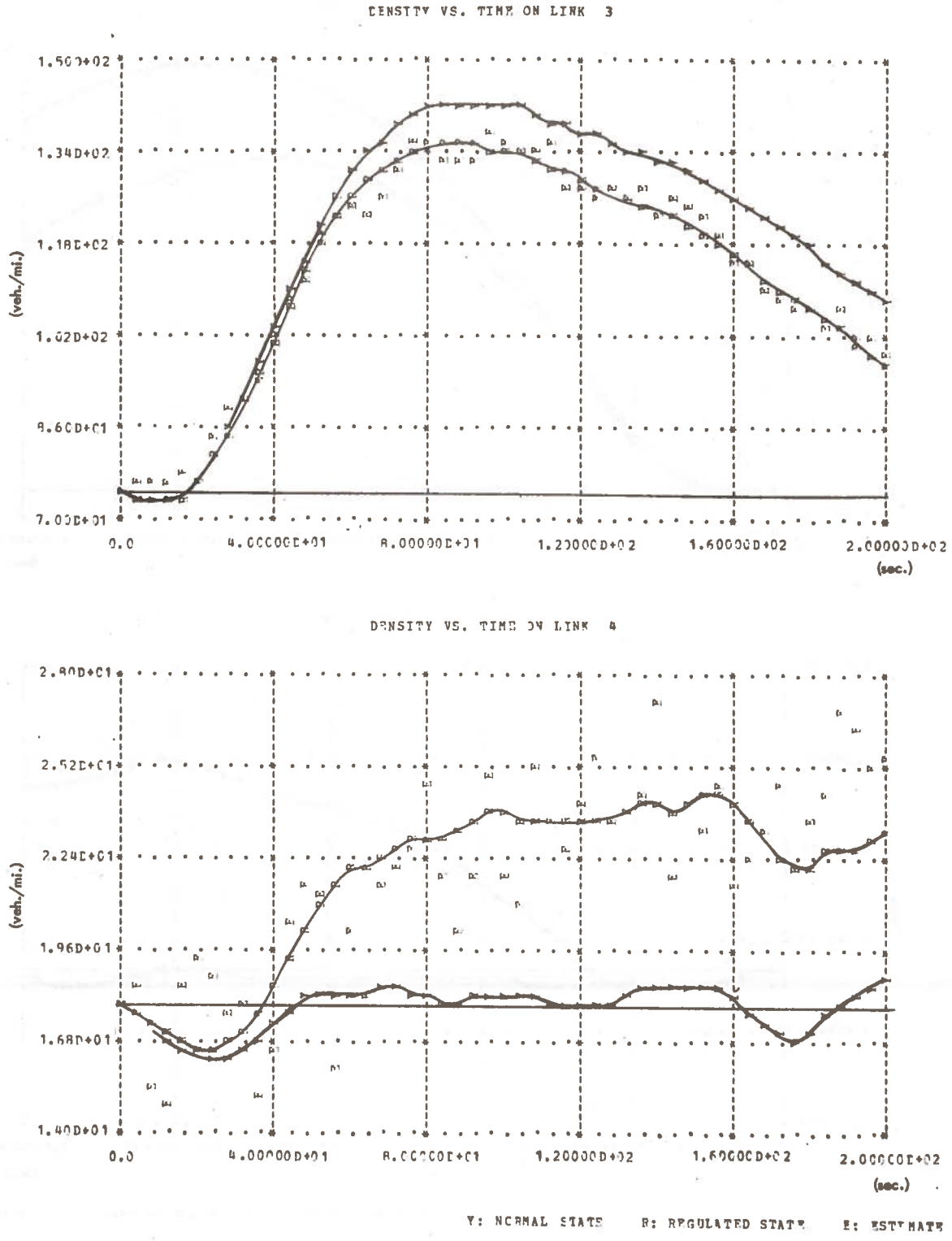

Figure 4.4 DECENTRALIZED CONTROL SYSTEM RESULTS FOR EXAMPLE (DENSITY) (LINKS 3 and 4)

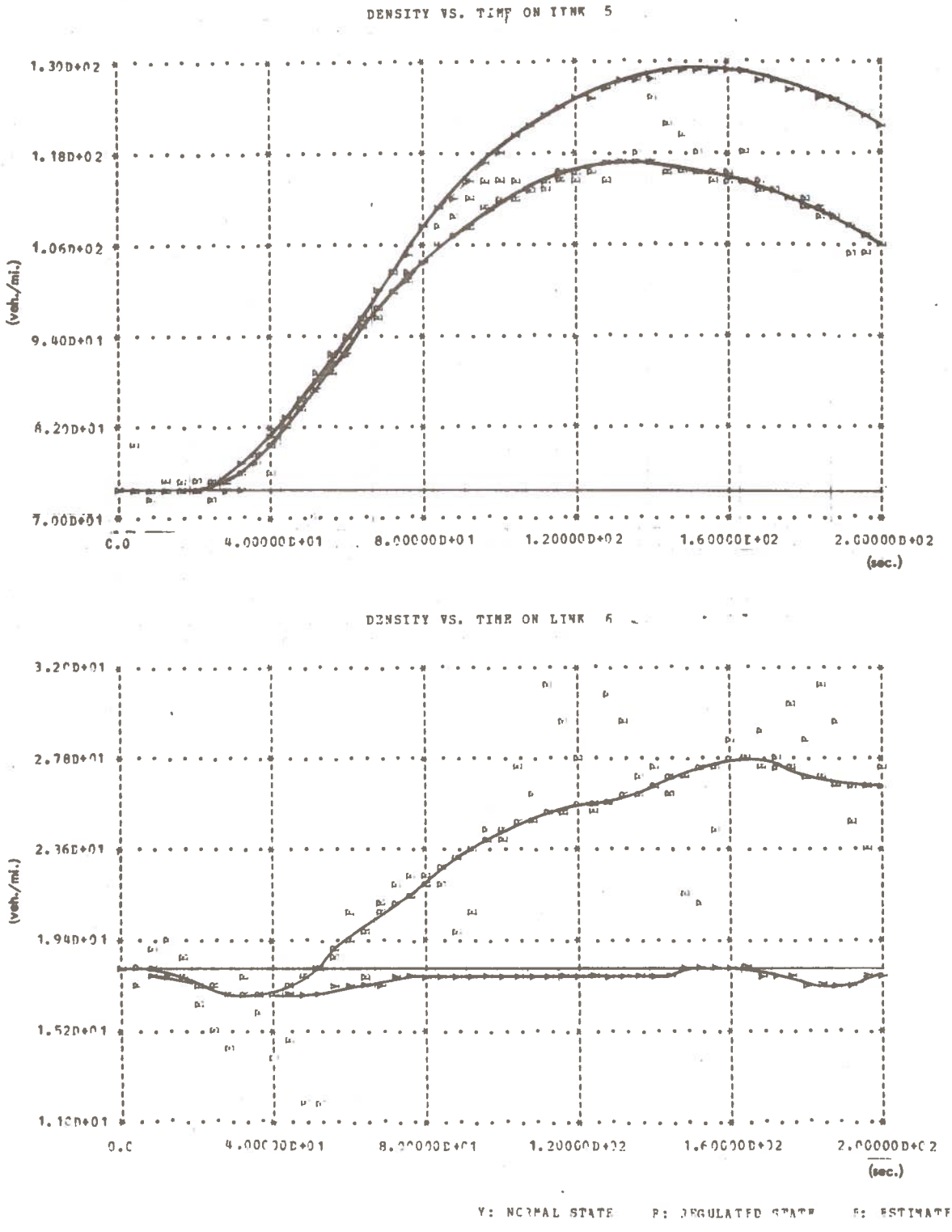

Figure 4.5 DECENTRALIZED CONTROL SYSTEM RESULTS FOR EXAMPLE (DENSITY) (LINKS 5 and 6)

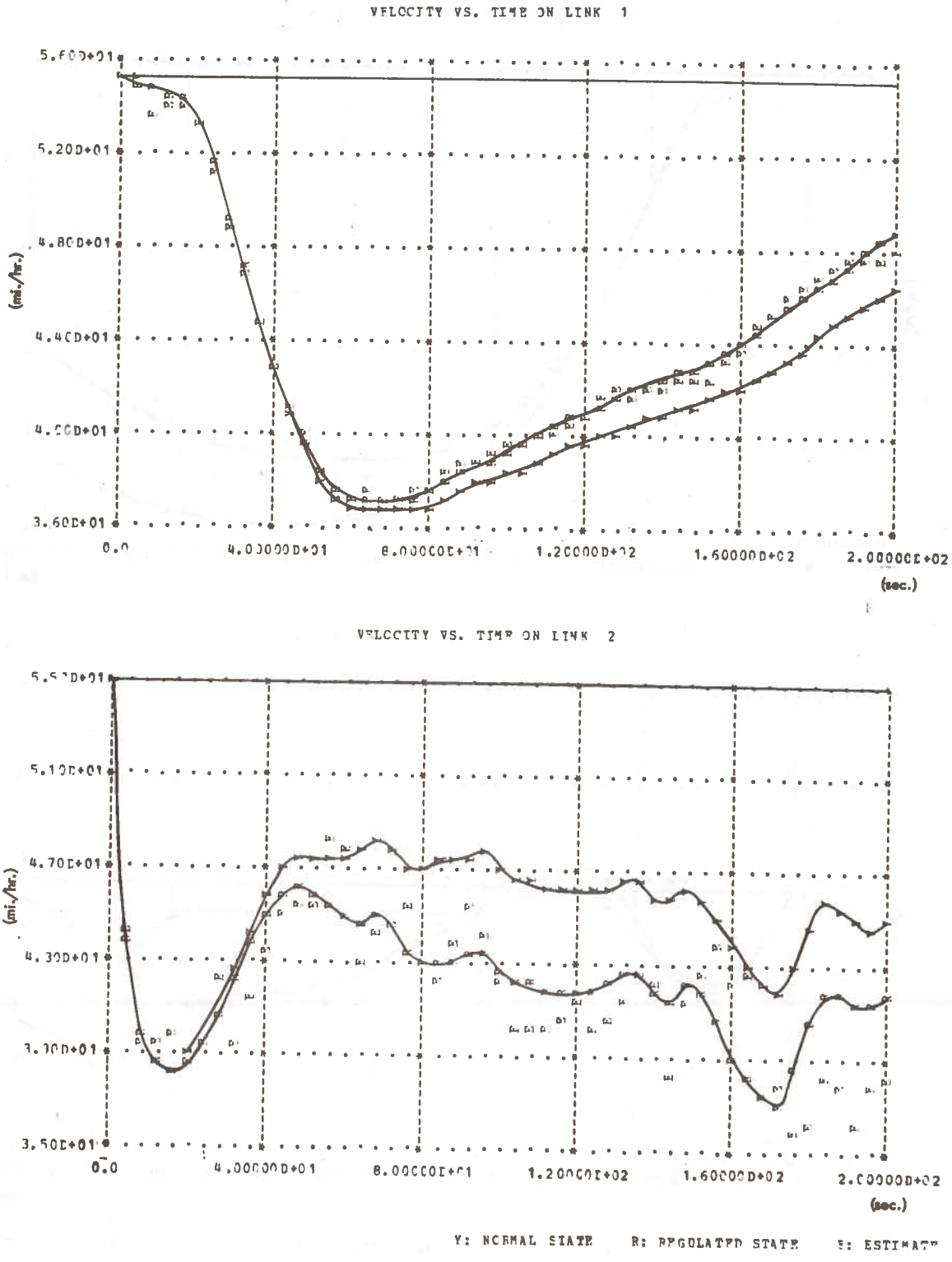

Figure 4.6 DECENTRALIZED CONTROL SYSTEM RESULTS FOR EXAMPLE (VELOCITY) (LINKS 1 and 2)

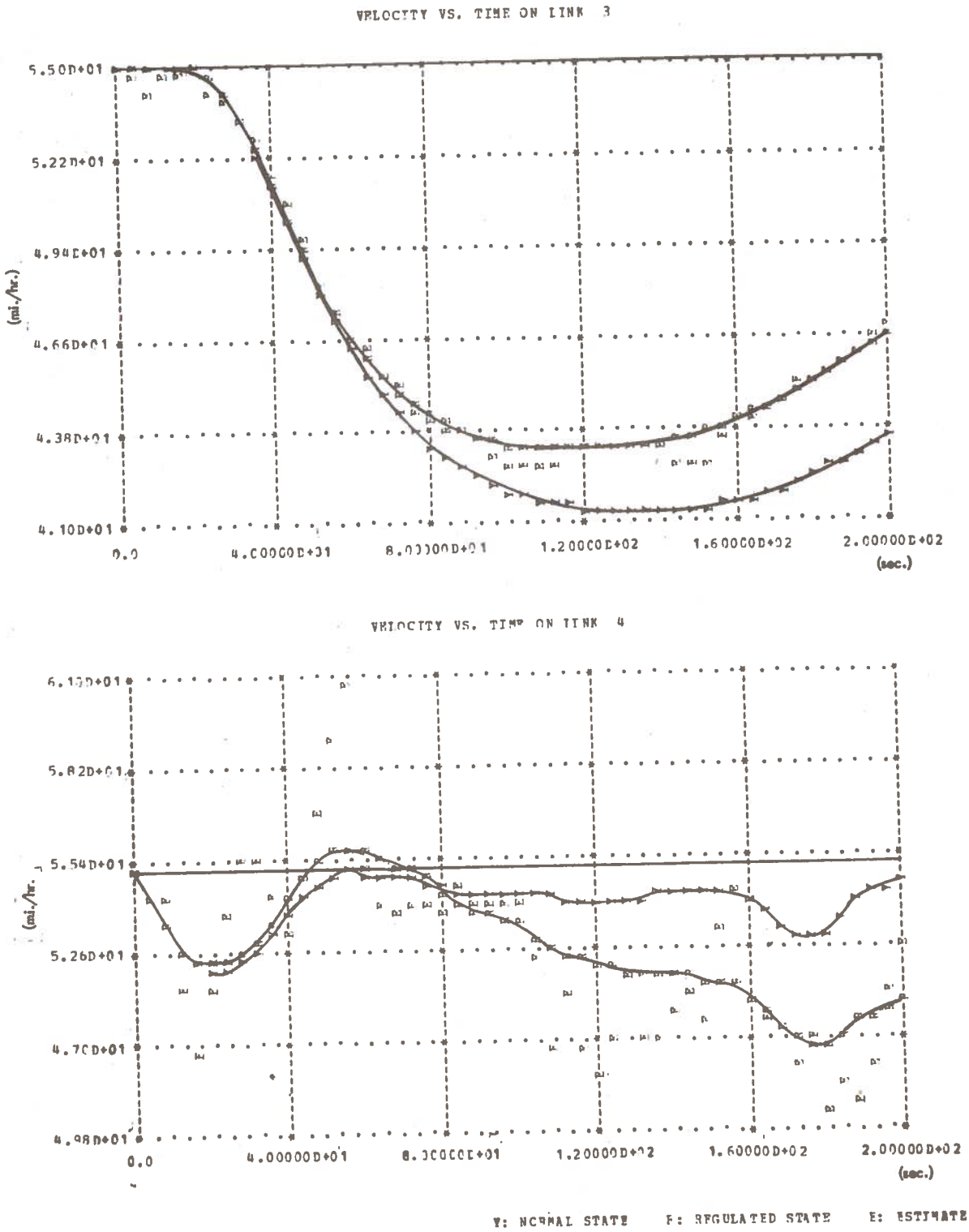

Figure 4.7 DECENTRALIZED CONTROL SYSTEM RESULTS FOR EXAMPLE (VELOCITY) (LINKS 3 and 4)

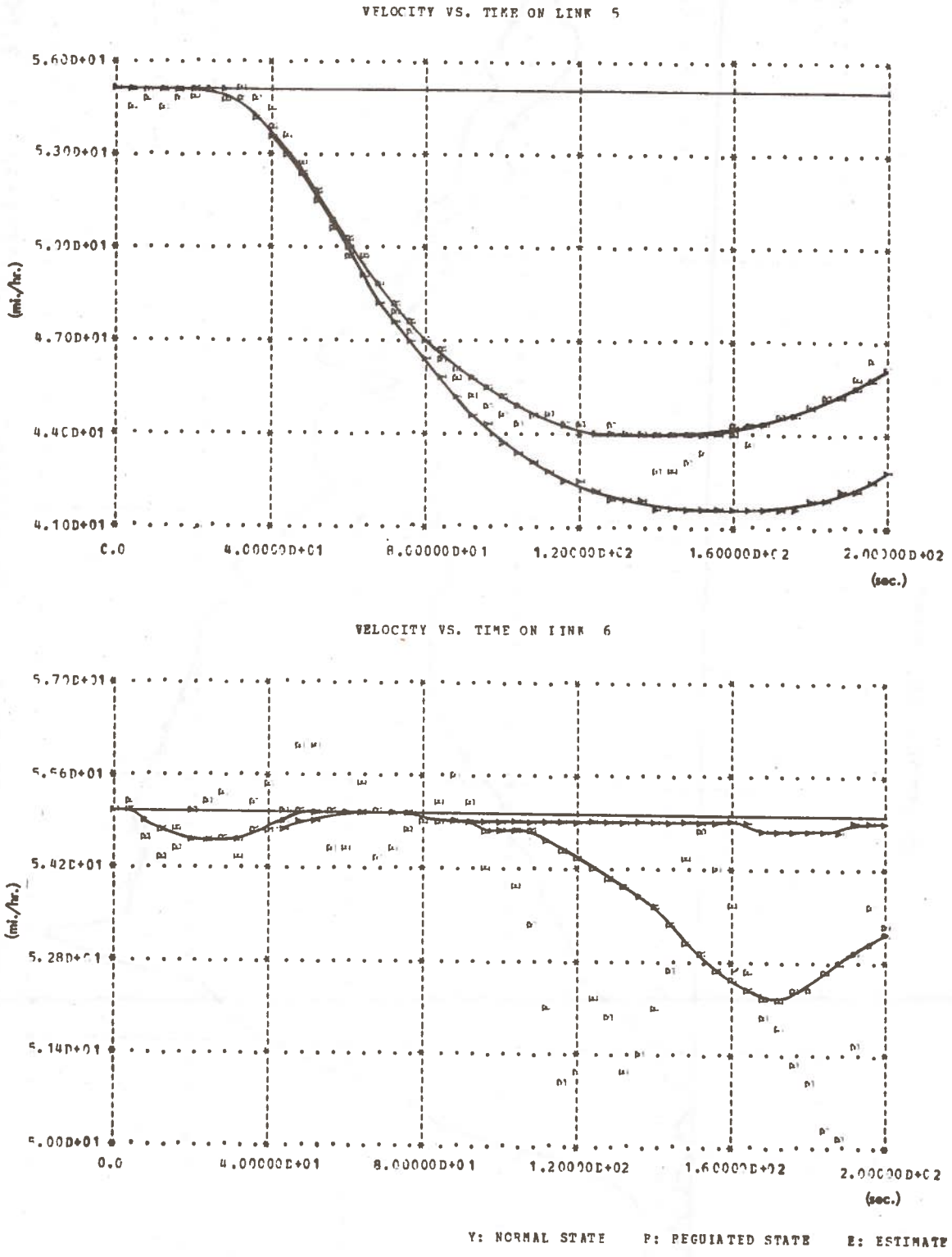

Figure 4.8 DECENTRALIZED CONTROL SYSTEM RESULTS FOR EXAMPLE (VELOCITY) (LINKS 5 and 6)

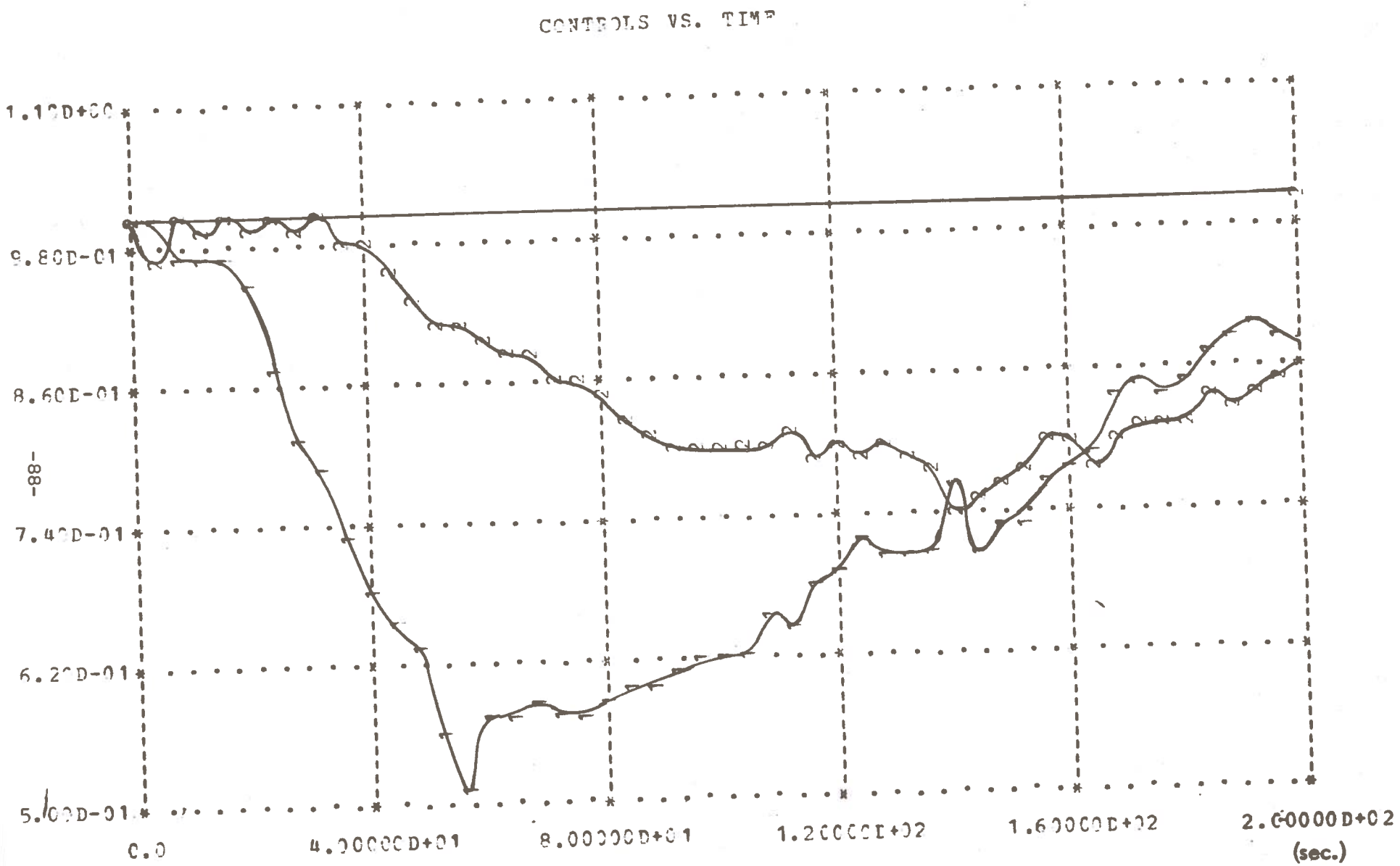

Figure 4.9 DECENTRALIZED CONTROL SYSTEM RESULTS FOR

The organization of the graphs is the same as in section 2. Figures 4.3 through 4.5 show the density-state variables on the links in the order that the links appear in the corridor. Figures 4.6 through 4.8 show the velocity-state variables on the links in the same order. The graph of the controls appears in figure 4.9.

We can see immediately that the qualitative behavior of the state variables on all the links is very much the same as in the centralized solution. The estimates also behave the same as they do in the centralized solution. Thus, the numerical results (table 4.3) are virtually indistinguishable from the centralized solution.

There are two differences, however, in the behavior of the two solutions, and the differences are much what we may expect. First, let us study the graph of the controls (figure 4.9). Although the curve for the first control (controller A) is almost identical to the first control of the centralized solution (figure 2.13), the magnitude of the control is approximately 20 percent less in the decentralized solution. The second control (controller B) behaves quite differently from the centralized solution. In the centralized solution, control 2 achieves its maximum value at the end of the flow pulse (t=52 seconds), and remains near that value until the system has almost recovered. In the decentralized solution, the control builds slowly to its maximum value (at t=140 seconds), and from then until the end of the experiment, is slightly greater than the centralized control.

The reasons for the behavior of the decentralized control are straightforward. The only knowledge that the second control has of the flow pulse is the effect on the density and velocity of links 5 and 6. Thus, it cannot anticipate the impact of the disturbance as control 2 of the centralized solution did. By the time it reaches its maximum value, the density on link 5 is greater and the velocity on link 5 lower than they are in the centralized solution (see figures 2.9, 2.12, 4.5, and 4.8), which requires control 2 to exert more energy than in the centralized solution.

Control 1 appears to be more conservative in the decentralized solution than in the centralized solution. The magnitudes of the elements of the

Table 4.3

COMPARISON OF CENTRALIZED AND DECENTRALIZED SOLUTIONS FOR SAMPLE CORRIDOR

Estimated State	Statistical Covariance		Percent Degradation
	Centralized	Decentralized	
Density Link 1 (ρ_1)	1.60	1.67	4.4
Velocity Link 1 (v_1)	0.0362	0.0309	-14.6
Density Link 2 (ρ_2)	1.75	1.80	2.9
Velocity Link 2 (v_2)	0.901	1.21	34.3
Density Link 3 (ρ_3)	1.70	1.63	-4.1
Velocity Link 3 (v_3)	0.0313	0.0288	-8.0
Density Link 4 (ρ_4)	0.937	0.988	5.4
Velocity Link 4 (v_4)	0.618	0.794	28.5
Density Link 5 (ρ_5)	1.51	1.49	-1.3
Velocity Link 5 (v_5)	0.0444	0.0472	6.3
Density Link 6 (ρ_6)	1.89	1.92	1.6
Velocity Link 6 (v_6)	0.495	0.451	-8.9
COST ($\hat{J}$)*			
OPEN LOOP	5.15582×10^5	5.15582×10^5	0
CLOSED LOOP	4.74092×10^6	4.75457×10^6	0.288

*See section 2.4: $\hat{J} = \sum_{t=0}^{T-1} \{[\underline{x}(t)-\underline{x}_0]'\underline{X}_1[\underline{x}(t)-\underline{x}_0]+[\underline{u}(t)-\underline{u}_0]'\underline{S}_2[\underline{u}(t)-\underline{u}_0]\}$.

feedback-gain matrix for controller A are smaller than the corresponding elements in the centralized solutions. Also, errors in the states of controller B do not contribute to control 1 as they do in the centralized solution. These two facts explain the the lower-control energy that is applied in the decentralized solution. Control 1 can still anticipate the effect of the flow pulse in the decentralized solution, and thus, it behaves qualitatively in the same manner as in the centralized solution.

In spite of the differences in the actions of the controls, the quantitative behavior of the state variables is almost the same for the decentralized solution as for the centralized solution. Generally, the densities on the main freeway are slightly higher and the velocities slightly lower for the decentralized solution. Consequently, the densities on the secondary freeway are slightly lower and the velocities higher for the decentralized solution. Also, the disruption of flow on link 6 is delayed for the decentralized solution. This is a direct consequence of behavior of control 2.

An interesting comparison between the centralized and decentralized solutions can be made with the flows versus density graphs in figure 4.10. Figure 4.10 is an enlarged duplicate of figure 2.15 with the operating point of the decentralized controller added. We can see that the decentralized controller tries to use the unused capacity of the secondary freeway just as the decentralized controller does. It is not quite as successful in this attempt, but does well enough that the statistical costs for both solutions are close.

In concluding this section, we note that the situation we have given the controller is not a simple one. The input flow during the pulse is more than twice the capacity of the main freeway. During the disturbance on the freeway, the state deviations are large enough to invalidate the assumption of linearity. Yet, the control system still works well.

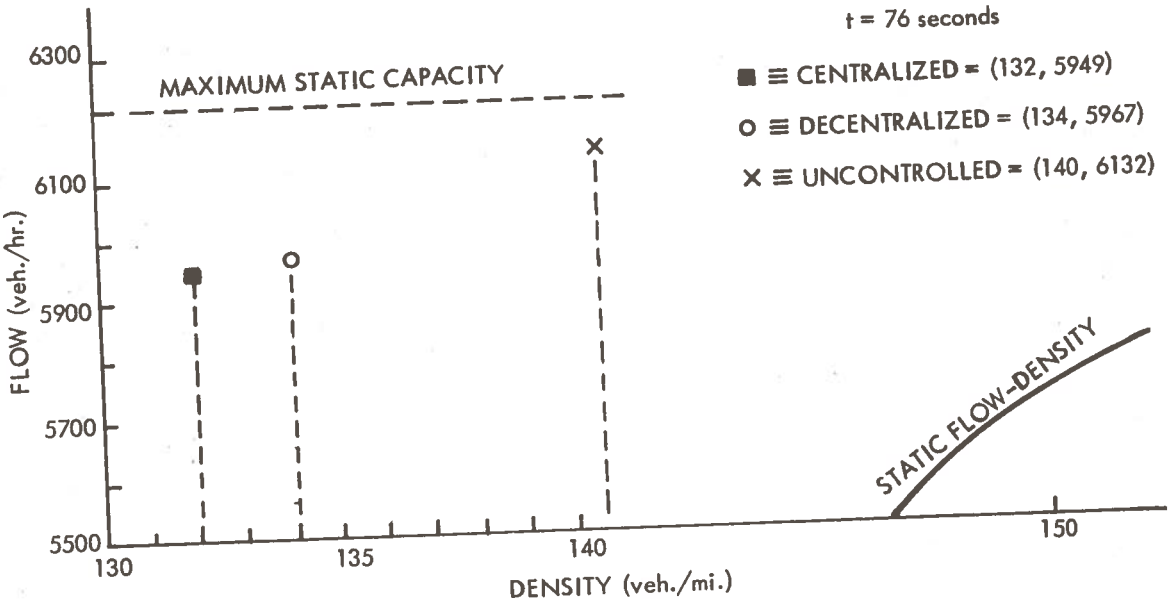

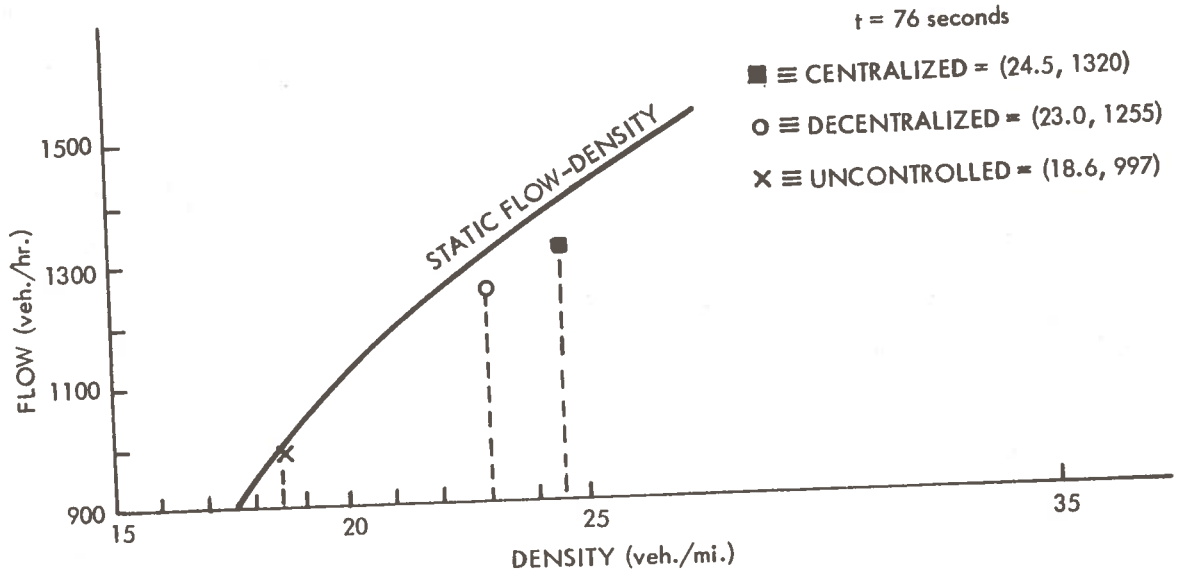

Figure 4.10 COMPARISON OF FLOW DEMANDS ON CORRIDOR

5. CONCLUSIONS

The objective of this report is to develop and evaluate a systematic approach to the design of a suboptimal decentralized control system, and to apply the approach to a freeway corridor. The results of section 4 indicate that the control system designed by the method presented in section 3 has worked well for the traffic model that has been used. A brief summary of the philosophy leading to the design method is given in the next few paragraphs.

The approach that is used to develop the design method has consisted of two parts. In the first part, a centralized solution has been developed using the LQG regulator approach. To use the LQG method, several assumptions have to be made concerning the properties of the system. Although the development of the control system indicated that some of the assumptions were not satisfied, the control system worked well for the particular traffic model used, as was seen in the example of section 2.4.

The centralized LQG control system design has two important desirable properties:

(a) The feedback law is linear, which makes compuation of the control from the estimate easy.

(b) The estimator structure is logical and is composed of two parts. The first part propagates the estimate with the system dynamics. The second part is an appropriately weighted feedback of the difference between the true and the expected measurements.

The implemented centralized solution also has two undesirable properties:

(1) The filter gain must be computed on-line (because of the use of the extended Kalman filter).

(2) All the measurements must be available to the central processor, necessitating a prohibitive amount of communication.

In formulating the design approach for the decentralized controller, we have tried to keep the desirable properties, eliminate the undesirable properties, and still retain as much as possible the performance of the centralized solution.

To do this, we have fixed the filter and feedback law to be linear, preset the decentralized structure of the system, and restricted the quantities communicated between controllers only to the most important estimates. We are then able to formulate the problem as a constrained static minimization.

The results of section 4 have indicated that this method of decentralized control design works well for the sample freeway corridor, assuming that the freeway model is valid. The design also needs to be tested for other situations (such as high-density conditions, high-noise levels, etc.).

The method of solution of the constrained static minimization problem needs to be improved. The sample corridor with 12 state variables and 12 estimates caused the storage of the static minimization to approach practical system limits. The problem is caused by the size of the Lyapunov equation which has to be solved repeatedly.

There are several possible ways to approach this problem. The most obvious, and the most researched, approach is to find an alternative to the direct method for solving the Lyapunov equation. As seen in section 3.3, most of the methods developed to date cannot take advantage of the sparsity of the system matrix, or the repeated substitution of the driving matrix with the same system matrix. The remainder suffer from numerical accuracy problems.

Another approach may be to solve the problem for many smaller ones, and then, to connect the results to obtain the overall solution. This approach may work well for the freeway-corridor problem. The corridor can be first decomposed into its decentralized structure. The controllers can be taken in groups of three starting with the beginning of the corridor. Each time a group of them is solved, the solution for the middle controller is kept. The middle controller then becomes the first controller of the next group, the last controller becomes the middle controller, and the next controller in the corridor is added to form the next group of three. This procedure is continued until the the corridor is reached, and may be iterated. Questions concerning convergence and performance of the resulting solutions need to be considered before it can be used.

A third approach to increasing the size of the problem which can be handled

by the method of section 3.3 may be to assume that the separation principle holds. The filter and control gains may be calculated independently, thus reducing the dimension of the Lyapunov equation to be solved by one-half.

As a final remark, we emphasize that all the results obtained for the sample freeway corridor are only as valid as the model. The literature has shown that the qualitative behavior of this model agrees with the physical behavior of freeways, but the model has only been validated in limited real-life situations. Until further study is done, the model's validity, and thus the validity of the decentralized control system which implicitly assumes the accuracy of the model, is open to question.

With this qualification in mind, we can examine the contribution of this report more closely. The method used to design a decentralized control system is not affected by the model; only the resulting design is. Thus, this method can be applied to many systems for which accurate models are available, and the resulting design will work for the original system. When a valid freeway model is developed (or the present model is verified), the same design method can be used.

6. BIBLIOGRAPHY

M. Athans, "The Role and Use of the Stochastic Linear-Quadratic-Gaussian Problem in Control System Design," IEEE Trans. Automatic Control, Vol. AC-16, Dec. 1971.

S. Barnett and C. Storey, "Solution of the Lyapunov Matrix Equation", Electronics Letters, Vol. 2, Dec. 1966.

S.P. Bingulac, "An Alternate Approach to Expanding PA + A'P = -Q", IEEE Trans. Automatic Control, Vol. AC-15, Feb. 1970.

A.E. Bryson and Y.C. Ho, Applied Optimal Control, Blaisdell, Waltham, MA., 1969.

C.H. Carpenter, "Come Control and Communication Aspects of Stochastic Systems", S.M. Thesis, Dept. E.E., M.I.T., May 1972.

C.F. Chen and L.S. Shieh, "A Note on expanding PA + A'P = -Q", IEEE Trans. Automatic Control, Vol. AC-13, Feb. 1968.

C.Y. Chong, "On the Stochastic Control of Coupled Linear Systems", S.M. Thesis, E.E., M.I.T., Sept. 1970.

C.Y. Chong and M. Athans, "On the Periodic Coordination of Linear Stochastic Systems", Proc. IFAC 6th Intl. Congress, Aug. 1975.

E.J. Davison and F.T. Man, "The Numerical Solution of A'Q + QA = -C," IEEE Trans. Automatic Control, Vol. AC-13, Aug. 1968.

R. Fletcher and M.J. Powell, "A Rapidly Convergent Descent Method for Minimization", The Computer Journal, Vol. 6, 1963.

D.C. Gazis, R. Herman, and R.B. Potts, "Car Following Theory of Steady State Traffic Flow", Operations Research, Vol. 7, 1959.

S.B. Gershwin, "Dynamic Stochastic Control of Freeway Corridor Systems; Volume I Steady State Optimal Traffic Assignment Using the Accelerated Gradient Projection Method," Electronic Systems Laboratory Report ESL-R-609, M.I.T., 1975.

K. Glover, "Structural Aspects of System Identification", Ph.D. Thesis, Dept. E.E., M.I.T., 1973.

H. Greenberg, "An Analysis of Traffic Flow", Operations Research, Vol. 7, 1959.

G. Hadley, Nonlinear and Dynamic Programming, Addison-Wesley, Reading, MA., 1964

P. Hagander, "Numerical Solution of A'S + SA + Q = 0", Information Sciences, Vol. 4, 1972.

J.A. Heinen, "A Technique for Solving the Extended Lyapunov Equation", Proc. of the IEEE, Vol. 59, Feb. 1971.

P.K. Houpt, "Decentralized Stochastic Control of Finite State Systems with Application to Vehicular Traffic Flow", Ph.D. Thesis, Dept. E.E., M.I.T., Nov. 1974.

P.K. Houpt and Athans, "Dynamic Stochastic Control of Freeway Systems; Volume I: Summary," Electronic Systems Laboratory Report ESL-R-608, M.I.T., 1975.

L. Isaksen, "Systems Approach to Traffic Responsive Ramp Metering Control of Urban Freeways", Ph.D. Thesis, U.S.C., 1971.

L. Isaksen and Y.J. Payne, "Regulation of Freeway Traffic", 1972 JACC Proc.

A.H. Jazwinski, Stochastic Processes and Filtering Theory, Academic Press, N.Y., N.Y., 1970.

D.L. Kleinman, "An Iterative Technique for Ricatti Equation Computations", IEEE Trans. Automatic Control, Vol. AC-13, Feb. 1968.

M.J. Lighthill and G.C. Whitham, "On Kinematic Waves II: A Theory of Traffic Flow on Long Crowded Roads", Proc. Royal Soc. (London) Ser. A, Vol. 229, 1955.

O.L. Mangasarian, Nonlinear Programming, McGraw-Hill, N.Y., N.Y., 1969.

J.N. Mather, "Solutions of Generic Linear Equations", Dynamical Systems, M.M. Peixoto, ed., Academic Press, New York, N.Y., 1973.

T.R. McCalla, Introduction to Numerical Methods and Fortran Programming, Wiley, New York, N.Y., 1967.

C. Moler and G. Forsythe, Computer Solution of Linear Algebraic Systems, Prentice Hall, Englewood Cliffs, N.J., 1967.

G.F. Newell, "Nonlinear Effects in the Dynamics of Car Following", Operations Research, Vol. 9, 1961.

D. Orlhac, M. Athans, J. Speyer, and P.K. Houpt, "Dynamic Stochastic Control of Freeway Corridor Systems; Volume IV: Estimation of Traffic Variables Via Extended Kalman Filter Methods", Electronic Systems Laboratory Report ESL-R-611, M.I.T., 1975.

M.J. Powell, "An Efficient Method for Finding the Minimum of a Function of Several Variables without Calculating Derivatives", The Computer Journal, Vol. 7, 1964.

H.J. Rome, "A Direct Solution to the Linear Variance Equation of a Time Invariant Linear System," IEEE Trans. Automatic Control, Vol. AC-14, Oct. 1969.

N.R. Sandell, P. Varaiya, and M. Athans, "A Survey of Decentralized Control Methods for Large Scale Systems", Proc. Engineering Foundation, Conference on Systems Engineering, Henniker, N.H., Aug. 1975.

M. Singleton and J.E. Ward, "Dynamic Stochastic Control of Freeway Corridor Systems' Volume V: A Comparative Study of Various Types of Vehicle Detectors", Electronic Systems Laboratory Report ESL-R-612, M.I.T., 1975.

P.G. Smith, "Numerical Solution of the Matrix Equation Ax + xA' + B = 0", IEEE Trans. Automatic Control, Vol. AC-16, June 1971.

W. Thompson, H.J. Payne, and L. Isaksen, "Design of a Traffic REsponsive Control Systems for a Los Angeles Freeway", Proc. IEEE, 1972, Int. Conf. on Cyb. and Soc.

R.S. Varga, Matrix Iterative Analysis, Prentice-Hall, Englewood Cliffs, N.J., 1962.

H.S. Witsenhausen, "A Counterexample in Stochastic Optimal Control", SIAM J. Control, Vol. 6, 1962.

W.M. Wonham, "Random Differential Equations in Control Theory", Probabilistic Methods in Applied Mathematics, Vol. II, A.T. Barucha-Reid, ed., Academic Press, N.Y., 1969.

APPENDIX A: DIRECT METHOD FOR SOLVING LYAPUNOV EQUATIONS

The matrix Lyapunov equation:

$$\underline{A}\,\underline{\Sigma} + \underline{\Sigma}\,\underline{A}' + \underline{Q} = 0, \tag{A.1}$$

is actually a set of n(n+1)/2 independent linear equations (assuming that $\underline{A}$ is non-singular, and that no two poles are symmetric about the origin) in the same number of unknowns. There are several systematic methods (see Chen and Shieh [1968] and Bingulac [1970]) for writing the linear system of equations from equation (A.1). The method we will use is a modified version of the method proposed by Chen and Shieh.

By using this method, equation (A.1) can be written as:

$$\overline{\underline{A}}\,\underline{\Sigma}_v = -\underline{Q}_v, \tag{A.2}$$

where:

$\overline{\underline{A}}$ ≡ expanded version of $\underline{A}$,

$\underline{\Sigma}_v$ ≡ n(n+1)/2 vector consisting of the upper-triangular-half of $\underline{\Sigma}$ stored row-wise,

$\underline{Q}_v$ ≡ n(n+1)/2 vector consisting of the upper-triangular-half of $\underline{Q}$ stored row-wise.

There are many ways to solve equation (A.2) (see Moler and Forsythe [1967]). The most effective method for many situations is the L-U decomposition method.

From linear algebra, we know that any square nxn matrix $\underline{A}$ can be written as:

$$\underline{A} = \underline{L}\,\underline{U}, \tag{A.3}$$

where:

$\underline{L}$ ≡ nxn lower triangular matrix with 1's along the diagonal.

$\underline{U}$ ≡ nxn upper triangular matrix .

Substituting (A.3) into the linear equation:

$$\underline{A}\,\underline{x} = \underline{b}, \tag{A.4}$$

we get:

$$\underline{L}\,\underline{U}\,\underline{x} = \underline{b}. \tag{A.5}$$

Let:

$$\underline{U}\,\underline{x} = \underline{y}. \tag{A.6}$$

Substituting (A.6) in (A.5) gives the equation:

$$\underline{L}\,\underline{y} = \underline{b}. \tag{A.7}$$

The pair of equations (A.6) and (A.7) can easily be solved since $\underline{L}$ in lower triangular equation (A.7) can be solved for $\underline{y}$ by using forward substitution. Then, equation (A.6) can be solved for $\underline{x}$ using back substitution since $\underline{U}$ is upper triangular. The total number of operations involved in the L-U decomposition is about n^3, while n^2 operations are needed for the forward and back substitutions.

Applying this method to solve equation (A.2) results in approximately n^6 operations for the L-U decomposition and n^4 for the substitution because the matrix $\underline{\bar{A}}$ is $[n(n+1)/2] \times [n(n+1)/2]$. The number of operations can be reduced considerably by taking advantage of the sparsity properties of $\underline{\bar{A}}$ to eliminate multiplications involving zeroes. We have found empirically that for the 12-state freeway-corridor problem the L-U decomposition is on the order of n^4 operations rather than n^6.

The actual algorithm for solving equation (A.2) is designed to

(a) use an optimal ordering algorithm to determine the optimal order for processing the rows and columns of $\underline{\bar{A}}$. This is done only once if the location of the non-zero elements of $\underline{\bar{A}}$ remains unchanged,

(b) perform the L-U decomposition symbolically: i.e., to determine the positions of the non-zero elements in L and U. Again, this step is performe only once if the locations of the non-zero elements of $\underline{\bar{A}}$ remain unchanged,

(c) perform the L-U decomposition numerically. This step is repeate every time the non-zero elements of $\underline{\bar{A}}$ change their values,

(d) use forward and back substitutions to solve $\underline{\Sigma}_v$. This step is th only step that needs to be executed if only $\underline{Q}_v$ changes.

LINEARIZED SYSTEM MATRIX A_o:

-3.06D-02	-8.12D-02	0.0	0.0	0.0	0.0	0.0	0.0	0.0	0.0	0.0	0.0
5.06D-02	-2.00D-01	0.0	0.0	-5.06D-02	0.0	0.0	0.0	0.0	0.0	0.0	0.0
0.0	0.0	-3.06D-02	-1.01D-02	0.0	0.0	0.0	0.0	0.0	0.0	0.0	0.0
0.0	0.0	2.06D-01	-2.00D-01	0.0	0.0	-2.06D-01	0.0	0.0	0.0	0.0	0.0
3.06D-02	8.12D-02	0.0	0.0	-3.06D-02	-8.12D-02	0.0	0.0	0.0	0.0	0.0	0.0
0.0	3.06D-02	0.0	0.0	5.06D-02	-2.31D-01	0.0	0.0	-5.06D-02	0.0	0.0	0.0
0.0	0.0	3.06D-02	1.01D-02	0.0	0.0	-3.06D-02	-1.01D-02	0.0	0.0	0.0	0.0
0.0	0.0	0.0	3.06D-02	0.0	0.0	2.06D-01	-2.31D-01	0.0	0.0	-2.06D-01	0.0
0.0	0.0	0.0	0.0	3.06D-02	8.12D-02	0.0	0.0	-3.06D-02	-8.12D-02	0.0	0.0
0.0	0.0	0.0	0.0	0.0	3.06D-02	0.0	0.0	0.0	-2.31D-01	0.0	0.0
0.0	0.0	0.0	0.0	0.0	0.0	3.06D-02	1.01D-02	0.0	0.0	-3.06D-02	-1.01D-02
0.0	0.0	0.0	0.0	0.0	0.0	0.0	3.06D-02	0.0	0.0	0.0	-2.31D-01

LINEARIZED INPUT MATRIX B_o:

0.0	0.0
0.0	0.0
0.0	0.0
0.0	0.0
2.26D+00	0.0
0.0	0.0
-2.26D+00	0.0
0.0	0.0
0.0	2.26D+00
0.0	0.0
0.0	-2.26D+00
0.0	0.0

OBSERVATION MATRIX C_o:

1.00D+00	0.0	0.0	0.0	0.0	0.0	0.0	0.0	0.0	0.0	0.0	0.0
0.0	0.0	1.00D+00	0.0	0.0	0.0	0.0	0.0	0.0	0.0	0.0	0.0
0.0	0.0	0.0	0.0	1.00D+00	0.0	0.0	0.0	0.0	0.0	0.0	0.0
0.0	0.0	0.0	0.0	0.0	0.0	1.00D+00	0.0	0.0	0.0	0.0	0.0
0.0	0.0	0.0	0.0	0.0	0.0	0.0	0.0	1.00D+00	0.0	0.0	0.0
0.0	0.0	0.0	0.0	0.0	0.0	0.0	0.0	0.0	0.0	1.00D+00	0.0

LINEAR FEEDBACK GAIN MATRIX G_o:

2.30D-03	1.92D-04	-7.94D-04	4.70D-04	5.25D-03	-3.51D-04	-8.62D-03	-2.93D-04	1.58D-03	-2.76D-04	-8.97D-04	-1.51D-07
6.96E-04	1.52D-04	2.27D-04	8.75D-05	1.61D-03	1.92D-04	-4.57D-04	4.79D-04	4.76E-03	-6.77D-04	-7.36D-03	3.07D-04

FINAL EXTENDED KALMAN GAIN MATRIX H :

5.15D-01	0.0	1.38D-02	0.0	6.76D-05	0.0
-3.77D-02	0.0	-1.16D-02	0.0	3.06D-04	0.0
0.0	5.13E-01	0.0	1.38D-02	0.0	9.80D-04
0.0	-2.03D-02	0.0	-9.21D-02	0.0	-1.19E-02
1.09E-02	0.0	5.18D-01	0.0	9.38D-03	0.0
-8.96D-03	0.0	-3.82D-02	0.0	-7.63D-03	0.0
0.0	1.38D-02	0.0	5.07D-01	0.0	1.46D-02
0.0	-1.67D-03	0.0	-5.16D-02	0.0	-9.28D-02
6.76D-05	0.0	9.38D-03	0.0	5.25D-01	0.0
-3.80E-04	0.0	-5.97D-03	0.0	-6.62D-02	0.0
0.0	9.80D-04	0.0	1.46D-02	0.0	5.12D-01
0.0	-3.57D-04	0.0	-1.38D-02	0.0	-1.44D-01

DECENTRALIZED FEEDBACK GAIN FOR CONTROLLER A:

0.158463D-02	0.149074D-03	0.313606D-03	-0.237515D-04	0.473421D-02	-0.435586D-03
-0.682637D-02	0.115597D-03				

DECENTRALIZED FEEDBACK GAIN FOR CONTROLLER B:

0.516333D-02	-0.729205D-03	-0.178864D-02	-0.736903D-03

DECENTRALIZED FILTER GAIN FOR CONTROLLER A:

0.513672D+00	0.0	0.117321D-01	0.0
-0.362271D-01	0.0	-0.142583D-01	0.0
0.0	0.519685D+00	0.0	0.109814D-01
0.0	-0.540823D-01	0.0	-0.782439D-01
0.117321D-01	0.0	0.515557D+00	0.0
-0.478706D-02	0.0	-0.350580D-01	0.0
0.0	0.109814D-01	0.0	0.510768D+00
0.0	-0.646907D-02	0.0	-0.594544D-01

DECENTRALIZED FILTER GAIN FOR CONTROLLER B:

0.522768D+00	0.0
-0.656641D-01	0.0
0.0	0.516650D+00
0.0	-0.133427D+00

APPENDIX D: REPORT OF INVENTIONS

This report represents a breakthrough in the development of a theory for a decentralized control strategy applicable to a large-scale transportation network.

However, there are no inventions or other patentable items.

OFFICIAL BUSINESS
PENALTY FOR PRIVATE USE, $300

U.S.MAIL

POSTAGE AND FEES PAID
U. S. DEPARTMENT OF TRANSPORTATION
518